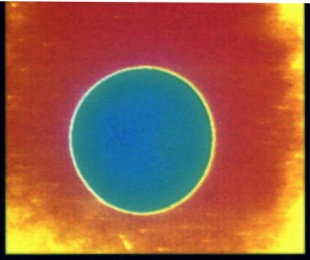

Structure and function of aquaporins

in health and disea

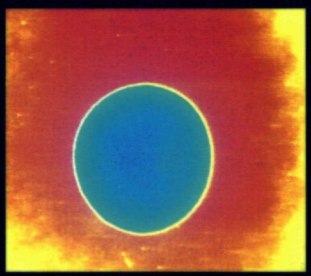

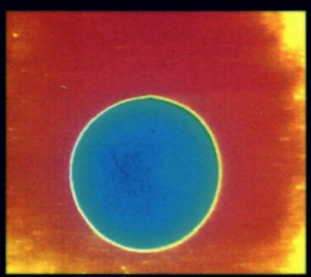

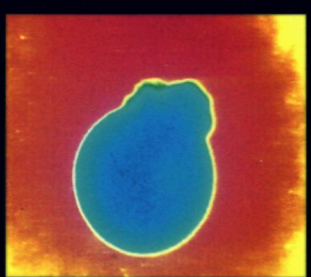

Sabine M. Mulders

Structure and function of aquaporins in health and disease

Cover illustration: video images of oocytes

CIP-gegevens Koninklijke Bibliotheek, Den Haag
Mulders, Sabine Marie-Antoinette

Structure and function of aquaporins in health and disease.
Sabine M. Mulders.-Ill. Thesis University of Nijmegen.
-With ref.-With summary in Dutch
ISBN 90-9010904-8

Structure and function of aquaporins in health and disease

Een wetenschappelijke proeve
op het gebied van de Medische Wetenschappen

Proefschrift

ter verkrijging van de graad van doctor
aan de Katholieke Universiteit Nijmegen,
volgens besluit van het College van Decanen
in het openbaar te verdedigen
op vrijdag 10 oktober 1997
des namiddags om 3.30 uur precies

door
Sabine Marie-Antoinette Mulders
geboren op 5 april 1969 te Silvolde

Promotor
Prof. Dr. C.H. van Os
Co-promotor
Dr. P.M.T. Deen

Manuscriptcommissie
Prof. Dr. R.A. Koene
Prof. Dr. J.J.H.H.M. de Pont
Prof. Dr. E.J.J. van Zoelen

The research presented in this thesis was performed at the Department of Cell Physiology, Faculty of Medical Sciences, University of Nijmegen, and supported by the Dutch Science Foundation, division of Life Sciences (NWO-SLW-810-405-16.2)

Voor mijn ouders

Contents

Chapter 1

Introduction

Eur J Clin Invest 26, 1041-1050 (1996)
(adapted and updated version)

Water crosses most cell membranes by simple diffusion through the lipid bilayer. However, in certain cell membranes water permeability is much higher than can be explained by diffusion alone, indicative of channel-mediated water transport. The biophysical properties of these water filled pores in biological membranes have been studied for decades and this cumulated in an accurate description of water channel properties [47]. There are several parameters which provide useful information about the presence of a facilitated water-transporting pathway. The osmotic water permeability coefficient (P_f, in μm/s), which is defined as the net flow of volume across a membrane in response to a hydrostatic or osmotic driven force, enables us to quantify water transport in time. A P_f higher than ~30 μm/s is indicative of channel-mediated water transport. The P_f of a membrane containing water channels exceeds the diffusional water permeability (P_d), which results in a P_f/P_d ratio greater than unity. Another parameter is the activation energy (E_A, in kcal/mol). Generally, E_A is >8 kcal/mol for water movement by a channel-independent diffusion through the lipid bilayer and ~4 kcal/mol for water movement through aqueous pores. So, a membrane with a high water permeability, a P_f/P_d ratio larger than unity, and a low E_A is likely to contain water channels. In spite of this knowledge, the molecular identification of water channels took place only recently and was due to a serendipitous discovery. Denker *et al.* [37] copurified a 28 kDa protein together with a 32 kDa Rhesus antigen from human red blood cells and this discovery led to the cloning of the first molecular water channel, CHIP28 [139]. CHIP28 appeared to be a member of the MIP-family of intrinsic membrane proteins, named after the first cloned protein of this family, the major intrinsic protein (MIP) of lens fiber cells [57]. The molecular fingerprint of MIP family members consists of two repeats, presumably the result of an ancient gene duplication event [132]. Each repeat is characterized by a very conserved region in which an NPA-box (asparagine-proline-alanine) is unchanged from bacteria to mammals (Fig. 1). Due to this property, new family members were discovered by homology cloning using RT-PCR and primers corresponding to these conserved sequences [44,55,62, 68,74,98,144].

It is now clear that genes coding for MIP proteins are ubiquitous in nature. All current MIP family members derived from two divergent bacterial paralogues, one a glycerol facilitator, the other a water channel [133]. Water channels were found in mammals, plants, insects and bacteria [133]. For the functional characterization of water channels, the *Xenopus* oocyte expression system has played a dominant role, merely because the osmotic swelling test of oocytes expressing water channels is of appealing simplicity. cRNA encoding water channels is injected into *Xenopus* oocytes (~1 mm diameter), which results in the synthesis of large amounts of water channels (Fig. 2). After three days the oocytes are placed in a hypotonic medium. If water channels are present in the plasma membrane, water will quickly enter and the swelling of the oocyte is recorded by a video-imaging system.

For MIP family members that were proven to be water-selective, a new more appropriate name was chosen and since then water channels discovered in mam-

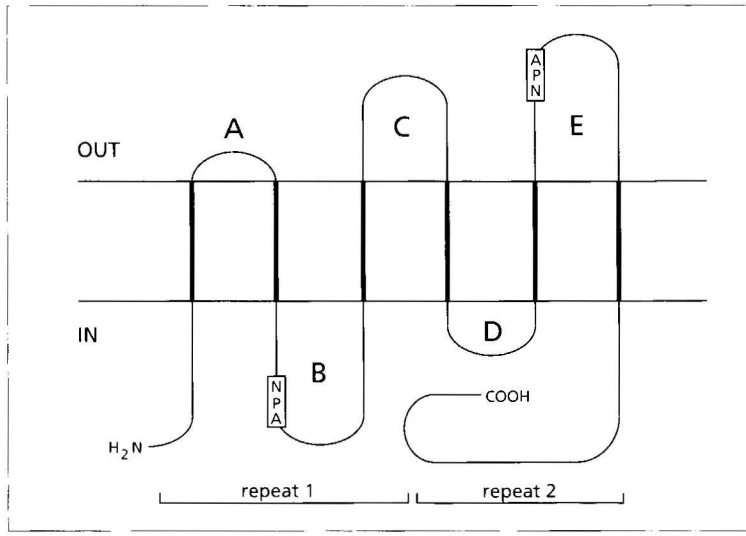

Fig. 1 Proposed topology of the aquaporins. The molecule consists of six transmembrane segments, connected by loops A to E, with cytoplasmic amino- and carboxy termini. Indicated are the two repeats and the highly conserved NPA boxes.

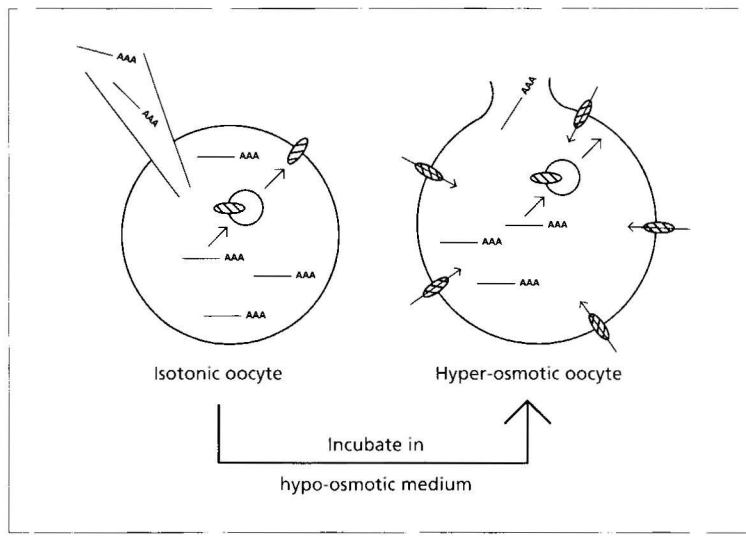

Fig. 2 Schematic drawing of the injection of oocytes. *Xenopus* oocytes are isolated by digestion with collagenase A, and oocytes of stage V or VI are selected. One day after isolation, oocytes are injected with 1 to 20 ng of cRNA encoding AQPs. Ater three days, the oocyte has translated the cRNA into protein, and water permeability of the oocyte is measured in a standard swelling assay. The swelling assay is based on the rate of swelling in response to dilution of the extracellular solution.

malian tissues have been rebaptized as aquaporins 0 through 5, in the rank order of their discovery [3]. This thesis is restricted to the mammalian aquaporins, and is focussed on the relationship between the structural features of these aquaporins and their function.

Aquaporin 0

The major intrinsic protein (MIP) in the fiber cell membranes of the bovine lens was the first member of this channel family to be identified [57]. MIP constitutes over 60% of the membrane protein of lens fiber cells. Initially, MIP was thought to be the gap junction protein of the lens, but expression in *Xenopus* oocytes revealed that MIP does not form gap junctions like connexins [165]. Reconstituted into planar lipid bilayers, MIP functions as an ion channel [45,113], and it was suggested that, as a voltage gated ion channel, it could help to minimize the extracellular fluid in the lens and maintain lens transparency [45]. Mice with mutations in MIP suffer from congenital cataract, which corroborates that MIP has an important function in ion and water homeostasis of lens fiber cells and in maintenance of lens transparency [158,159]. In this thesis it is described that MIP functions as a weak water channel in oocytes and MIP is now also named AQP0.

Aquaporin 1

The identification of CHIP28 as the first molecular water channel AQP1 initiated an avalanche of new information that substantially increased our understanding of water homeostasis of the body in general and renal water transport in particular. Expression of AQP1 in *Xenopus* oocytes dramatically increased the rate of osmotic swelling [140]. The selectivity of AQP1 was proven in reconstitution studies. Proteoliposomes containing AQP1 were highly water permeable with unchanged permeabilities for urea and protons [196]. One group reported glycerol permeation through AQP1 [1], but this observation has not been confirmed by others. Recently, Yool *et al.* reported a forskolin-induced cation conductance in oocytes expressing AQP1 [194]. However, other groups have not been able to reproduce these results [2,30,48,134,153,182].

AQP1 has been shown to be expressed in an ever increasing number of tissues. In kidney, it is expressed in apical and basolateral membranes of proximal tubules, the thin descending limb of Henle and in vasa recta. Furthermore, AQP1 is expressed in red blood cells, lens epithelium, corneal endothelium, ciliary body and iris, nonfenestrated capillary endothelial cells, the apical microvilli of the choroid plexus, parts of the male reproductive tract, red pulp in spleen, gallbladder epithelium, and cholangiocytes in liver. Others also reported expression in alveolar epithelial cells and bronchial epithelium, colonic epithelial crypt cells, pancreatic acinar cell epithelium, salivary gland epithelium and the basolateral membrane of sweat glands, endocardium and syncytial trophoblast cells of placenta (For review, see [148]), and in the inner ear [164].

In red blood cells, AQP1 is thought to be needed to overcome the large osmotic dif-

ferences in the hypertonic kidney medulla. In kidney, 180 liters of glomerular filtrate is formed each day, of which 80-90% is reabsorbed in the proximal tubule and the descending limb of Henle's loop, where AQP1 is expressed. Furthermore, AQP1 could play a role in the secretion and uptake of aqueous humor and corneal hydration in the eye [125,163], in the formation of cerebrospinal fluid in brain [125], and in secretion of bile [125,146]. Recently, it was shown that in rat cholangiocytes, secretin stimulates ductal bile secretion by increasing AQP1 water channels in the plasma membrane [103]. The molecular mechanism responsible for the regulated membrane trafficking of AQP1 in cholangiocytes is still unknown.

In lung, AQP1 is expressed in the peribronchial vasculature and the visceral pleura. This location suggests that AQP1 may play an important role in water absorption in the lung at birth, when the lung has to be cleared from fluids and be prepared for alveolar gas exchange [80]. Indeed, AQP1, together with AQP4 and AQP5, showed a sharp increase in expression in rat lung in the perinatal period [171]. Additionally, the expression of AQP1 in rat lung is increased by corticosteroids, which are known to improve pulmonary functions in premature human infants, consistent with the possible role of AQP1 in perinatal lung water clearance [80].

Epithelial cells lining cysts in autosomal dominant polycystic kidney disease have been found to express AQP1 [164]. AQP1 may play a role in fluid secretion into these cysts and this is corroborated by the simultaneous presence of CFTR in apical membranes of these cyst cells [61].

Every year, many patients diagnosed with head or neck cancer receive radiation therapy, which often destroys salivary secreting acinar cells of salivary glands as a side-effect. In rats, an increased fluid secretion was observed after adenoviral-mediated transfer of the AQP1 cDNA to irradiated salivary glands, suggesting that AQP1 gene transfer may have potential as a therapeutic approach for the treatment of postradiation salivary hypofunction [36].

AQP1 gene defects

Mutations in AQP1 leading to a non-functional water channel were expected to have severe clinical or even lethal consequences, since AQP1 is expressed in a wide variety of tissues throughout the whole body. However, when it appeared that the Colton blood group antigens result from an alanine-valine polymorphism at residue 45 in the first extracellular loop of AQP1, a world wide search was started for individuals who are negative for the Colton blood group antigens ($Co\ a^-/b^-$) [143]. This search revealed 5 individuals, and from 3 women blood and urine samples could be collected. In these individuals, an exon deletion, a nucleotide insertion and a missense mutation resulted in the disruption of the protein, leading to the absence of AQP1. Surprisingly, however, these individuals appeared to be healthy, suggesting the existence of compensatory mechanisms and denying the anticipated vital importance of AQP1 [143]. Recent studies have revealed a slightly reduced life span and deformability of their erythrocytes [107], but, until now, a thorough assessment of renal function has not been accomplished. Furthermore, these individuals were expected to have eye problems like glaucoma, and a deficient cerebrospinal fluid production, but no apparent clinical manifestations were observed.

The existence of red cells with a specific deficiency of AQP1 protein in Colton-null individuals provides an opportunity to assess the contribution of AQP1 to the diffusional (P_d) and osmotic (P_f) water permeabilities of red cells. In addition, the exact P_f/P_d ratio will permit calculation of the aqueous pathway through AQP1 [47]. Low molecular weight solutes do not permeate through AQP1, indicative for a small pore, in which water only moves in single file. Mathai *et al.* [107] used red cells of these extremely rare Colton-null phenotype individuals and determined that AQP1 contributes for more than 85% to the total osmotic pathway. The AQP1-mediated P_f/P_d ratio turned out to be 13 and this ratio predicts the length of the aqueous channel within AQP1 to be 36Å, which is shorter than the estimated 50Å width of the lipid bilayer.

In contrast to these Colton-negative individuals, who are apparently not in need of a functional AQP1, CAPD patients seem to benefit from a functional AQP1, since the presence of AQP1 in peritoneal capillaries facilitates water efflux into the peritoneal dialysate [131].

Aquaporin 2

Soon after the cloning of AQP1, a second water channel was cloned from renal collecting ducts, where AQP1 was not detected [55]. In this part of the kidney, vasopressin-dependent reabsorption of the remaining 10-20% of the glomerular filtrate not reabsorbed by the proximal nephron takes place. With immunohistochemistry AQP2 was localized exclusively to the principal cells of the cortical and outer medullary collecting duct (CD) and to inner medullary CD cells [55,123]. Additionally, quantitative ELISA, RT-PCR and *in situ* hybridization showed that AQP2 and the V_2 receptor are also highly expressed in arcades, which connect deep and mid-cortical nephrons to cortical collecting ducts [81]. The use of immuno-electron microscopy techniques revealed that most of AQP2 is present in small endosomal vesicles in the subapical region of principal cells [123]. In the absence of arginine-vasopressin, AVP, the apical membrane has a low permeability for H_2O, but admission of AVP results in a rapid increase in P_f. Wade *et al.* [183] originally postulated that the rapid increase in P_f occurred by a membrane shuttle mechanism. Binding of AVP to the V_2 receptor increases cAMP which results in a fusion of intracellular membrane compartments with the apical membrane. Withdrawal of AVP results in endocytosis and restoration of a low water permeability of the apical membrane (Fig. 3).

Conclusive evidence has now been provided for the shuttle hypothesis by following the redistribution of AQP2 after AVP admission in isolated collecting ducts in normal and in Brattleboro rats and in transfected LLC-PK1 cells [79,106,122,149,191]. Nielsen *et al.* [122] examined the role of AVP in perfused collecting ducts of rat, using high-resolution immuno electron microscopy. They measured the labeling density of AQP2 in the apical membrane and intracellular vesicles before and after AVP admission and confirmed the shuttle hypothesis. Others [149,191] reached the same conclusion from *in vivo* studies in Brattleboro rats, who lack vasopressin synthesis, and where AQP2 is only present in subapical vesicles. AVP infusion

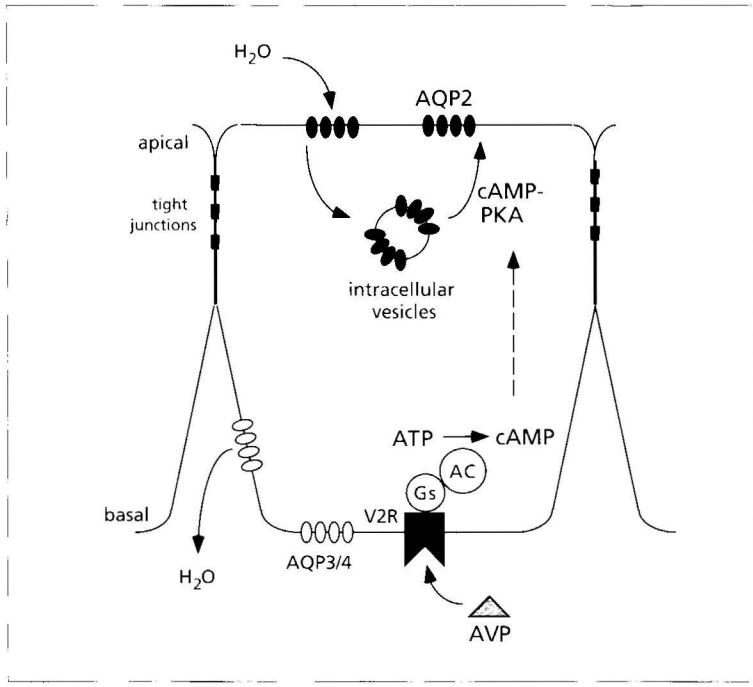

Fig. 3 Distribution of AQP2, AQP3 and AQP4 in collecting duct principal cells. Vasopressin (AVP) binds to the V_2 receptor (V2R). Subsequently, heterotrimeric G-proteins (Gs) mediate activation of adenylyl cyclase (AC), which induces the conversion of ATP into cAMP. cAMP activates protein kinase A (PKA), which results in phosphorylation of AQP2 in subapical vesicles which consequently fuse with the apical membrane. Water enters the cell through AQP2 in the apical membrane, and leaves the cell through AQP3 and/or AQP4 in the basolateral membrane.

caused a marked redistribution of AQP2 to the apical membrane. In normal rats, the fraction of AQP2 in the plasma membrane relative to that in intracellular vesicles increased 2-fold after infusion of the V_2 receptor agonist 1-desamino-8-D-arginine vasopressin (dDAVP) and this increase was even larger when the rats were water-loaded for 12 h before dDAVP infusion [106]. Katsura *et al.* [79] transfected LLC-PK_1 cells with AQP1 or AQP2 expression constructs (tagged with a C-myc epitope). AQP1 transfection conferred a constitutively two-fold higher P_f to LLC-PK_1 cells but the P_f of AQP2 transfected cells only increased after AVP treatment. Forskolin treatment induced a similar redistribution of AQP2 to the plasma membrane as AVP. The ultimate proof for the reversibility of AQP2 shuttling was provided by experiments in which LLC-PK_1 cells were treated with the protein synthesis inhibitor cycloheximide. Repetitive admission and withdrawal of vasopressin indicated that AQP2 molecules can be recycled at least 3 times without being degraded in the lysosomal compartment [79]. Immunolocalization studies, however, showed that AQP2 was inserted into the basolateral membrane rather than into the apical membrane. This unphysiological targeting may be due to the C-myc epi-

tope which could influence the routing of AQP2, or is inherent to AQP2 expression in LLC-PK cells. Recently, Valenti *et al.* [172] and Deen *et al.* [34] reported stably transfected cell lines (human collecting duct cells and MDCK cells, respectively) in which AQP2 translocates to the apical membrane upon vasopressin stimulation, which reflects the normal physiological situation.

In addition to the short term regulation by vasopressin, the urinary concentration ability is also regulated by a long term process. When dehydrated Brattleboro rats were treated for 5 days with AVP infusion, the expression level of AQP2 increased nearly three-fold [40]. After thirsting normal rats for 48 hours, the amount of AQP2 mRNA [99] and the AQP2 protein expression [40,64,123]increased several-fold. When dehydrated rats were treated with a V_2 receptor antagonist the increase in AQP2 expression was completely abolished, indicating that this increase is mediated by the V_2 receptor [64].

To study the effect of cAMP on the AQP2 gene, the 5' flanking region of the human AQP2 gene was isolated and its promoter activity was measured by a CAT assay. It was shown that the AQP2 promoter region contains a cAMP responsive element (CRE), which directed increased transcription after elevation of intracellular cAMP levels. This suggests that cAMP is an important regulator of AQP2 gene expression [170].

In addition to an effect of AVP on AQP2 expression and insertion into the apical membrane, it was investigated whether AVP regulates the water pore in AQP2 directly by phosphorylation of the protein kinase A (PKA) consensus site Ser256. Kuwahara *et al.* [85] treated AQP2 expressing oocytes with forskolin and cAMP and observed a 50% increase in P_f without an increase in plasma membrane expression, while a S256A mutant AQP2 could not be stimulated by cAMP. *In vitro* phosphorylation studies confirmed AQP2 phosphorylation by PKA of the S256 residue [85]. In contrast to this study, Lande *et al.* [88] were unable to find an effect of phosphorylation of AQP2 containing endosomes on the P_f of the isolated endosomes. They concluded that phosphorylation of AQP2 does not modify water permeation through AQP2 but that phosphorylation may modulate the distribution of AQP2 between plasma membrane and intracellular vesicle compartments. This was further corroborated in transfected LLC-PK_1 cells, where vesicles containing AQP2-S256A were not able to fuse with the plasma membrane, confirming that PKA phosphorylation of AQP2 is required for regulated exocytosis [54,78].

The molecular machinery needed for AVP dependent vesicle trafficking in the collecting duct cell is not yet understood in detail. Vesicle associated membrane proteins, VAMPs, play a role in membrane vesicle targeting in the endocytosis of synaptic vesicles in neuronal cells (SNARE hypothesis) [49]. It was shown that two VAMP homologues, VAMP-2/synaptobrevin [124,162] and cellubrevin [73], colocalize with AQP2 in intracellular vesicles. This strongly suggests that VAMPs are involved in vasopressin-regulated targeting of AQP2. In addition, the demonstration of expression of the vesicle targeting protein syntaxin-4, which binds VAMP-2 with high affinity, in the apical membrane of collecting duct principal cells supports the view that these proteins could play a role in AQP2-vesicle targeting to the apical membrane [102]. Others showed that a Rab3-like protein, a protein also

involved in regulated exocytosis, is co-purified with AQP2 containing vesicles [93]. The glucose transporter from adipocytes, GLUT4, contains a dileucine internalization sequence which is critical for endocytosis of the GLUT4 protein [24]. The C-terminus of AQP2 also contains two dileucine motifs in a palindromic sequence which is absent in AQP1 [79]. Both GLUT4 and AQP2 are internalized in clathrin-coated pits, indicating that a similar mechanism may be involved in internalization. However, recently it was shown that these dileucine motifs are not involved in AQP2 targeting (D. Brown, personal communication).

AQP2 and diseases

Congenital nephrogenic diabetes insipidus

The exclusive localization of AQP2 in kidney medulla and its regulation by AVP resulted in the hypothesis that this water channel accounts for the facultative reabsorption of the approximately sixteen liters of pro-urine which daily reach the collecting duct. The final evidence for this assumption was the detection of AQP2 gene mutations in patients with hereditary nephrogenic diabetes insipidus (NDI) [31,178]. This disease is characterized by the inability of the kidney to concentrate urine in response to AVP. In most patients, NDI is caused by mutations in the V_2 receptor gene, a form which is inherited as an X-linked recessive trait. In a few families, however, NDI shows an autosomal mode of inheritance. Mutations in the AQP2 gene have recently been found in such families [10,16,31,66,129,130,178] (Fig. 4).

Patients with a mutation in the AQP2 gene show the same clinical phenotype as those with a V_2 receptor mutation, but can be distinguished from patients with a V_2 receptor defect by their normal extra-renal response to the V_2 receptor agonist 1-desamino-8-D-arginine vasopressin (dDAVP) [179]. The functional consequences of several amino acid substitutions found in patients with autosomal recessive NDI, have been studied in *Xenopus laevis* oocytes [28,178]. Expression of mutant AQPs did not result in an increase of P_f compared to water-injected oocytes. Further studies on the fate of these mutant aquaporins in *Xenopus* oocytes have shown that they are retarded in the endoplasmic reticulum (ER), and consequently impaired in their transport to the plasma membrane, in some cases combined with a lower stability of the mutant proteins [28].

Kanno *et al.* [77] studied AQP2 excretion into urine and quantified urinary AQP2 by a radioimmunoassay. In healthy volunteers and patients with central diabetes insipidus, AQP2 was found to increase in response to AVP, but not in patients with X-linked and non-X-linked NDI. They suggested that this assay might be used for detection of NDI patients and their differentiation from patients with central diabetes insipidus. However, a high AQP2 level was detected in urine of an NDI patient with a non-sense V_2 receptor mutation [35] and this shows that delineation of NDI from central diabetes insipidus will not be as simple as suggested and is certainly inferior to the performance of a dDAVP-test. Moreover, the latter procedure not only discriminates between central and nephrogenic diabetes insipidus, but also between the two genetic forms of NDI [179].

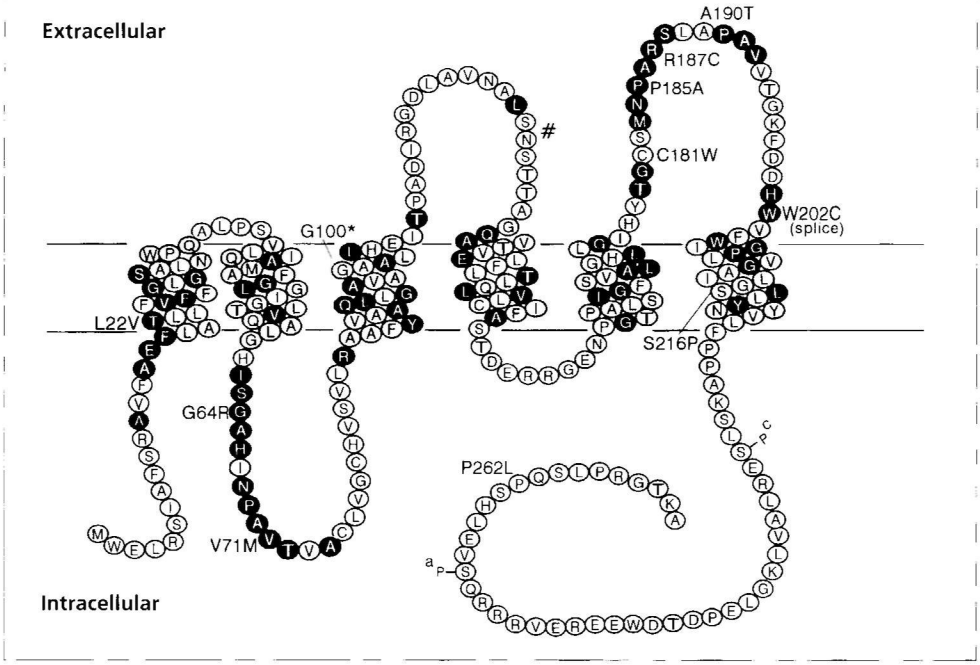

Fig. 4 Proposed topology of AQP2. Missense mutations, the site of a frame shift mutation (#) and a mutation in the splice site (splice) found in the AQP2 gene of nephrogenic diabetes insipidus patients are indicated. Amino acids which are conserved in at least 9 out of 17 members of the MIP family are indicated by filled symbols. Consensus sequences for potential phosphorylation sites for protein kinase A (P^a) and protein kinase C (P^c) are indicated. Mutations were taken from [10,16,31,66,129,130,178]

Acquired nephrogenic diabetes insipidus

A well-known cause of acquired nephrogenic diabetes insipidus is chronic lithium therapy. Lithium is thought to exert this side-effect by interfering with the post-V_2 receptor pathway, although the exact mechanism of inhibition has remained unknown. Marples *et al.* [104] found a decrease in AQP2 expression in renal medulla of rats after chronic lithium infusion. Cessation of lithium infusion or dDAVP treatment for a week reversed this down-regulation only partially, consistent with the clinical observation of slow recovery from lithium-induced NDI. Other polyuric states which have been associated with reduced expression of AQP2 are those observed during hypokalemia, after release of bilateral ureteral obstruction and in experimental nephrotic syndrome [4,52,105]. In addition, Takahashi *et al.* [166] found that AQP2 expression is reduced in the polyuria accompanying chronic renal failure, a factor which might contribute to the urinary concentrating defect. Another condition in which, probably in addition to medullary wash-out, reduced expression of AQP2 could be involved is the initially reduced response to dDAVP, which is often observed in patients with central diabetes insipidus. Abnormal expression of AQP2 has not only been associated with polyuria, but also with

pathological water retention. An increase of AQP2 expression has been observed in kidneys of cirrhotic rats which correlated with the volume of ascites [5], in experimental rat models of syndrome of inappropriate secretion of antidiuretic hormone (SIADH) [53], and in congestive heart failure [127,190]. Whether the increased expression of AQP2 is a primary event, or caused by increased levels of ADH, is yet unknown.

Aquaporin 3

The basolateral membrane of collecting duct cells exhibits a constitutive high water permeability, and in the search for this basolateral, AVP-independent water channel, three groups reported the cloning of a new member of the MIP family [44,68,98]. The new water channel was called AQP3, although Ma *et al.* [98] called it the glycerol intrinsic protein (GLIP) because they failed to show any water transport through GLIP. In contrast to other AQPs, AQP3 is also permeable for small solutes like urea and glycerol, albeit to a much smaller degree than water. AQP3 is present in the basolateral membrane of collecting duct principal cells [68,98], with almost no AQP3 present in intracellular vesicles, suggesting that this water channel is not regulated by membrane shuttling [42]. In thirsted rats or Brattleboro rats infused with AVP, a 1.5 to 3-fold increase in abundance of mRNA and protein in the kidney was observed [42,69,168]. In the 5' flanking region of the AQP3 gene, the presence of SP1 and AP2 *cis* regulatory elements has been demonstrated, which have been associated with cAMP-mediated transcriptional regulation [67]. In the terminal IMCD of kidney, AQP3 may play a role in antidiuresis as an exit pathway for urea. Outside the kidney, AQP3 has been localized in the basal membrane of tracheal epithelial cells, in the conjunctival epithelium in eye, in the basolateral membrane of villus epithelial cells in the colon and in brain ependymal cells [50]. With an RNase protection assay AQP3 was also detected in transitional epithelium of urinary bladder and skin epidermis [106].

Defects in AQP3 may contribute to nephrogenic diabetes insipidus. The observation, however, that the basolateral membranes of the inner medullary collecting duct contains some AQP2 [123] and abundant AQP4 [50] suggests that an AQP3 defect will not be as severe as mutations in AQP2.

Aquaporin 4

In view of the high transcellular water permeability of lung alveoli, Hasegawa *et al.* [62] assessed whether other aquaporins than AQP1 are involved. They isolated a rat lung cDNA encoding a novel, mercurial-insensitive water channel (MIWC), which was also found to be strongly expressed in brain, eye and colon. Jung *et al.* [74] isolated an AQP4 from brain, which was identical to MIWC, except for one functionally important amino acid. AQP4 mRNA was demonstrated to be present in brain and, to a lesser extent, in eye, kidney, intestine and lung. In rat brain this fourth aquaporin is present in ependymal cells lining the aquaduct, glial cells forming the edge of cerebral cortex and brainstem, Purkinje cells of the cerebellum, in the hypo-

thalamic area where vasopressin secretory neurons are located and in astrocytes of brain and spinal cord [50,51,62,74]. Also, expression has been reported in epithelial cells in stomach, intestine, ciliary body and various exocrine glands [50,176]. Assessment of the localization of AQP4 in kidney revealed its exclusive presence in basolateral membranes of collecting duct principal cells. No influence of thirsting on the level of AQP4 expression was found [167]. AQP4 contains a PKA consensus sequence in loop B, suggesting a possible regulation mechanism by phosphorylation [62,74]. The tissue-specific distribution of AQP4 suggests that AQP4 is a component of orthogonal arrays of particles (OAPs), which are square arrays of membrane-associated particles visualized by freeze-fracture electron microscopy [51].
The expression of AQP4 at certain sites of the brain raises the question what clinical consequences a defect in this water channel might have. Based on its presence in the vasopressin secretory neurons of the hypothalamus, AQP4 has been suggested to be an osmoreceptor [74]. This hypothesis implicates that in case of a defect in the AQP4 gene, hyperosmolality will result in an inappropriate release of vasopressin and thus might cause some form of hereditary central diabetes insipidus. Expression of AQP4 in the ependymal lining of the aquaductal system and at the base of the brain suggests that AQP4 can play an important role in the reabsorption of cerebro spinal fluid, implicating that the possibility of other clinical consequences, e.g. a disturbance of liquor drainage, needs to be considered as well. However, a recently developed AQP4 knock-out mouse appeared free of symptoms related to disturbances in central osmoregulation [100].

Aquaporin 5

A fifth AQP was cloned from rat submandibular gland [144]. AQP5 expressed in *Xenopus* oocytes conferred a mercury sensitive water permeability. Northern analysis showed the presence of an AQP5 transcript in submandibular and sublingual salivary glands, in the lacrimal gland, and in the eye, trachea and lung [144]. Based on amino acid identity, AQP5 is more closely related to AQP2 than to the constitutively active water channels AQP1, AQP3 and AQP4. Furthermore, the cytoplasmic loop D of AQP5 contains a PKA consensus site, similar to the PKA consensus site in the C-terminus of AQP2. Like insertion of AQP2 into the apical membrane is regulated by AVP, AQP5 may be regulated by the autonomic nervous system, which controls the production of tears and saliva [144].
Based on its tissue distribution, AQP5 is thought to play an important role in generation of saliva, tears and pulmonary secretion and has been postulated to be involved in conditions such as the Sjögren syndrome, an autoimmune disease causing lack of tear and saliva formation [144].

Aquaporin 6, 7, 8, 9, etc.?

The existence of several tissues with high water permeabilities in which none of the known water channels are expressed, like the retinal pigmented epithelium, parotid, pancreas, and sweat glands, suggests the presence of yet unidentified aquapor-

ins. Recently, 3 new aquaporins have been cloned, and they will probably not be the last mammalian aquaporins to be discovered. Only of one of these aquaporins, AQP7, the functional characteristics have been studied [70]. AQP7 is a mercury insensitive water channel which also transports urea and glycerol, and shows the closest homology to AQP3. It is predominantly found in testis, with minor expression in kidney, intestine, retina and heart [70].

Gene organization and chromosomal localization

Only recently the genomic organization and localization of all 6 human aquaporins are fully understood. These six AQPs consist of 263 to 341 amino acids (Fig. 5), which are encoded by mRNAs of 1019 to 4060 bases (Fig. 6). AQP2 and AQP4 mRNAs have been reported to be poly-adenylated at different positions and AQP4 is thought to be transcribed from different promoters resulting in different N-terminal amino acid stretches [97,170,192](Fig. 5). AQP0, AQP2 and AQP5, which are most similar (Fig. 5), are located on chromosome 12q13, forming an aquaporin gene cluster [33,90,150] (Fig. 6). Recently, a new human MIP homolog has been cloned which also maps to chromosome 12, and is probably part of the aquaporin gene cluster. This homolog, called hKID, is expressed exclusively in kidney, it is upregulated in response to dehydration, and is not permeable to water, urea or glycerol [101].

The genes for AQP1, AQP3 and AQP4 are localized on different chromosomes (Fig. 6). AQP1 has been assigned to chromosome 7p14-p15 [32]. The gene for AQP3 was originally localized to chromosome 7q36 [71], but this was later corrected by Mulders *et al.* [119] and confirmed by Ishibashi *et al.* [72]. Localization is now agreed on chromosome 9p12-p21. AQP4 was originally mapped to chromosome 18q22 [192], but this was later corrected to 18q11.2-12.1 [97].

Based on the amino acid identity between all six AQPs, it is clear that the AQPs originate from a common ancestor. Of the six AQPs, AQP3, which is functionally different from the others, has diverged most (Fig. 5) and has, in contrast to the others, a high identity to the glycerol facilitator protein (GlpF) of *E. coli.* The evolutionary distance of AQP3 from the others is also reflected in its genomic structure (Fig. 6). The genes for AQP0, AQP1, AQP2 and AQP5 are comprised of four exons, of which the first repeat of the molecule is encoded by exon 1, while the second repeat is encoded by exon 2 through 4 [90,114,137,170,192](Fig. 5). AQP4 also contains four exons, but, in contrast to the other aquaporins, Lu *et al.* reported that it contains an additional exon with an alternative coding initiation sequence upstream of exon 1, which was called exon 0 [97]. Consequently, AQP4 contains two translation start sites, resulting in two proteins differing 22 amino acids in size [97], suggesting alternative transcription as a mechanism of AQP4 regulation (Fig. 5). Others [192] also reported transcription of AQP4 to be alternatively started from an upstream fifth exon, although this sequence was different from that reported by Lu *et al.* [97]. Since this divergent sequence was based on a cDNA obtained by PCR, which might introduce errors, this fifth exon was not found in their genomic fragments, and the distance to exon 1 was not established, a PCR artifact or a ligation of

Fig. 5 Alignment of human aquaporin 0 through 5. The conserved NPA boxes are underlined. The exon boundaries (E1-E6) are indicated above the sequences for AQP0, AQP1, AQP2, AQP4 and AQP5 and below the sequences for AQP3. For AQP4, the boundary between exon 0 and exon 1 is indicated. In the sequence of AQP4, the two start methionines are underlined. The order of AQP sequences is on basis of amino acid identity. Data were taken from [67,90,97, 114,137,170,192].

a different cDNA onto that of AQP4 during the cDNA synthesis must be considered a likely explanation.

The genomic structure of AQP3 is completely different from the others. The AQP3 gene comprises of six exons [67] (Fig. 6). All AQP genes, except that of AQP3, have identical exon-intron boundaries and are spliced after a full codon triplet. The AQP3 gene is only spliced at a complete triplet after the first and fourth exon (Fig. 6). These data place AQP3 in a different evolutionary branch from other aquaporins [68,133].

Structure-function relationship of aquaporins

Hydrophobicity plots predicted that MIP family members have six hydrophobic domains which can form the transmembrane regions, with intracellular amino-

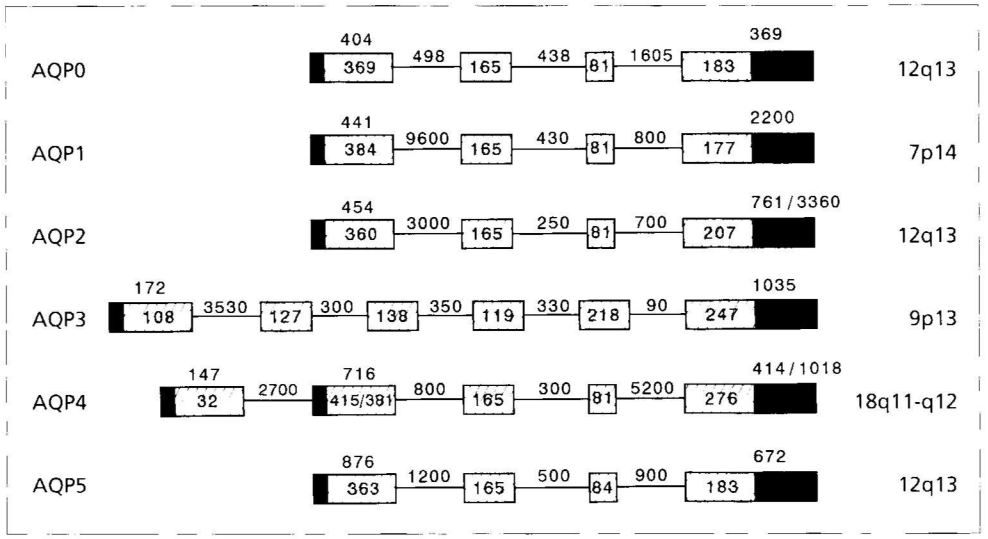

Fig. 6 Genomic structure and chromosomal localization of aquaporin 0 through 5. Exons are indicated by rectangles, introns by lines. Within the exons the untranslated regions are solid and the coding sequences are shaded. Numbers within exons give the number of nucleotides encoding protein, while those above exons also contain the nucleotides of untranslated regions. Numbers above the lines give the lengths of the introns. Data were taken from [32,33,67,90,97,114,119,137,150,170].

and carboxy-termini. The six bilayer spanning domains are connected by 5 loops (loop A to E) (Fig. 1). The molecule consists of two repeats of three transmembrane domains each, that are oriented at 180° towards each other [132]. Each repeat contains the conserved NPA box, in loops B (intracellular) and loop E (extracellular) (Fig. 1). Since AQP1 was the first discovered water channel, it is the water channel whose structure has been studied most intensively. AQP1 resides in the membrane as a homotetramer [161,180]. Nevertheless, every monomer appeared to function as an independent channel [75,156]. This is consistent with radiation inactivation studies which revealed that the functional unit of water channels in proximal tubules and erythrocytes is about 30 kDa, which is in agreement with the molecular size of AQP1 [174,175]. It was shown that only one monomer is glycosylated at an asparagine residue in loop A (N42) [161], although other experiments suggest that two out of four monomers in each membrane-associated tetramer are glycosylated [176,177]. The requirement for tetrameric structures is not yet understood; it may provide stability of the proteins in the plasma membrane.

The hydrophobicity-based molecular structure of AQP1 of 6 transmembrane domains was confirmed by partial proteolysis after insertion at different sites of an E1 epitope tag sensitive to chymotrypsin, without affecting the biological activity of the molecule [142]. Water transport through AQP1 can be inhibited by binding of mercury to cysteine 189, located in loop E next to the NPA motif [141,197]. The location of the mercury-sensitive cysteine of AQP1 in loop E, the N-glycosylation

site of AQP1 in loop A, and the N-glycosylation sites of AQP2, -3, -4, and -5 in loop C [44,55,62,68,74,144] support the extracellular localization of these loops. However, Skach *et al.* proposed a different topology model for AQP1 at the endoplasmic reticulum [160].They performed experiments in oocytes in which specific translocation initiation and termination events were studied by expressing AQP1 truncated molecules containing a reporter of translocation, and determined the reporter topology by protease sensitivity. From these experiments it was concluded that AQP1 has a four transmembrane-spanning topology as it emerges from the ribosome. These surprisingly different results may suggest a potentially complex mechanism of AQP1 biogenesis. The same authors showed that this is not a general characteristic of aquaporins, since AQP4 was shown to have a 6 transmembrane topology at the endoplasmic reticulum [155].

When the mercury-sensitive cysteine in loop E of AQP1 was replaced by a serine (C189S), and a cysteine was introduced at position 73 in cytoplasmic loop B, it was observed that water permeation became mercury-sensitive again [75]. This suggested that both position 189 and position 73 are located close to the water pore, indicating that loops B and E are essential for water transport. Jung *et al.* [75] proposed the so-called hourglass model in which loops B and E fold back into the membrane and together form the water pore (Fig. 7A). Four subunits form together a tetramer, with the six bilayer-spanning helices predicted to be located on the outside of the tetramer and the water pore located in the center of the tetramer (Fig. 7B).

AQP1 can be reconstituted into highly ordered two-dimensional (2D) crystals that exhibit native biological activity [186]. Structural analysis of 2D crystals revealed that AQP1 is in the membrane in tetramers which are asymmetric with respect to the membrane, with four major protrusions on the inside and a large central cavity on the outside of the cell [185,187]. High resolution 3D maps of AQP1 determined by electron crystallography showed that each AQP1 monomer consists of six alpha helices, representing the transmembrane regions, which are surrounding a substructure within the cylinder which is presumably formed by loops B and E [9,19,91]. Detailed 3D maps of AQP1 can gain insight into the molecular structure of the water pore. Merging these structural data with the known primary sequence of AQP1 and results from site-directed mutagenesis studies might reveal the final answer to the structure of the water pore.

The topology model of AQP2 is similar to that of AQP1. AQP2 is also glycosylated, but at position N124 located in the third loop. Bai *et al.* [6] inserted an N-glycosylation motif (NTS motif) into the hydrophylic loops of the non-glycosylated mutant of AQP2 (N124D). Only when the NTS motif was inserted in the first or fifth hydrophylic loop, the protein was glycosylated, which indicates that loops A, C, and E are extracellular. The mercury sensitive cysteine of AQP2 resides at position 181 in loop E next to the NPA motif, as in AQP1. Introduction of a cysteine in loop B (A65C) of a mercury insensitive AQP2 molecule (C181A), made AQP2 mercury sensitive by only 16%. Furthermore, they showed that amino acid substitutions of asparagine 123 in loop C decreased water permeability and that cysteine residues introduced in loop C (H122C or N123C) or loop D (G154C, D155C,

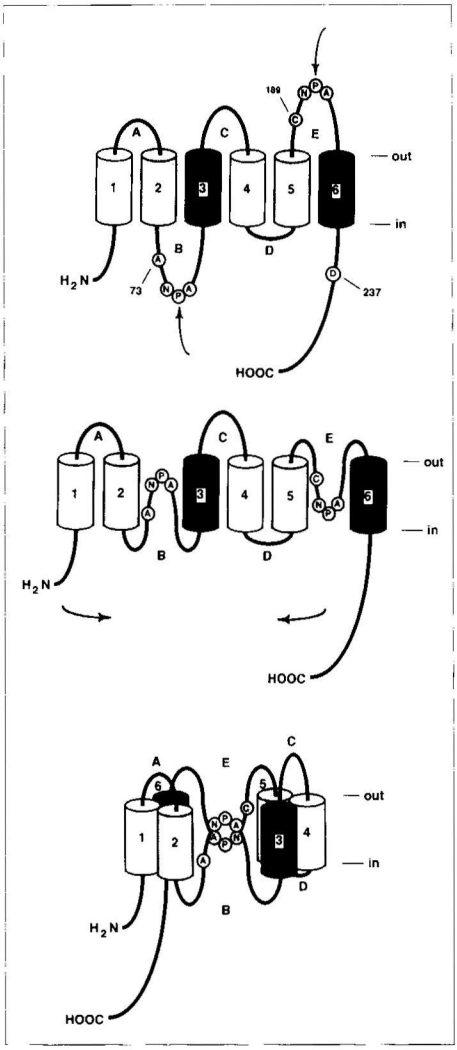

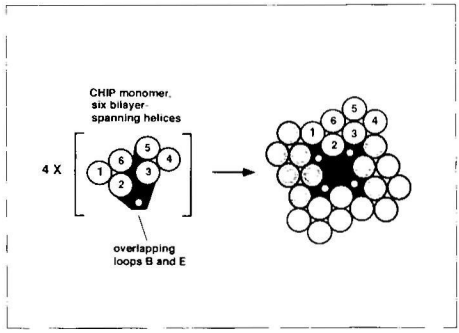

B

Fig. 7A The hourglass model (Figure derived from [75]). Functional model for AQP1 as proposed by Jung *et al.* [75]. According to this model, the very conserved loops B and E fold back into the membrane and form together the pore through which water transport takes place. **B** Oligomerization of four subunits forming a tetramer with a deep central depression containing four water channel pores.

N156C) in a C181A mutant induced partial mercury sensitivity, indicating that loop C and D may be closely located near the water pore. Since similar experiments have not been performed with AQP1, results can not be compared. Mutations in loop B and E of AQP2 did not alter water channel function and therefore, Bai *et al.* [6] concluded that the functional model for AQP2 may be different from the AQP1 hourglass model, since for AQP2 loops C and D also play a critical role in water transport.

AQP3 is the only mammalian water channel that is not only permeable for water, but also for small solutes like urea and glycerol [44,68,98]. The MIP family derived from two bacterial paralogues: one a water channel, the other a glycerol facilitator.

The evolutionary tree of the aquaporins indicate that aquaporins 1, 2, 4, and 5 originate from the aquaporin, while AQP3 has highest homology with the glycerol facilitator [133]. Loops C and E of AQP3 are substantially longer than loops C and E of other aquaporins. This insertion of extra amino acids is conserved in all glycerol facilitator proteins, and may be related to functional differences. The water permeability of AQP3 is mercury-sensitive, although no cysteine is present near the second NPA motif like in AQP1 and AQP2. Sasaki *et al.* [152] showed that the cysteine at position 11 is the mercury sensitive site in AQP3. When a cysteine was introduced at positions 212 or 213 in the E loop, mercury sensitivity was introduced. When the larger amino acid tryptophan was introduced at these sites, both water permeability and glycerol permeability were inhibited. From these site-directed mutagenesis studies and mercury inhibition studies, it was concluded that water and glycerol share the same pore. However, Echevarria *et al.* [43] showed that for water, the Arrhenius activation energy (E_A) was 3 kcal/mol, whereas the E_A for urea and glycerol was >12 kcal/mol. The sulfhydryl reagent pCMBS abolished the water permeability of AQP3, without inhibiting the glycerol permeability. In addition, phloretin inhibited the water permeability of AQP3, without affecting glycerol or urea permeability. From these results it was concluded that water does not share the same pathway with glycerol and urea in AQP3 [43].

AQP4 is the only water channel that is not sensitive to mercury inhibition, and introduction of a cysteine at the known mercury-sensitive site did not induce mercury-sensitivity [74]. To further investigate the mercury-insensitivity of AQP4, Shi *et al.* [157] individually mutated residues 69 to 74 and 187 to 190, located next to the conserved NPA motifs, into a cysteine. Introduction of a cysteine at residue 70, 71, 72, 73 and 189 conferred mercury sensitivity. The introduction of the larger amino acid tryptophane at the sites 72 and 188 completely abolished water permeability without affecting plasma membrane expression, indicating that these residues are located near the water pore. When the cRNAs encoding G72W and A188W AQP2 proteins were co-injected with wildtype AQP4 cRNA, water permeability was only slightly increased, compared to control oocytes. The authors concluded from this surprising finding that AQP4 monomers are not independently functional as was shown for AQP1 [157].

Aim and outline of this thesis

The original aim of this project was to study the structure-function relationship of CHIP28, which was later renamed AQP1. At the start of this study, the discovery of AQP1 took place only one year ago, and opened an exciting new field of research. Consequently, many groups took part in this field of research, trying to understand water channel function and searching for new water channel homologs. This created an enormous advance in knowledge about these channels with their intriguingly simple, but important function. When aquaporins 2 through 5 were cloned, each with distinct tissue distributions and, in the case of AQP3, different transport characteristics, the question arose how the different transport characteristics between aquaporins can be explained, and why we need more than one water channel

homolog. To be able to answer these questions, we need to know more about the structure-function relationship of aquaporins. In this thesis, the structure-function relationship of several aquaporins is studied using *in vitro* mutagenesis and subsequent expression of these proteins in *Xenopus* oocytes.

In chapter 2, the water channel characteristics of the major intrinsic protein (MIP) of lens, which was thought to be an ion channel, are studied and compared to AQP1. In chapter 3, the predictions of the hourglass model that loops B and E are essential for water transport characteristics are studied, by exchanging loops B and E among three aquaporins with different transport characteristics: AQP0, AQP2 and AQP3. Chapter 4 describes three new mutations in the AQP2 gene causing autosomal recessive NDI, which provide valuable information about the structure-function relationship of AQP2. Chapter 5 describes how a study, originally started to solve routing problems of endoplasmic reticulum-retarded AQP2 proteins, unmasked an unexpected difference between the mercury-sensitive cysteine of AQP1 and AQP2. In chapter 6, a mutation in the C-terminus of the AQP2 gene is reported that causes an autosomal dominant form of NDI and experiments are described to address the molecular cause of dominant NDI in this patient.

A general discussion and a summary of this thesis is given in chapters 7 and 8.

Chapter 2

Water channel properties of major intrinsic protein of lens

Sabine M. Mulders •
Gregory M. Preston ••
Peter M.T. Deen •
William B. Guggino •••
Carel H. van Os •
Peter Agre ••

• Department of Cell Physiology,
University of Nijmegen, The Netherlands
•• Departments of Biological Chemistry, Medicine, and
••• Physiology, Johns Hopkins University
School of Medicine, Baltimore, U.S.A.

J Biol Chem 270, 9010-9016 (1995)

Summary

The functions of major intrinsic protein (MIP) of lens are still unresolved; however the sequence homology with channel-forming integral membrane protein (CHIP) and other aquaporins suggests that MIP is a water channel. Immunolocalizations confirmed that *Xenopus* oocytes injected with bovine MIP cRNA express the protein and target it to the plasma membrane. Control oocytes or oocytes expressing MIP or CHIP exhibited small, equivalent membrane currents that could be reversibly increased by osmotic swelling. When compared with water-injected control oocytes, the coefficient of osmotic water permeability (P_f) of MIP oocytes was increased 4-5 fold with a low Arrhenius activation energy, while the P_f of CHIP oocytes increased > 30 fold. To identify structures responsible for these differences in P_f, recombinant MIP proteins were expressed. Analysis of MIP-CHIP chimeric proteins revealed that the 4 kDa cytoplasmic domain of MIP did not behave as a negative regulator. Individual residues in MIP were replaced by residues conserved among the aquaporins, and introduction of a proline in the 5th transmembrane domain of MIP raised the P_f by 50%. Thus oocytes expressing MIP failed to exhibit ion channel activity and consistently exhibited water transport by a facilitated pathway that was qualitatively similar to the aquaporins but of lesser magnitude. We conclude that MIP functions as an aquaporin in lens but the protein may also have other essential functions.

Introduction

Major intrinsic protein (MIP) is a 26 kDa protein expressed exclusively in lens fiber cells where it comprises over 60% of the membrane protein. The cDNA encoding MIP was isolated from a bovine lens cDNA library, and hydrophobicity plots predicted that MIP is an integral membrane protein with cytoplasmic amino and carboxyl termini and six bilayer-spanning domains [57]. MIP reconstituted into liposomes exhibits voltage dependent channels permeable to ions and small molecules that may be closed by Ca^{2+} and calmodulin [56,128,135,154]. In planar lipid bilayers, MIP forms single channels of various conductances (up to 3 nano-siemens) and a weak selectivity for anions [45]; Nodulin-26, a homologous protein from soy bean root nodules was recently shown to behave similarly [189]. In spite of these studies with reconstituted MIP protein, studies of MIP in native membranes or expressed in oocytes have failed to confirm a physiologic function for MIP. For example, although MIP was initially considered to be the gap-junction protein, immunological, biochemical and electrophysiological studies failed to identify electric coupling of lens fiber cells via MIP [165].

MIP was the first identified member of an ancient family of membrane proteins from diverse organisms that now includes more than 20 members. Several MIP family members from animal and plant tissues were shown to function as water-selective membrane channels and are now referred to as the 'aquaporins' [22]. The purification and cDNA cloning of the 28 kDa channel-forming integral membrane protein, CHIP [37,139], a MIP homolog from red cells and renal proximal tubules, permitted the first demonstration of a molecular water channel [140]. CHIP is now designated aquaporin-1 (AQP1), and cDNAs encoding four other aquaporins have subsequently been isolated from diverse mammalian tissues [55,62,68,74,144].

The hourglass model was recently proposed to merge structural and functional features of the aquaporins [75]. The model describes two tandem repeats with the first and second half of the molecule oriented at 180° to each other, and each half contains the sequence asparagine-proline-alanine (NPA) in intracellular loop B and extracellular loop E. In the hourglass model, it was predicted that loop B and loop E fold back into the membrane, forming a single water-selective pore. The striking sequence homology with the aquaporins suggests that MIP may also be involved in water movement through the lens fiber cell membranes. In this report, we investigated the water transporting capacities of MIP using the *Xenopus* oocyte expression system, and water channel properties qualitatively similar to the aquaporins were observed.

Materials and methods

- *Plasmid DNA mutagenesis, DNA sequencing, and in vitro RNA synthesis*

Standard molecular procedures were used [151]. The bovine MIP coding sequence [57] flanked 5' and 3' by *Xenopus* ß-globin gene untranslated sequences [165] was transferred into pBluescript II KS (Stratagene) following digestion with *Hind* III and *Xba* I. The CHIP expression vector was constructed as described [140]. These

constructs served as templates for site-directed mutagenesis reactions using the Muta-Gene phagemid in vitro mutagenesis kit (Bio-Rad). Table I lists the mutants used in this study. The location of mutations within the MIP polypeptide are illustrated in Figure 1.

The chimeric protein vectors CHIP-MIP-1 and MIP-CHIP-1 were constructed by inserting a *Bam* HI restriction site at Val-112 of MIP and Thr-120 of CHIP, resulting in the insertion of the amino acids aspartic acid and proline. MIP(V112*Bam*) and CHIP(T120*Bam*) were digested with *Bam* HI, the 5' half of CHIP was ligated to the 3' half of MIP (CHIP-MIP-1), and the 5' half of MIP to the 3' half of CHIP (MIP-CHIP-1). The chimeric protein vectors MIP-CHIP-2 and CHIP-MIP-2 were constructed using the megaprimer polymerase chain reaction method [8] exchanging at Arg-226 of MIP and Arg-234 of CHIP, using the following antisense primers:

MIP-CHIP-2: 5'-GTCTGTGAGGTCACTGCTG/CGAGGGAAGAGGAGAAAG-3'

CHIP-MIP-2: 5'-CTCAGAAACACTCTTGAGC/CGTGGGGCCAGGATGAAG-3'

The chimeric protein, MIP-CHIP (loop A), contains the first exofacial loop (A) of CHIP (amino acids 34-51) in place of the first exofacial loop of MIP (amino acids 33-43), and was constructed with an 82 base pair insertional-substitutional oligonucleotide primer (not shown) in a site-directed mutagenesis reaction. All mutations were confirmed by enzymatic nucleotide sequencing (U.S. Biochemical Corp.).

Capped RNA transcripts were synthesized *in vitro* using T3 RNA Polymerase with *Xba* I-digested MIP, CHIP, or mutant expression vector DNA, and the RNA was purified as described [193].

- *Preparation of oocytes and measurement of P_f*

Female *Xenopus laevis* were anesthetized on ice, and stage V and VI oocytes were removed and prepared [96]. The day after isolation, oocytes were injected with either 50 nl of water or 0.5-25 ng of cRNA in 50 nl of water. Injected oocytes were maintained for 2-3 days at 18°C prior to osmotic swelling, membrane isolation, or voltage clamp experiments. Oocyte swelling was performed at 22°C following transfer from 200 mosM (osm_{in}) to 70 mosM (osm_{out}, CHIP) or either 70 or 20 mosM (osm_{out}, MIP) modified Barth's solution diluted with water. Sequential oocyte images were digitized at 5 sec intervals for a total of 1 minute, and the volumes of the sequential images were calculated as described [141]. The change in relative volume with time, $d(V/V_0)/dt$, was fitted by computer to a quadratic polynomal, and the initial rates of swelling were calculated. The osmotic water permeability (P_f, μm/s) was calculated from osmotic swelling data between 5 and 10 s, initial oocyte volume (V_0=9 x 10^{-4} cm^3), initial surface area (S = 0.045 cm^2) and the molar ratio of water (V_w = 18 cm^3 / mol) [198] using the formula:

$$P_f = [V_0 \times d(V / V_0) / dt] / [S \times V_w \times (osm_{in} - osm_{out})]$$

- *Oocyte membrane isolation and immunoblot analysis*

Total oocyte membranes [141] and plasma membranes [184] were isolated from groups of 4-30 oocytes, solubilized in 1.25% (wt/vol) SDS at 60°C for 10 minutes, electrophoresed into 12% SDS-polyacrylamide gels [86], transferred to nitrocellulose [25], incubated with a 1:10,000 dilution of anti-MIP antibody, or a 1:1,000 dilution of anti-CHIP antibody [161], and visualized using the ECL Western blot-

MIP constructs	Wild type amino acid/codon	Mutant amino acid/codon
MIP (V112Bam)	Val-112/GTC	Val-Asp-Pro/GTggatccC
MIP(C14V)	Cys-14/TGT	Val-14/GTT
MIP(V160P)	Val-160/GTG	Pro-160/CCA
MIP(A181C)	Ala-181/GCA	Cys-181/TGT
MIP(S243V/S245E)	Ser-Glu-Ser-245/AGTgagTCC	Val-Glu-Glu/GTTgagGAA
CHIP constructs	**Wild type amino acid/codon**	**Mutant amino acid/codon**
CHIP(T120Bam)	Thr-120/ACT	Thr-Asp-Pro/ACggatccT
CHIP(D131P)	Asp-131/GAT	Pro-131/CCT
CHIP(P169A)	Pro-169/CCC	Ala-169/GCC
Chimeric constructs	**Amino acids**	**Total amino acids**
MIP-CHIP (loop A)	MIP(1-32)-CHIP(34-51)-MIP(44-263)	270
MIP-CHIP-1	MIP(1-112)-CHIP(121-269)	263
MIP-CHIP-2	MIP(1-226)-CHIP(235-269)	261
CHIP-MIP-1	CHIP(1-120)-MIP(113-263)	273
CHIP-MIP-2	CHIP(1-234)-MIP(227-263)	271

Table 1 Site-specific mutations, insertional mutations, and chimeric constructs of MIP and CHIP.

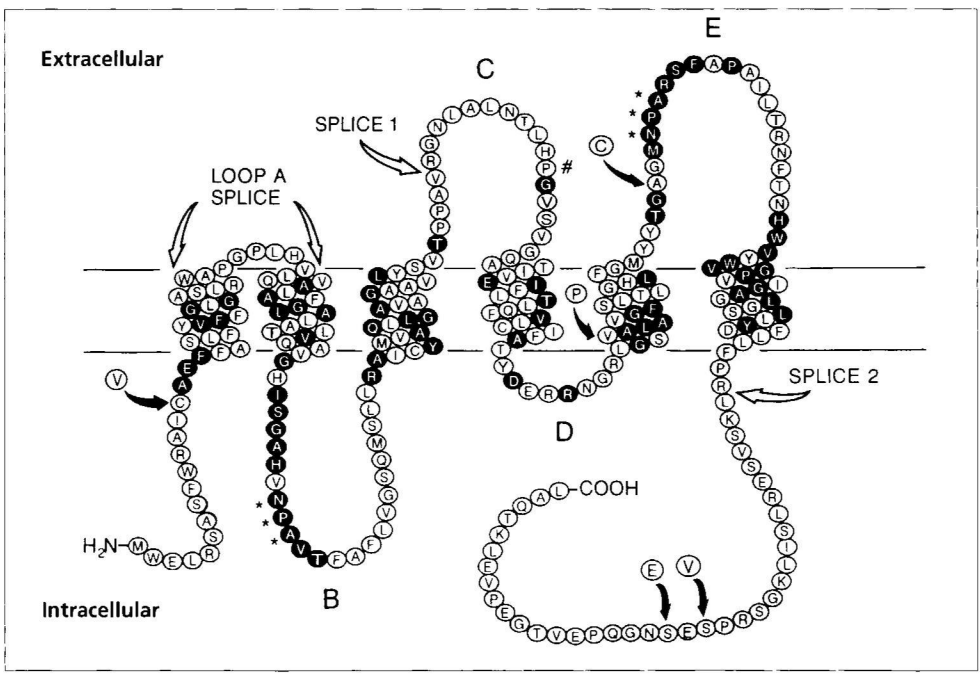

Fig. 1 Membrane topology of MIP showing sites targeted for mutagenesis and domain exchanges in this study. Splice 1 is the splice site for MIP-CHIP-1 and CHIP-MIP-1; splice 2 is the splice site for MIP-CHIP-2 and CHIP-MIP-2. The proline introduced in CHIP at position Asp-131 is indicated with #. NPA motifs are indicated with *asterisks*. *Filled symbols* indicate amino acids that are conserved in more than half of the members of the MIP family from bacteria, yeast, plants and animals [145].

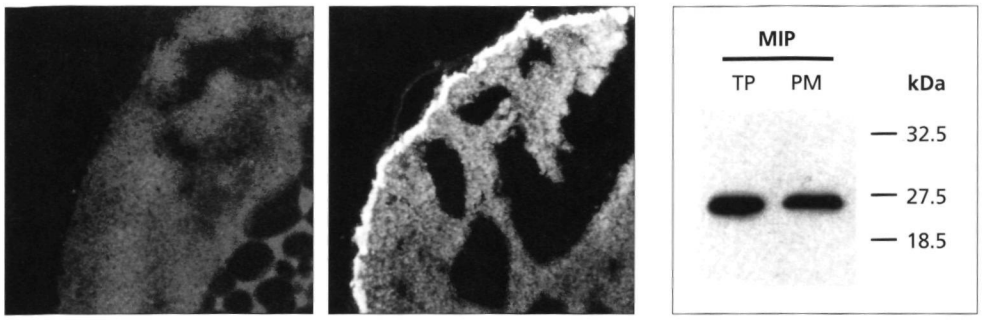

Fig. 2A Immunofluorescence microscopy of control oocytes and oocytes expressing MIP. Frozen sections were prepared from *Xenopus* oocytes injected with 50 nl of water or 50 nl of water containing 10 ng of MIP cRNA and probed with anti-MIP antibody (see 'Materials and Methods'). Note strong labeling of plasma membrane and negligible labeling of cytoplasm of the oocyte expressing MIP. **B** Immunoblot of total protein (TP, equivalent of 0.2 oocytes) and plasma membranes (PM, equivalent of 15 oocytes) from oocytes expressing MIP. SDS-PAGE immunoblot was incubated with a polyclonal antibody directed against the carboxyl terminus of MIP.

ting detection system (Amersham Corp.). Molecular weights were determined relative to the mobility of prestained SDS-PAGE standards (Bio-Rad).

◆ *Anti-MIP antibody*

A synthetic peptide corresponding to the 15 carboxyl-terminal amino acids of bovine MIP (PEVTGEPVELKTQAL) [57] was coupled to keyhole limpet haemocyanin. Rabbits were injected with 400 μg of conjugated synthetic peptide mixed with Freund's complete adjuvant. After 4 weeks, and every three weeks thereafter, the rabbits were boosted with 200 μg of conjugated synthetic peptide mixed with incomplete Freund's adjuvant. The produced anti-MIP antiserum was tested for specificity and cross-reactivity by an enzym-linked immunosorbent assay.

◆ *Immunolocalization of MIP in Xenopus oocytes*

Oocytes were frozen for immuno-fluorescence microscopy in Tissue-Tek mounting medium (Miles Inc.). Sections of 5 μm were cut by cryostat, collected on gelatin-coated slides and fixed at room temperature for 5 minutes in 1% (wt/vol) periodate-lysine-paraformaldehyde fixative (PLP) [110]. Sections were washed three times with TBS (0.9% NaCl, 25 mM Tris, pH 7.4) and incubated overnight at 4°C with anti-MIP antibody at a dilution of 1:1,000 in TBS containing 10% (vol/vol) goat serum. After three washes with TBS, the sections were incubated for 1 hour at 37°C with affinity-purified fluorescein isothiocyanate-labelled goat-anti-rabbit IgG (Sigma Immuno Chemicals) at a dilution 1:50 in TBS containing 10% (vol/vol) goat serum. After three more washes in TBS, the sections were embedded in Mounting Medium (Sigma) and analyzed by immunofluorescence microscopy.

◆ *Electrophysiology*

Studies were carried out as described [140] using a two-micro electrode voltage clamp with Clampex software. Water- and cRNA-injected oocytes were voltage-

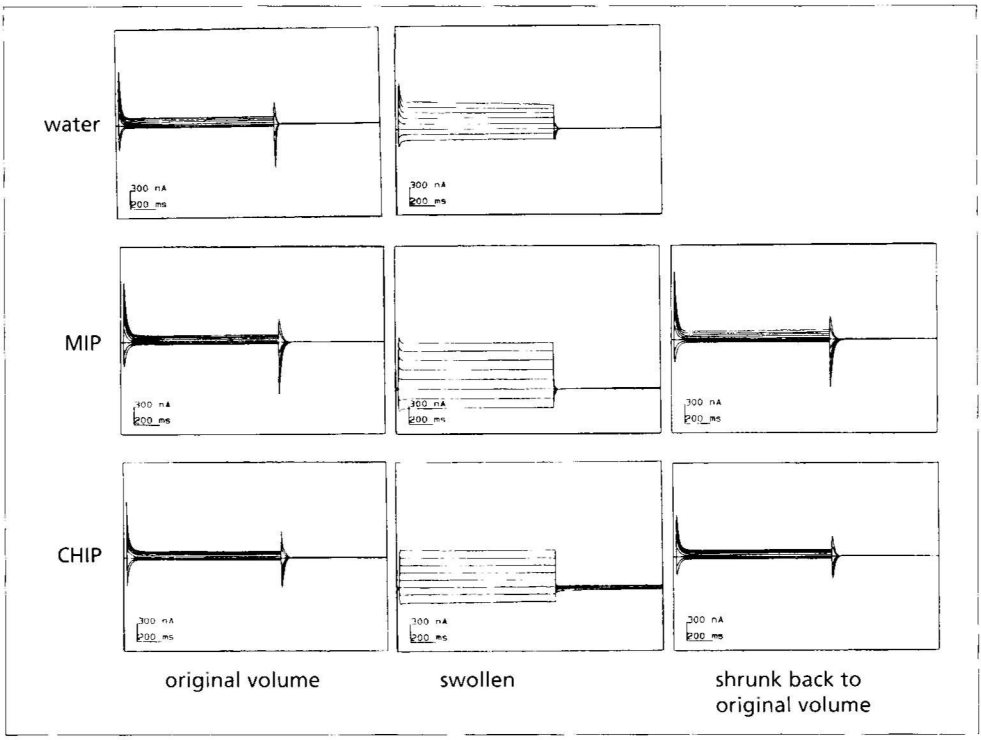

Fig. 3 Membrane ion conductance. Voltage clamp was used to measure currents at voltages from -90 mV to +50 mV of water-injected control oocytes, oocytes injected with 25 ng of MIP cRNA, or oocytes injected with 0.5 ng of CHIP cRNA. The currents were determined in 200 mosM Modified Barth's Solution (MBS). The oocytes were swollen by replacing MBS with a hypotonic medium, and current measurements were repeated. Control oocytes were placed in H_2O, and the current was measured after 30 minutes. Oocytes expressing MIP and CHIP were placed in MBS diluted from 200 to 70 mosM, and currents were measured after 20 and 30 seconds. Oocytes were shrunk back to their normal volume by replacing the hypotonic medium with isotonic MBS, and currents in oocytes expressing MIP and CHIP were measured after 8 minutes.

clamped at a holding membrane potential of -70 mV, repolarized to -90 mV and depolarized to +50 mV in 20 mV step intervals. The membrane potential was returned to the holding potential between each step.

Results

Oocytes from *Xenopus laevis* have provided the standard system for expression of water channels and measurement of their functional activity by a swelling assay (see Materials and Methods). Expression of MIP and insertion of the protein into the oocyte plasma membrane was studied by immunofluorescence microscopy of frozen sections. Oocytes injected with MIP cRNA showed a strong anti-MIP immunolabelling of the plasma membrane, whereas the cytoplasm showed only

weak immunostaining (Fig. 2A). Immunoblot analysis of isolated oocyte plasma membranes also showed a single strong signal at 27 kDa, confirming that MIP is targeted to the plasma membrane (Fig. 2B)

It was reported that MIP reconstituted into planar lipid bilayers forms channels with high conductance [45]. The hypothesis that MIP is an ion channel was tested by measuring the conductance of oocyte membranes expressing MIP with a two-microelectrode voltage clamp. In the absence of osmotic swelling, no differences in conductance were measured in oocytes injected with water, MIP cRNA, or CHIP cRNA (Fig. 3). The oocytes were placed in a hypotonic medium, and, after being osmotically swollen to a similar size, membrane currents were again measured. Oocytes injected with water, MIP cRNA, or CHIP cRNA exhibited a similar increase in conductance. After replacing oocytes in isotonic buffer to cause shrinkage to the initial volume, the conductance decreased again to the initial values, although the shrinking process for water-injected oocytes was too slow for analysis (not shown).

Osmotic water permeability (P_f) of *Xenopus* oocytes was measured in hypotonic medium three days after injection with 50 nl of water, or 10 ng of MIP or CHIP cRNA. Water-injected control oocytes swelled minimally ($P_f = 10 \pm 3.2$ μm/s). Oocytes injected with MIP cRNA displayed a 4-5 fold increase in water permeability above the basal level of control oocytes ($P_f = 45 \pm 8.2$ μm/s). A more than 30 fold increase in P_f was exhibited by oocytes injected with the same amount of CHIP cRNA ($P_f = 351 \pm 43$ μm/s, Fig. 4, A and B). Although the P_f of MIP injected oocytes was only ~15% of CHIP-injected oocytes, the MIP-injected oocytes had significantly greater P_f than the control oocytes ($p < 0.05$, Fig. 4A), a difference that was consistently reproduced in each of 14 independent experiments.

Water transport through aqueous channels is characterized by a low Arrhenius activation energy, which is equivalent to diffusion of water in bulk solution ($E_A \sim 4$ kcal/mol), whereas diffusion of water through lipid membranes is characterized by a high value ($E_A > 10$ kcal/mol) [47]. Water permeability of oocytes injected with 25 ng MIP cRNA was measured at multiple temperatures; consistent with facilitated water transport, the activation energy was low ($E_A = 3.9$ kcal/mol $\pm$ 1.4 kcal/mol, average of 4 experiments, Fig. 5). Indicative of diffusional water movement, the activation energies of water-injected oocytes were measured in two experiments ($E_A = 10$ and 18 kcal/mol).

Domains of MIP and CHIP that might be of importance for the specific functional characteristics of the two proteins were exchanged, and the functional consequences were measured (Table 1, Fig. 1). The MIP-CHIP (loop A) chimera represents a MIP molecule with residues 33-43 in loop A replaced by the residues 34-51 from the loop A of CHIP. The MIP-CHIP-1 and CHIP-MIP-1 chimeras contain the amino-terminal half of one molecule and the carboxyl-terminal half of the other spliced at a site in loop C where the tandem repeats are normally joined. The MIP-CHIP-2 and CHIP-MIP-2 chimeras are spliced at a site in the carboxyl-terminal cytoplasmic domains of the molecules. When membranes of oocytes expressing each of these constructs were analyzed by immunoblot, polypeptides of the anticipated size were identified, and the levels of expression were comparable with

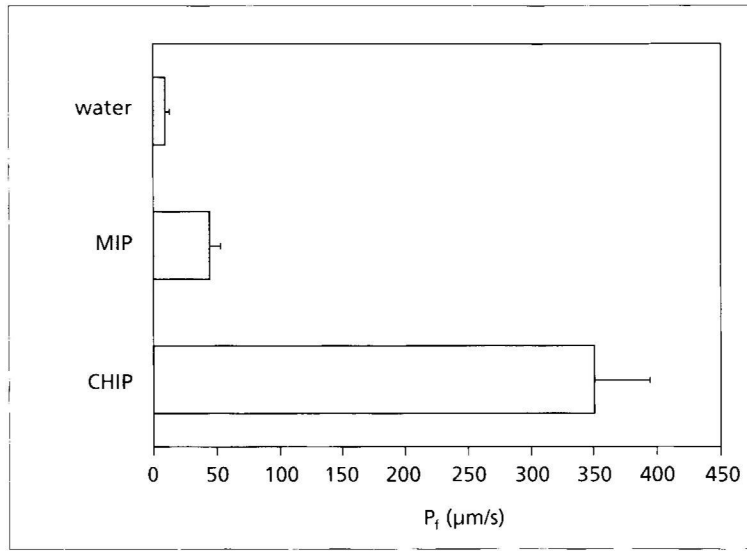

A

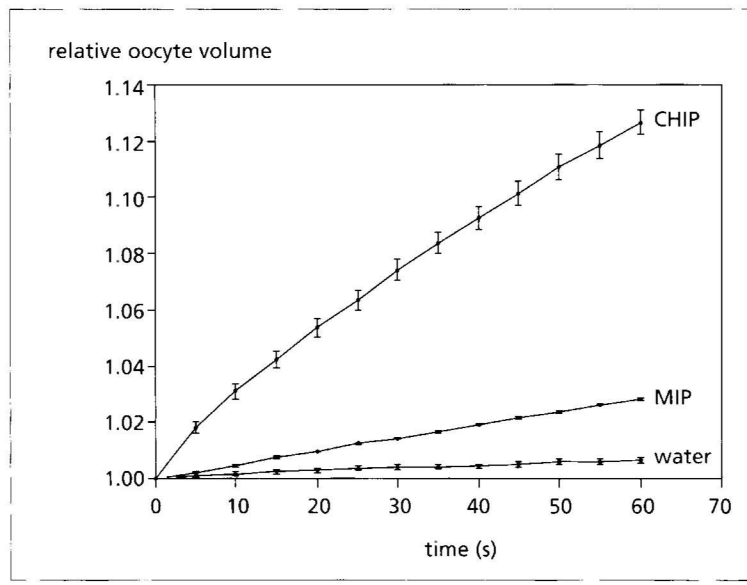

B

Fig. 4A Increased osmotic water permeability of *Xenopus* oocytes expressing MIP and CHIP. Oocytes were injected with water or 10 ng of *in vitro* transcribed cRNA encoding MIP or CHIP. After 72 hours, P_fs were determined by videomicroscopic measurement of the rate of swelling after transfer to hypotonic medium. Shown are the means ± SD for 8 oocytes. **B** Time-dependent osmotic swelling of oocytes injected with water or 10 ng of cRNA encoding MIP or CHIP. Shown are the means from 5 traces ± SE.

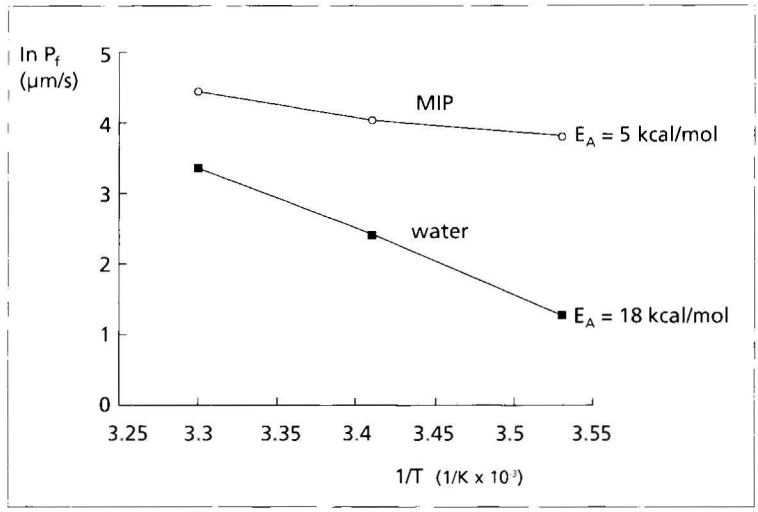

Fig. 5 Arrhenius activation energy (E_A) of osmotic water permeabilities of control oocytes and oocytes expressing MIP. The E_A was determined by measuring the P_f at 10, 20, and 30°C. Control oocytes were injected with water and MIP oocytes were injected with 25 ng of MIP cRNA. In this experiment, each point represents 7-10 control oocytes or 11-15 MIP oocytes.

oocytes expressing native MIP and CHIP proteins (not shown).

Unlike all of the known aquaporins, MIP does not contain a potential N-glycosylation site in either loop A or loop C, and no glycosylation of MIP was detected when the polypeptide was expressed in oocytes (Fig. 2B). The MIP-CHIP (loop A) construct contains the CHIP glycosylation site at residue asparagine 42 in loop A. Despite the presence of a potential glycosylation site, oocytes expressing this construct still did not exhibit an increase in P_f, and immunoblots revealed a 27-kDa polypeptide but not higher molecular mass bands, indicating that N-glycosylation had still not occurred (not shown).

Oocytes expressing MIP-CHIP-1 and CHIP-MIP-1 chimeras did not exhibit a significant increase in P_f above water-injected controls, suggesting that these chimeric proteins cannot form functional water channels. Oocytes expressing MIP-CHIP-2 also exhibited P_fs similar to control oocytes. In contrast, oocytes expressing CHIP-MIP-2 were found to have P_fs similar to oocytes expressing wild-type CHIP (Fig. 6), indicating that the carboxyl-terminal cytoplasmic domain of MIP does not interfere with the water-transporting domains of CHIP.

Unlike CHIP, the increase in water permeability induced by MIP expression is not blocked by $HgCl_2$. A putative mercury-sensitive cysteine residue was introduced into MIP at position 181 which conforms to the mercury-sensitive cysteine 189 in CHIP, but the substitution MIP(A181C) did not confer mercury-sensitivity to MIP (Fig. 7). The cysteine at position 14 in the amino-terminal domain of MIP was replaced by a valine, since other aquaporins do not contain a cysteine at this position, but the P_f of C14V mutant MIP was not different from wild-type MIP

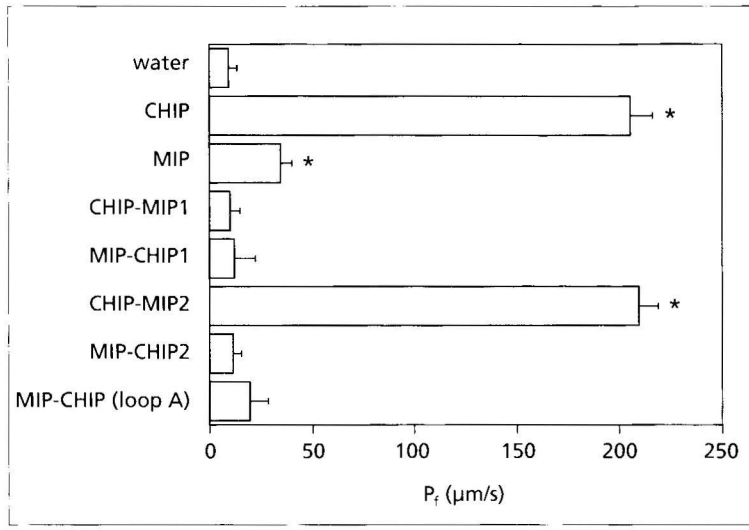

Fig. 6 Osmotic water permeability of oocytes expressing chimeric MIP-CHIP proteins. P_f was determined from oocytes injected with water or 10 ng cRNA encoding MIP, CHIP, or the indicated MIP-CHIP chimeric proteins. Shown are the means ± SD of 5 oocytes. * $p<0.05$ compared to water-injected control oocytes.

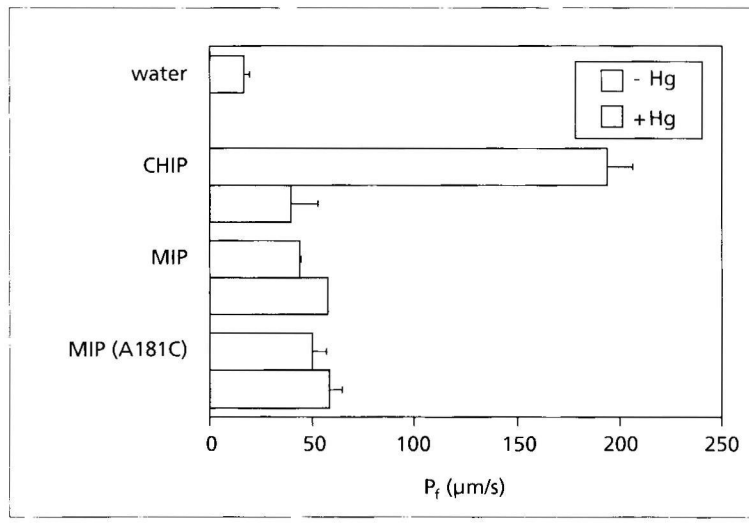

Fig. 7 Osmotic water permeability and Hg^{2+} inhibition of oocytes expressing CHIP, MIP, or MIP(A181C). Oocytes were injected with 1 ng of CHIP cRNA or 10 ng of MIP cRNA or 10 ng of MIP(A181C) cRNA. P_f was determined without pretreatment (open bars) or after 5 minutes in buffer containing 3 mM $HgCl_2$, followed by swelling in the presence of $HgCl_2$ (solid bars). Shown are the means ± SD of 5 oocytes.

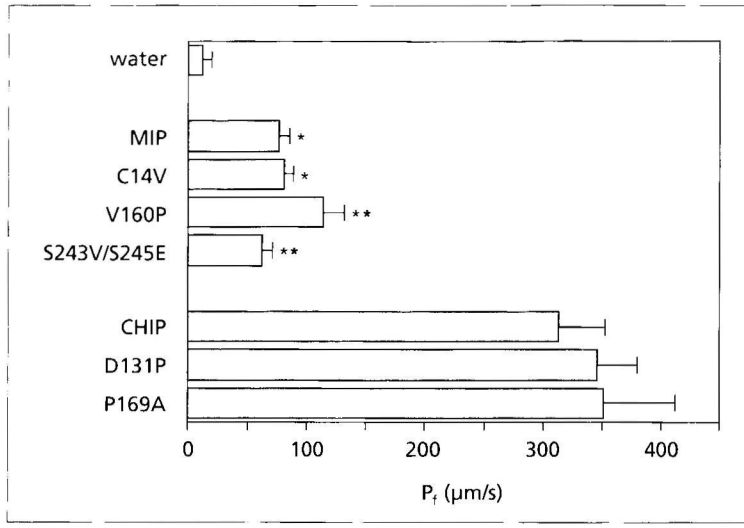

A

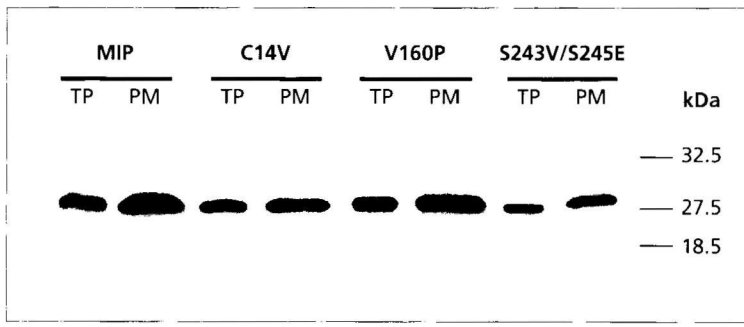

B

Fig. 8 Osmotic water permeability of oocytes expressing MIP and CHIP mutants. **A** Oocytes were injected with water or 25 ng of cRNA encoding MIP, MIP(C14V), MIP(V160P), MIP(S243V, S245E), or 5 ng of cRNA encoding CHIP, CHIP(D131P), or CHIP(P169A). The P_f was measured three days after injection. Shown are the means ± SD. * $p<0.05$ compared with water-injected oocytes, ** $p<0.05$ compared with wild-type MIP. **B** Immunoblot comparison of total protein (TP, equivalent of 0.2 oocytes) or plasma membranes (PM, equivalent of 20 oocytes) from oocytes expressing MIP or the indicated MIP mutants. SDS-PAGE immunoblot was incubated with a polyclonal antibody specific for the carboxyl terminus of MIP.

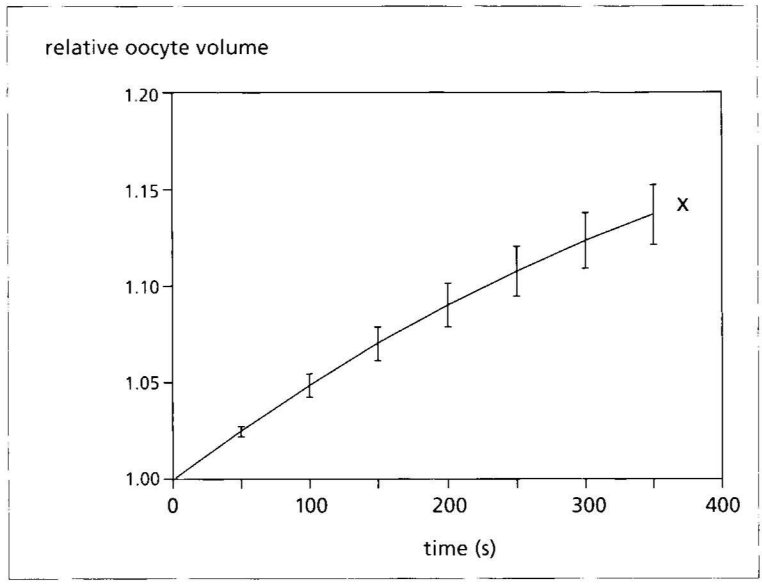

Fig. 9 Time-dependent osmotic swelling of oocytes expressing MIP. Three days after injection of 25 ng of MIP cRNA, oocytes were transferred to 20 mosM Modified Barth's Solution, and swelling was recorded until the oocyte burst (x). Shown are the means from 7 traces ± SE.

(Fig. 8A). MIP contains a proline in the second extracellular loop (residue 123 in loop C), a site where other members of the MIP family do not contain this residue. Introducing a proline at this position in CHIP (D131P) also did not change the P_f (Fig. 8A).

All known aquaporins except AQP4 contain a proline in the 5th transmembrane segment; no proline exists in the 5th transmembrane domain of MIP. When a proline was introduced in MIP (V160P), the substitution reproducibly enhanced the P_f by 50 ± 20% relative to the P_f of oocytes expressing wild-type MIP (Fig. 8A). Notably, the amount of MIP protein expressed in oocytes was not different after injection of equal amounts of MIP cRNA and MIP(V160P) cRNA (Fig. 8B). Although not large, this increase in P_f was confirmed in each of 5 different experiments. A 'gain of function' mutation suggests that the P_f of MIP can be increased by introducing subtle conformational changes in the molecule. Nevertheless, replacing the proline in CHIP at this position (P169A) to the corresponding residue of MIP had no measurable influence on the P_f of CHIP (Fig. 8A).

These results show that MIP exhibits a low P_f value which can be increased by introducing subtle changes in the molecule. One explanation may be that MIP needs to undergo an activation or structural rearrangement to function as a water channel, whereas CHIP is constitutively in the activated state. Two sites in the carboxyl-terminal cytoplasmic domain of MIP are phosphorylated *in vivo* [87]. Since these sites are not conserved in other members of the MIP family, the sites may play a role in regulation of MIP function. Mutation of the two putative phosphorylation sites to the corresponding residues in CHIP (S243V, S245E) slightly decreased the P_f

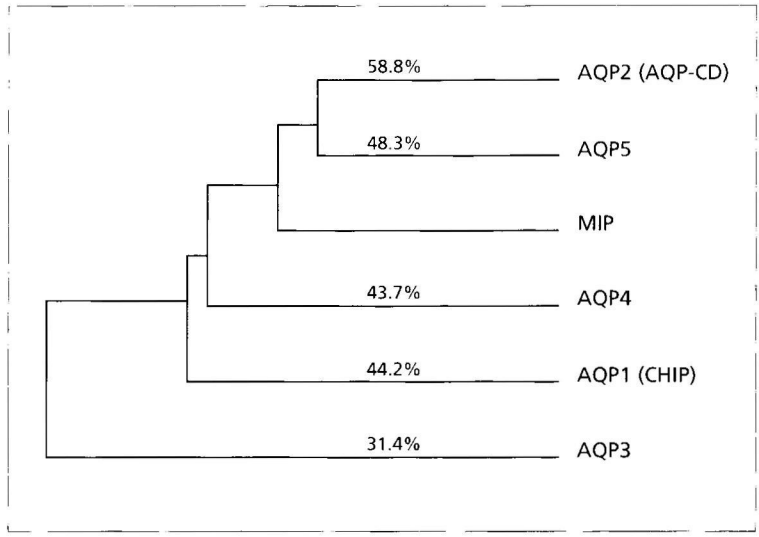

Fig. 10 Evolutionary tree of MIP and the mammalian aquaporins. The percentage of amino acid identity between MIP and the 5 mammalian aquaporins is indicated.

(Fig. 8A), but the amount of protein expressed was comparably reduced as compared with wild-type MIP by immunoblot (Fig 8B). The possibility of stretch-activation was also considered, but if it exists, it was not reproduced by simple increase in volume, since the rate of osmotic swelling did not increase with time (Fig. 9). Thus, if an activation step confers CHIP-level water permeability on MIP, the identity of this step remains unknown.

Discussion

Even though the cDNA encoding MIP was cloned more than a decade ago [57], the physiological roles of the protein are still not understood. Detailed studies of the homologous proteins MIP [45], Nodulin-26 [189], and preliminary studies with CHIP (J. Hall and P. Agre, unpublished) revealed large voltage-dependent conductances when reconstituted into planar lipid bilayers. Nevertheless, the magnitude of the currents in bilayers containing MIP was far above the conductances measured in normal lens [108,109]. Therefore, while the planar lipid bilayer studies are highly reproducible, their relevance to normal lens physiology remains uncertain. Moreover, the studies reported here (Fig. 3) and preliminary studies of other investigators [84] failed to confirm ion conductance by MIP expressed in oocytes.

Soon after the discovery that CHIP is a molecular water channel [140], several labs evaluated MIP and other homologous proteins for osmotic water permeability. One group reported that MIP is not a water channel [181], but apparently these investigators used the same techniques with which they failed to detect osmotic water permeability of AQP3 [98], a protein found by two other groups to exhibit

high P_f comparable with the other aquaporins [44,68]. The studies reported here document that oocytes expressing MIP exhibit osmotic water permeabilities 4-5 fold above control oocytes (Fig. 4) with activation energies identical to the aquaporins (Fig. 5). These observations are supported by preliminary studies of other investigators who also found an increase in P_f in oocytes expressing frog MIP [84] or bovine MIP [18]. MIP may contribute to the maintenance of lens transparency by enhancing uptake of intercellular water by adjacent lens fiber cells. The narrow geographic separation of lens fiber cells (which contain MIP) and lens epithelial cells (which contain CHIP) suggests functional cooperativity. Osmotic gradients provide the driving force for aquaporin-mediated water transport in kidney and most other tissues [125]. It is likely that hydrostatic forces move water through CHIP in endothelium of the proximal capillary bed [125], and a related process may occur for MIP when the lens shape is rapidly altered by contraction of muscles in the ciliary body to provide fine focus of the corneal image upon the retina.

A molecular explanation for why MIP is a weaker water transporter than the other aquaporins was sought, since the amino acid sequences of MIP and the aquaporins are strikingly similar [139,145](Fig. 10). MIP was expressed well in oocytes and was targeted to the plasma membrane (Fig. 2). Neither the phosphorylation sites nor the other residues in the carboxyl-terminal cytoplasmic domain of MIP appeared to function as restraints (Figs. 6 and 8), and several different residues and domains from CHIP were spliced into MIP without increasing the P_f (Figs. 6-8). Despite introduction of an N-glycosylation site, MIP-CHIP (loop A) was still not glycosylated, and introduction of the potential mercurial inhibition site in MIP (A181C) failed to confer sensitivity (Fig. 7). Likewise, when a cysteine was introduced into the mercury-insensitive AQP4, the recombinant protein also failed to demonstrate mercury-inhibitable P_f [74], implying that MIP and AQP4 are structurally different from CHIP near the extracellular side of the aqueous pore. Nevertheless, substitution of proline in the 5th bilayer-spanning domain yielded a 50 % increase in P_f (Fig. 8). This intriguing gain of function suggests that simple alterations in the bilayer-spanning domains can alter the conformation of MIP to more closely resemble CHIP. No loss of function was detected in the corresponding substitution (P169A) in CHIP; however, a small decrease in a high P_f should be more difficult to measure than a comparable increase in a low value. An alternative explanation may be that MIP requires a specific membrane organization, such as formation of orthogonal arrays, or a particular membrane environment which may be poorly reproduced in the oocyte expression system. For example, oocytes do not have plasma membranes with wavy junctions similar to lens fiber cells [195], and if this is important to the function of MIP, the water permeability studies may yield spuriously low values in oocytes.

Similar to other bilayer-spanning proteins, MIP may have multiple physiological functions, and it is possible that the primary role of MIP is not water transport. The red cell band 3 protein is the membrane anion exchanger (AE1), a cytosolic regulator of glycolytic enzyme activity, and the structurally important attachment site for ankyrin on the membrane [95]. MIP may also have a structural function, since the protein has been shown to enhance adhesion with membranes containing negative-

ly charged phospholipids [111]. Also, it is known that some proteins are expressed in lens where their function is unrelated to their functions in other tissues (e.g., crystallins) [26,136]. Thus the extremely high expression of MIP in lens may be far above the level needed for water permeability, since the abundance may be needed for an unrelated function.

A mutation has been identified in mice that may provide insight into other potential functions of MIP, since these mice develop cataracts prior to birth [115]. The *Cat* mouse mutation results in lower abundance of MIP mRNA with the major transcript being truncated, and MIP was not detectable in lens by immunocytochemistry [159]. The mutation is expressed as a dominant trait and has been mapped to the distal end of chromosome 10 [115], coincident with the MIP locus [58]. Mutations in genes encoding structural proteins usually produce dominantly inherited disorders, whereas mutations in transporters such as the CFTR are recessively inherited. Consistent with this, mutations in the AQP2 gene were recently identified in homozygotes and a compound heterozygote with severe nephrogenic diabetes insipidus, while the heterozygous relatives were unaffected [31,178]. Careful histological analysis of the early stages of disease in the *Cat* mouse may provide clues to the critical function of MIP, which is the first defect leading to the development of cataracts in this animal model.

Acknowledgements

We gratefully thank A. Hartog for performing immuno-cytochemistry of MIP in oocytes and Dr. R.J.M. Bindels for help in formulating a computer routine to analyse swelling curves of oocytes. We also thank James Hall, Richard Mathias, Paul Lampe and David Beebe for valuable discussions.

Chapter 3

The exchange of functional domains among aquaporins with different transport characteristics

Testing of the hourglass model

Sabine M. Mulders
Annemiete J. van der Kemp
Sylvie A. Terlouw
Hanneke A.F. van Boxtel
Carel H. van Os
Peter M.T. Deen

submitted

Summary

Aquaporins are transmembrane proteins which contain six bilayer spanning domains, connected by loops A through E. Loops B and E contain a conserved stretch of amino acids, called the NPA box. The hourglass model, the functional model for aquaporin 1, predicts that the intracellular loop B and extracellular loop E are essential for the formation of the water pore. To test the importance of loops B and E in the determination of the transport characteristics, we exchanged loops B and/or E between AQP0, AQP2, and AQP3. Detailed functional, immunoblot and immunocytochemical analyses of expression in *Xenopus* oocytes revealed that 6 out of the 9 chimeric aquaporin proteins were not functional, because the exchange of loops caused misrouting of these proteins. AQP0 with loop E of AQP2 was not impaired in its routing and yielded a water permeability (P_f) equal to wild-type (wt) AQP0. AQP2 with loop B of AQP0 was also routed normally and gave a P_f similar to wt AQP2. AQP0 with loops B and E of AQP2 (AQP0-2BE) did not yield an increase in P_f and was partly misrouted, but expression in the plasma membrane was clearly detectable. Since some mutant AQP2 proteins in nephrogenic diabetes insipidus conferred water permeability to oocytes, although they were hardly detectable in plasma membranes, AQP0-2BE expressing oocytes should yield an increase in P_f, when loops B and E of AQP2 would confer AQP2 water permeability to AQP0. We conclude that the water permeability of the aquaporin, in which loops B or E or both are exchanged for the corresponding loops of another aquaporin, is not influenced by these loops. Therefore, loops B and E might form the water pore, but other parts of the protein determine the characteristics of the channel.

Molecular water channels, or aquaporins, are a subset of the MIP family of transmembrane channel proteins. Family members are predicted to contain 6 transmembrane regions, connected by loops A through E (Fig. 1). Each molecule consists of two halves that are oriented 180° towards each other [145]. In the first intracellular loop (loop B) and the third extracellular loop (loop E), a conserved stretch of amino acids, the so-called NPA box is located. Until recently, 5 mammalian water channels have been cloned (AQP1 through 5) [44,55,62,68,74,98,139, 144]. The prototype of the family, the major intrinsic protein of the lens (MIP), which was discovered and cloned in 1984, appeared to be a weak water channel and is now also called AQP0 [117].

The topology and structure of AQP1, the first discovered water channel, has been the subject of many studies, and the 6 transmembrane topology model was convincingly confirmed [142]. The water flow through AQP1 can be blocked by mercury which binds to cysteine 189, located in loop E close to the second NPA box [141]. Substitution of larger amino acids for the mercury-sensitive cysteine resulted in a decreased water transport, indicating that this cysteine is located close to the water pore. Introduction of a cysteine near the first NPA box in a mercury insensitive mutant (A73C/C189S) restored mercury sensitivity. This observation was an important indication that led to a functional model for AQP1, called the hourglass model. This model implicates that loops B and E fold back into the membrane and form together the water pore [75].

AQP2 was demonstrated to have the same transmembrane topology as AQP1 [6]. Mutations in the gene coding for AQP2 have been shown to cause autosomal recessive nephrogenic diabetes insipidus (NDI). Results of functional studies with the encoded mutant AQP2 proteins found in NDI are in support of the hourglass model: mutations in the B and E loop resulted in misrouted water channels that were non-functional, whereas mutations in loop C and in the beginning of loop D also resulted in misrouted, but functional water channels [28,31,116,178].

Most aquaporins are selective for water, but some, in particular AQP3, also transport small solutes like urea and glycerol [68]. All current MIP family proteins are thought to derive from two divergent bacterial paralogues, one a glycerol facilitator, the other an aquaporin [133]. In contrast to the other aquaporins, AQP3 derived from a glycerol facilitator rather than an aquaporin. As a consequence of the larger evolutionary distance, AQP3 contains structural features that are different from the other aquaporins, in particular elongated C and E loops, which might be critical for transport of small solutes.

To gain more insight in the structure-function relationship of the aquaporins, we decided to test the predictions of the hourglass model by exchanging loops B and E among water channels with different characteristics: 1) AQP0, which is a weak, but water-selective channel; 2) AQP2, which is selective for water, and closely related to AQP0; and 3) AQP3, which transports water as well as urea and glycerol.

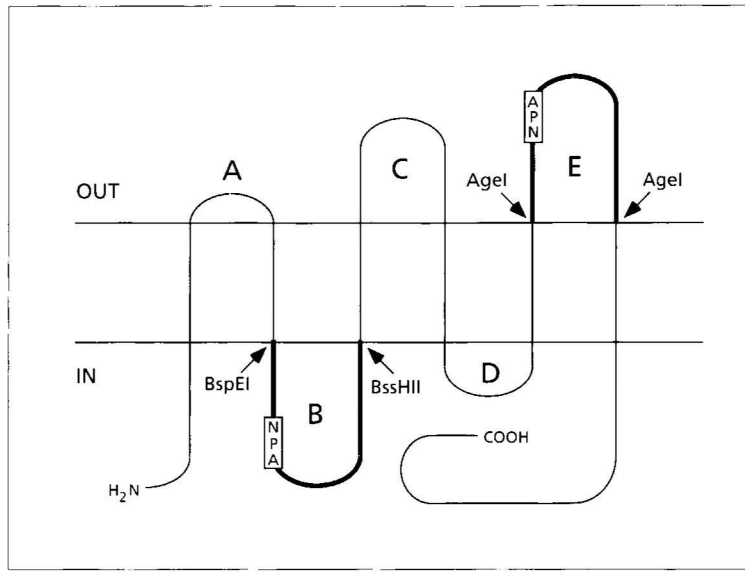

Fig. 1 General topology model of the aquaporins. The introduced restriction sites at the beginning and end of loops B and E, and the conserved NPA boxes in loops B and E, are indicated.

Construct	Wild-type amino acid/codon	Mutant amino acid/codon
AQP0 *Bsp*EI	Ser-Gly-64/agtgga	Ser-Gly-64/TCCgga
AQP0 *Bss*HII	Leu-Arg-Ala-86/cttcgtgcc	Leu-Arg-Ala-86/ctGcgCgcc
AQP0 *Age*I (1)	Thr-Gly-180/actggt	Thr-Gly-180/acCggt
AQP0 *Age*I (2)	Gly-Pro-Val-209/ggcccggtc	Gly-Pro-Val-209/ggAccggtc
AQP2 *Bsp*EI	Ser-Gly-64/agcggg	Ser-Gly-64/TCcggA
AQP2 *Bss*HII	Leu-Arg-Ala-86/ctccgagcc	Leu-Arg-Ala-86/ctGcgCgcc
AQP2 *Age*I (1)	Thr-Gly-180/accggc	Thr-Gly-180/accggT
AQP2 *Age*I (2)	Gly-Pro-Leu-209/ggacccctg	Gly-Pro-**Val**-209/ggaccGGtg
AQP3 *Bsp*EI	Ser-Gly-66/tctgga	Ser-Gly-66/tcCgga
AQP3 *Bss*HII	Ile-Lys-Leu-88/atcaagctg	**Leu-Arg-Ala**-88/TtGCGCGCg
AQP3 *Age*I (1)	Ser-Gly-198/tctggc	**Thr**-Gly-198/AcCggT
AQP3 *Age*I (2)	Pro-Ile-Val-235/cccatcgtc	**Gly-Pro**-Val-235/GGACCGgtc

Table 1 List of mutations that were introduced in AQP0, AQP2 and AQP3 to create the restriction sites. The nucleotide changes are depicted in upper case letters, the resulting amino acid substitutions are printed bold. The resulting restriction sites are underlined.

• *Introduction of the restriction sites*

To be able to exchange loops B and E between bovine AQP0 in the pXBGevI expression vector [117], human AQP2 in the pT7Ts expression vector [31], and rat AQP3 (kindly donated by M. Echevarria, Sevilla, Spain) in the pT7Ts expression vector, unique restriction sites were introduced at the beginning and end of loops B and E using the Altered sites II *in vitro* mutagenesis kit (Promega, Madison, WI). In all three constructs, a *Bsp*EI site was introduced at the beginning of loop B, a *Bss*HII site was introduced at the end of loop B, and *Age*I sites were introduced at the beginning and end of loop E (Fig. 1). The resulting sequences are listed in Table I. First, in every construct only two restriction sites were introduced (the *Bsp*EI and *Bss*HII sites, or both *Age*I sites). Then constructs containing all four introduced restriction sites were generated by ligating two halves of the cDNA containing two introduced restriction sites each, onto eachother. The clones that were identical to the wild-type cDNAs except for the transitions needed to create the restriction sites, were selected by sequence analysis [63].

• *Construction of AQP0 with loops B and/or E from AQP2, AQP2 with loops B and/or E of AQP0 and AQP2 with loops B and/or E of AQP3*

From the above-mentioned constructs the loops B of AQP0, AQP2, and AQP3 (each 65 bp) were isolated by low-melting point agarose gel electrophoresis after digestion with *Bsp*EI and *Bss*HII. Loops E from AQP0 (86 bp), AQP2 (86 bp) and AQP3 (110 bp) were acquired by the same technique, after digestion with *Age*I. Next, these fragments were cloned into the corresponding sites of the AQP0 or AQP2 constructs, in which the *Bsp*EI and *Bss*HII, or both *Age*I sites had been introduced.

AQP0 containing both loop B and loop E from AQP2 was constructed by ligating a 500 bp *Bgl*II-*Kpn*I fragment containing the first halve of AQP0 and loop B of AQP2 onto the second halve of AQP0 containing loop E of AQP2. The AQP2 constructs with both loops of AQP0 or AQP3 were created by ligation of *Bam*HI fragments of 500 bp of the second halve of AQP2 containing loop E of AQP0 or AQP3 into the AQP2 construct containing loop B of AQP0 or AQP3, respectively, from which these *Bam*HI fragments had been removed. Clones with proper orientation of inserts and proper reading frames were selected by endonuclease digestion and sequence analysis.

• *Transcription*

Constructs were linearized with *Sal*I (pT7Ts) or *Xba*I (pXBGevI) and *in vitro* transcribed using T7 RNA polymerase (pT7Ts) or T3 RNA polymerase (pXBGevI), according to Promega's (1991) Protocols and Principles guide, except that nucleoside triphosphates and 7-methyl-diguanosine triphosphate were used at a final concentration of 1 mM. The cRNAs were purified and dissolved in DEPC-treated milliQ water. The integrity of the cRNA was checked by agarose gel electrophoresis and the concentration was determined spectrophotometrically.

• *Water permeability*

Stage V and VI oocytes of *Xenopus laevis* were isolated and injected with water or 10

ng of cRNA. After incubation for three days in modified Barth's solution at 18°C, oocytes were analyzed in a swelling assay as described previously [31]. Oocyte swelling was performed at 22°C following transfer from 200 mosM to 70 mosM, or from 200 mosM to 20 mosM.

- *Isolation of oocyte lysates and membranes*

To determine the stability and size of the aquaporins, 8 oocytes were homogenized in 160 µl homogenization buffer A (HbA: 20 mM Tris (pH 7.4), 5 mM $MgCl_2$, 5 mM NaH_2PO_4, 80 mM sucrose, 1 mM EDTA, 1 mM DTT, 1 mM PMSF, 5µg/ml leupeptin and pepstatin) at 4°C at 3 days after injection. Subsequently, the lysates were centrifuged twice for 10 min at 125 g to remove yolk proteins. At the same day, plasma membranes were isolated from 25 oocytes according to Wall and Patel [184].

- *Immunoblotting*

Lysates or plasma membranes equivalent to 0.1 oocyte or 8 oocytes, respectively, were denatured for 30 min at 37°C in sample buffer (2% (wt/vol) SDS, 50 mM Tris (pH 6.8), 12% (vol/vol) glycerol, 0.01% (wt/vol) Coomassie Brilliant Blue, 100 mM DTT), electrophoresed through a 12% SDS-polyacrylamide gel [86] and transferred to nitrocellulose (Schleicher & Schuell, Dassel, Germany) as described previously [31]. Efficiency of protein transfer was checked by reversible staining of the nitrocellulose membrane with Ponceau Red. For immunodetection of AQP2, the nitrocellulose membrane was incubated with a 1:10,000 dilution of affinity-purified rabbit polyclonal antibodies directed against the 15 C-terminal amino acids of rat AQP2 [28]. For AQP0, a 1:10,000 dilution of affinity-purified rabbit polyclonal antibodies directed against the 15 C-terminal amino acids of bovine AQP0 [117] was used. As a secondary antibody, a 1:5,000 dilution of affinity-purified anti-rabbit IgG conjugated to horse radish peroxidase (Sigma, St. Louis, MO) was used. Proteins were visualized using enhanced chemiluminescence (Boehringer Mannheim, Germany).

Immunocytochemistry

At 3 days after injection, oocytes were stripped from remaining vitelline membranes and were incubated for 1 h in 1% wt/vol paraformaldehyde fixative (PLP) [110], dehydrated and embedded in paraffin. After blocking with 10% (vol/vol) goat serum in Tris-buffered saline (TBS), sections of oocytes expressing AQP2 proteins were incubated O/N at 4°C with affinity-purified polyclonal AQP2 antibodies diluted 1:500 in 10% (vol/vol) goat serum in TBS. Sections of oocytes expressing AQP0 proteins were incubated with a 1:500 dilution of affinity-purified polyclonal AQP0 antibodies in 10% (vol/vol) goat serum in TBS. After three washes for 10 min in TBS, the sections were incubated for 1 h in a 1:100 dilution of anti-rabbit IgG coupled to fluorescein isothiocyanate (FITC) (Sigma). The sections were again washed three times for 10 min, dehydrated by washing in 70-100% (vol/vol) ethanol and mounted in mowiol 4-88, 2.5% (wt/vol) NaN_3. Photographs were taken on Kodak EPH P1600X films with a Zeiss Axioskop microscope equipped with epifluorescent illumination.

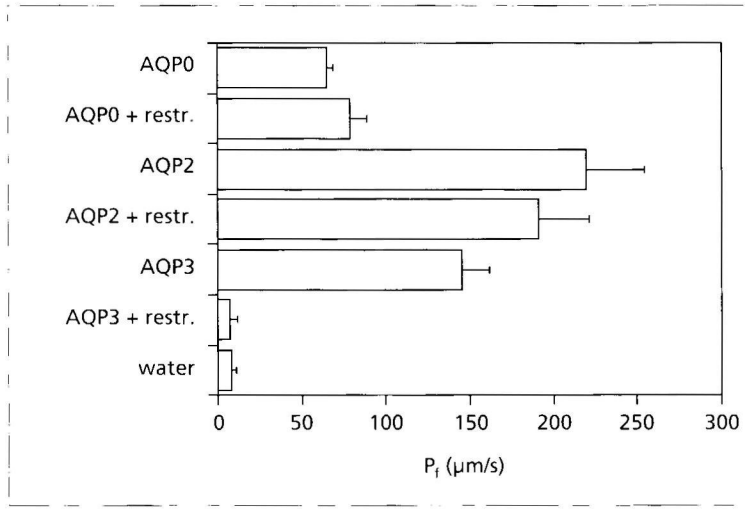

Fig. 2 Osmotic water permeability (P_f in μm/s) of oocytes. Oocytes were injected with water, or 10 ng of cRNA encoding wt AQP0, AQP2 or AQP3, or 10 ng of cRNA encoding these constructs after the 4 restriction sites had been introduced. Shown are means±SE.

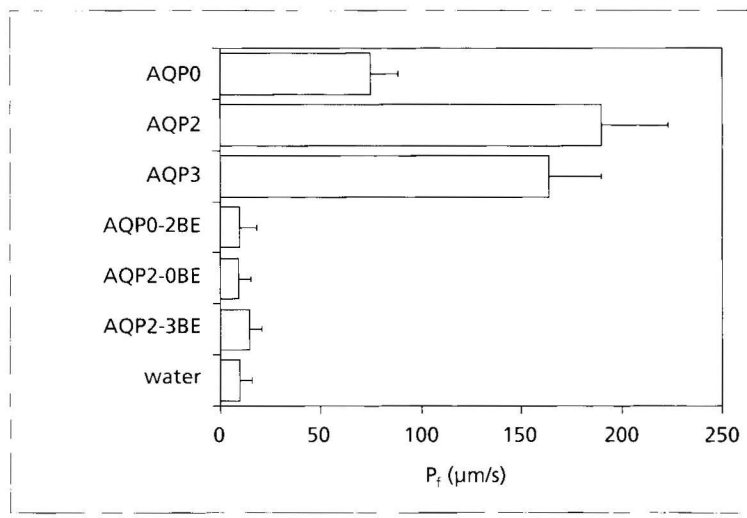

Fig. 3 Osmotic water permeability (P_f) of oocytes. Oocytes were injected with water, or 10 ng of cRNA encoding wt AQP0, wt AQP2, wt AQP3, AQP0 with loops B and E of AQP2 (AQP0-2BE), AQP2 with loops B and E of AQP0 (AQP2-0BE), or AQP2 with loops B and E of AQP3 (AQP2-3BE). Shown are means±SE.

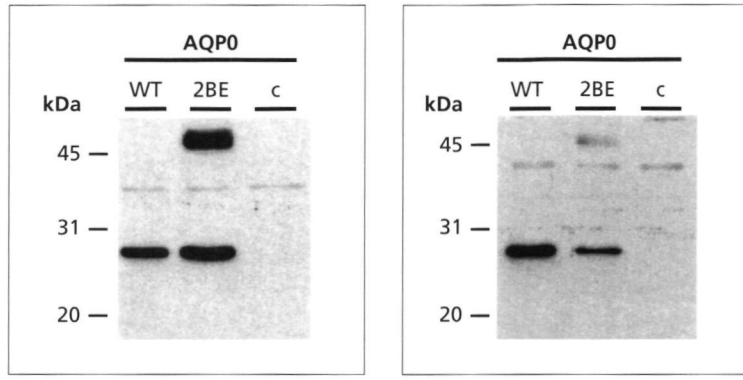

A B

Fig. 4 Immunoblot analysis of lysates (**A**) and plasma membranes (**B**) of oocytes expressing AQP0. Oocytes were injected with water (c) or 10 ng of cRNA encoding wt AQP0 or AQP0 with loops B and E of AQP2 (AQP0-2BE). Equivalents of 0.1 oocyte (lysates) or 8 oocytes (membranes) were separated by SDS-PAGE and immunoblotted. Proteins were visualized by chemiluminescence using AQP0 antibodies.

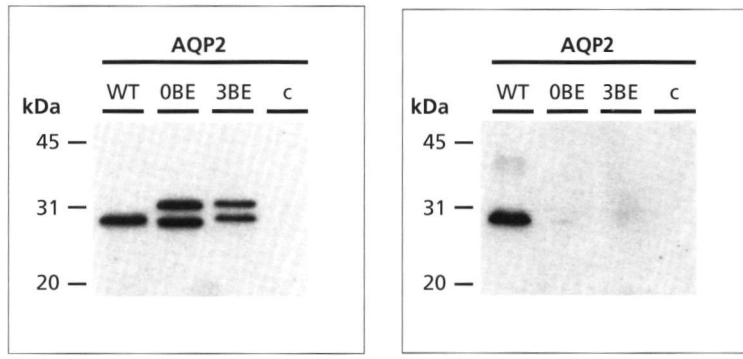

A B

Fig. 5 Immunoblot analysis of lysates (**A**) and plasma membranes (**B**) of oocytes expressing AQP2. Oocytes were injected with water (c) or 10 ng of cRNA encoding wt AQP2, AQP2 with loops B and E of AQP0 (AQP2-0BE), or AQP2 with loops B and E of AQP3 (AQP2-3BE). Equivalents of 0.1 oocyte (lysates) or 8 oocytes (membranes) were separated by SDS-PAGE and immunoblotted. Proteins were visualized by chemiluminescence using AQP2 antibodies.

To be able to exchange loops B and E between bovine AQP0, human AQP2 and rat AQP3, four restriction sites were introduced in each cDNA using *in vitro* mutagenesis. At the start and the end of loop B a *Bsp*EI and a *Bss*HII site were introduced, respectively, and in loop E, two *Age*I sites were introduced (Fig. 1 and Table 1). For AQP0, introduction of these restriction sites did not introduce changes at the protein level. For AQP2, a valine was substituted for a leucine at position 209. For AQP3, introduction of the restriction sites resulted in 6 amino acid substitutions (Ile86Leu, Lys87Arg, Leu88Ala, Ser197Thr, Pro233Gly, Ile234Pro) (Table 1). To test whether these amino acid substitutions affected function of the protein, these constructs were transcribed and obtained cRNAs were injected into *Xenopus* oocytes. Three days after injection, water permeability measurements revealed that wild-type (wt) AQP0 and AQP0 containing the restriction sites did not differ in function, as expected, and also wt AQP2 and AQP2-L209V yielded similar water permeabilities. However, AQP3 with the 6 amino acid substitutions was no longer functional (Fig. 2).

Based on these results, we decided to make the following constructs:

1. AQP0 with loops B and E of AQP2 (AQP0-2BE), AQP0 with loop B of AQP2 (AQP0-2B), AQP0 with loop E of AQP2 (AQP0-2E)
2. AQP2 with loops B and E of AQP0 (AQP2-0BE), AQP2 with loop B of AQP0 (AQP2-0B), AQP2 with loop E of AQP0 (AQP2-0E)
3. AQP2 with loops B and E of AQP3 (AQP2-3BE), AQP2 with loop B of AQP3 (AQP2-3B), AQP2 with loop E of AQP3 (AQP2-3E)

First, cRNAs from constructs in which both loops B and E had been replaced (AQP0-2BE, AQP2-0BE, AQP2-3BE) were injected into *Xenopus* oocytes. Swelling tests revealed that the water permeability of these oocytes was not increased above water-injected oocytes (Fig. 3). The absence of swelling of these oocytes is either due to the absence of the protein, or the presence of a non-functional, or misrouted protein. To investigate these possibilities, lysates and plasma membranes of these oocytes were prepared and subjected to immunoblotting. Lanes loaded with lysates of oocytes injected with cRNA coding for wt AQP0 or AQP0-2BE showed a 26 kDa band of similar intensity, indicating that both proteins are expressed in comparable amounts (Fig. 4A). The lane loaded with oocyte lysate of AQP0-2BE, however, showed an additional band at 45-50 kDa, which might represent aggregated AQP0 proteins. No signal was obtained in the lane loaded with a lysate of water-injected oocytes. Immunoblotting of plasma membranes isolated from these oocytes revealed that the expression of AQP0-2BE at the plasma membrane was less compared to wt AQP0 (Fig. 4B). Lysates of oocytes injected with cRNA encoding AQP2-0BE or AQP2-3BE both showed, beisdes the native AQP2 protein of 29 kDa, an additional band of ~32 kDa (Fig. 5A). This additional band has also been detected in NDI-related AQP2 mutants, and has been shown to represent a glycosylated form of AQP2 that is retarded in the endoplasmic reticulum (ER) [28]. Therefore, this finding indicates that these proteins are impaired in their routing to the plasma membrane. The bands representing AQP2-3BE run slightly higher, because loop E

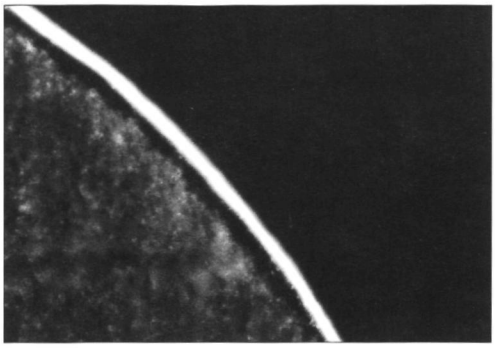

WT AQP0

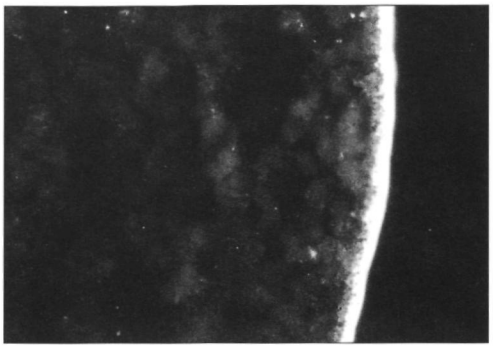

WT AQP2

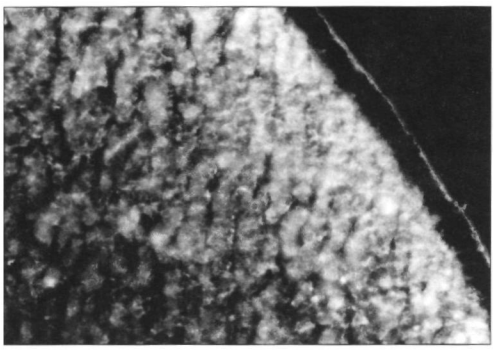

AQP0-2BE

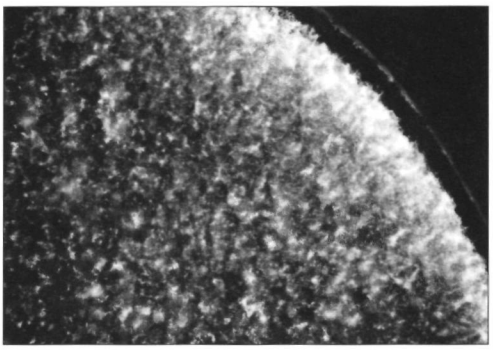

AQP2-0BE

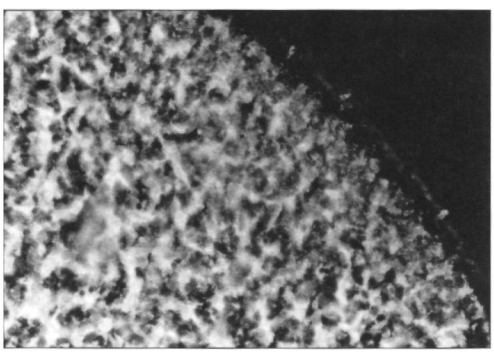

AQP0-2B

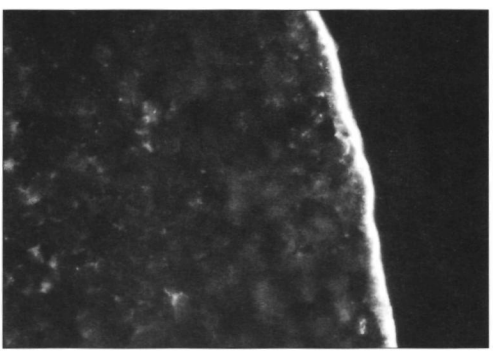

AQP2-0B

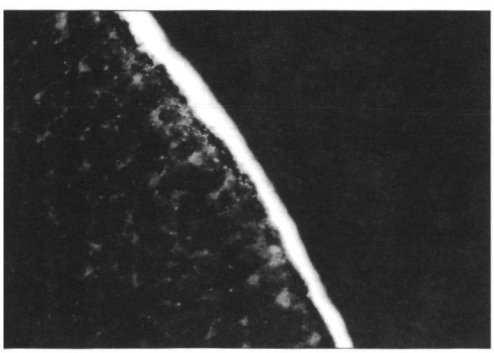

AQP0-2E

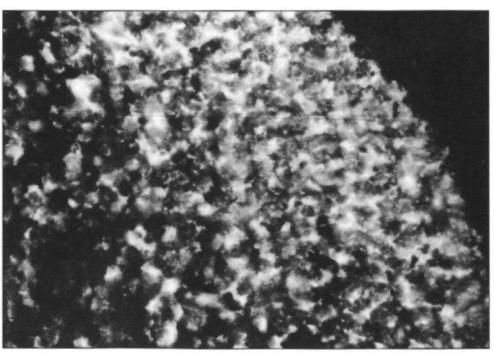

AQP2-0E

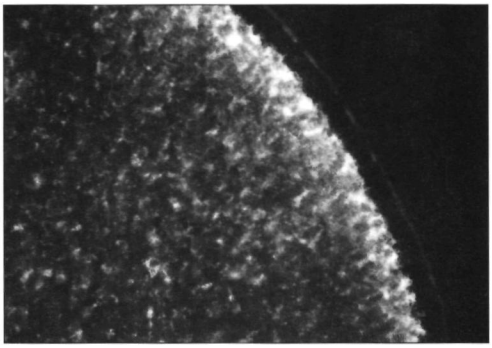

AQP2-3BE

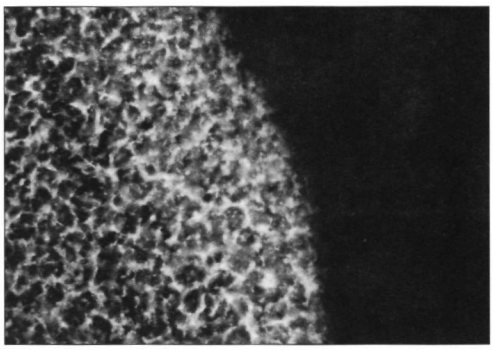

AQP2-3B

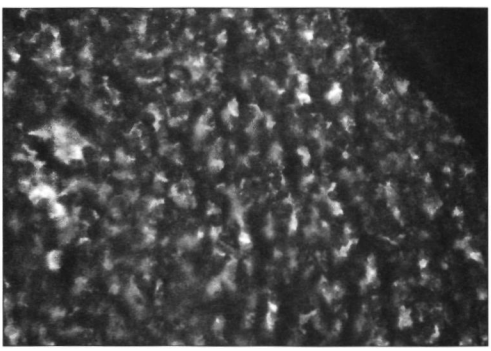

AQP2-3E

Fig. 6 Sections of oocytes. Oocytes were injected with cRNA encoding AQP0 or AQP2 proteins. AQP0 or AQP2 proteins were visualized with polyclonal AQP0 or AQP2 antibodies, respectively, and anti-rabbit IgG conjugated with FITC. Shown are wt AQP0, AQP0 with loops B and E of AQP2 (AQP0-2BE), AQP0 with loop B of AQP2 (AQP0-2B), AQP0 with loop E of AQP2 (AQP0-2E), wt AQP2, AQP2 with loops B and E of AQP0 (AQP2-0BE), AQP2 with loop B of AQP0 (AQP2-0B), AQP2 with loop E of AQP0 (AQP2-0E), AQP2 with loops B and E of AQP3 (AQP2-3BE), AQP2 with loop B of AQP3 (AQP2-3B), and AQP2 with loop E of AQP3 (AQP2-3E).

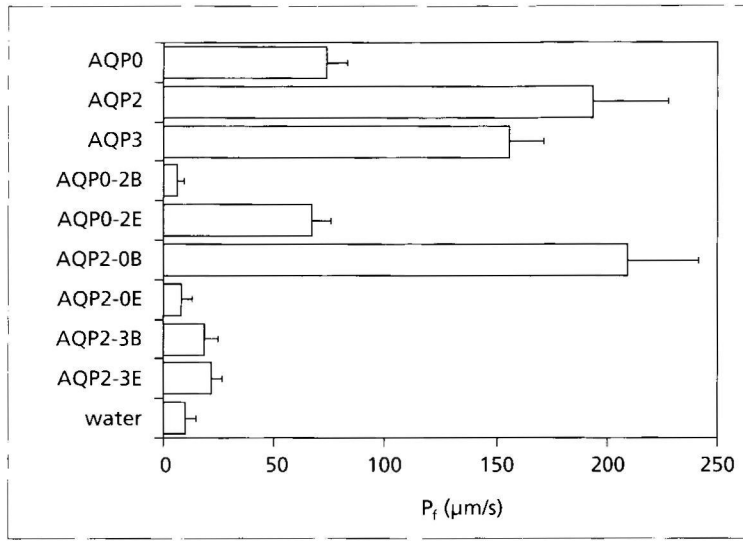

Fig. 7 Osmotic water permeability (P_f) of oocytes. Oocytes were injected with water, or 10 ng of cRNA encoding wt AQP0, wt AQP2, wt AQP3, or AQP0 with loop B of AQP2 (AQP0-2B), AQP0 with loop E of AQP2 (AQP0-2E), AQP2 with loop B of AQP0 (AQP2-0B), AQP2 with loop E of AQP0 (AQP2-0E), AQP2 with loop B of AQP3 (AQP2-3B), AQP2 with loop E of AQP2 (AQP2-3E). Shown are means±SE.

of AQP3 is eight amino acids longer than loop E of AQP0 or AQP2. Immunoblots of plasma membranes of these oocytes showed that AQP2-0BE or AQP2-3BE were not detectable in a plasma membrane fraction (Fig. 5B), which confirms the routing problem of these proteins. In sections of oocytes (Fig. 6) expressing wt AQP0 or wt AQP2, a clear, intense staining of the plasma membrane was observed. Oocytes expressing AQP0-2BE showed a diffuse cytoplasmic staining, with some staining of the plasma membrane. In sections of oocytes expressing AQP2-0BE or AQP2-3BE the proteins were distributed diffusely over the cytoplasm, and no plasma membrane staining could be detected. Water-injected oocytes did not yield any signal upon incubation with AQP0 or AQP2 antibodies (not shown).

Additionally, cRNAs of constructs in which only one loop had been replaced were injected into *Xenopus* oocytes. Swelling tests (Fig. 7) revealed that oocytes injected with cRNA encoding AQP0-2B did not give any increase in P_f, whereas oocytes expressing AQP0-2E revealed the same water permeability as oocytes expressing wild-type AQP0. Oocytes injected with cRNA encoding AQP2-0B had the same water permeability as oocytes expressing wt AQP2, but oocytes injected with cRNA encoding AQP2-0E did not show an increased water permeability. The water permeability of oocytes expressing AQP2-3B or AQP2-3E was not increased above water permeability of water-injected oocytes (Fig. 7).

To investigate the expression level and routing of these proteins, lysates and plasma membranes were prepared three days after injection, and were subjected to immunoblotting. Lanes loaded with lysates of oocytes expressing wt AQP0, AQP0-

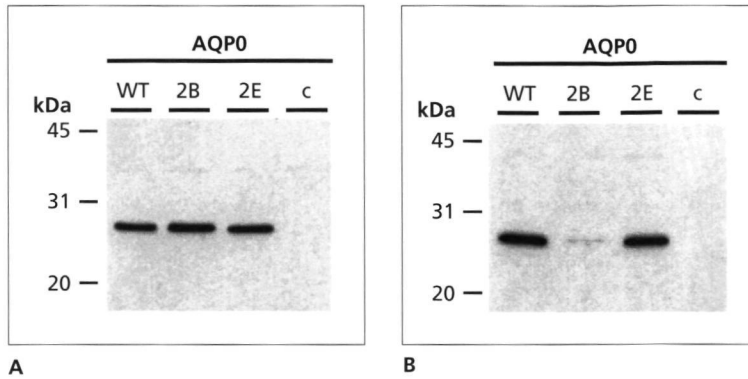

Fig. 8 Immunoblot analysis of lysates (**A**) and plasma membranes (**B**) of oocytes expressing AQP0 proteins. Oocytes were injected with water (c), or cRNA encoding wt AQP0, AQP0 with loop B of AQP2 (AQP0-2B) or AQP0 with loop E of AQP2 (AQP0-2E). Equivalents of 0.1 oocyte (lysates) or 8 oocytes (membranes) were separated by SDS-PAGE and immunoblotted. Proteins were visualized by chemiluminescence using AQP0 antibodies.

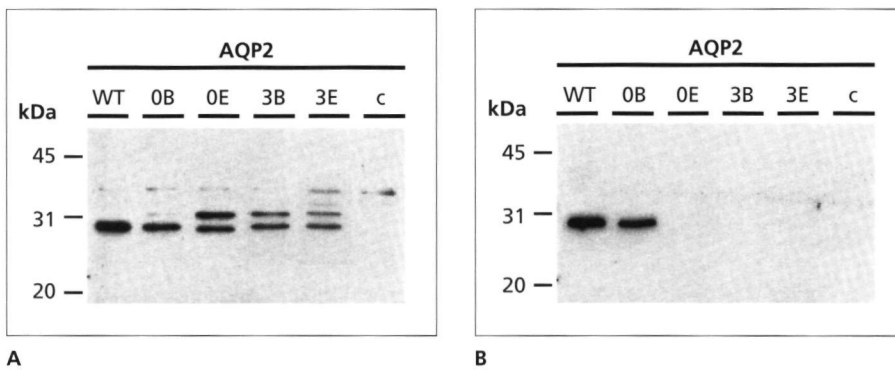

Fig. 9 Immunoblot analysis of lysates (**A**) and plasma membranes (**B**) of oocytes expressing AQP2 proteins. Oocytes were injected with water (c), or cRNA encoding wt AQP2, AQP2 with loop B of AQP0 (AQP2-0B), AQP2 with loop E of AQP0 (AQP2-0E), AQP2 with loop B of AQP3 (AQP2-3B), or AQP2 with loop E of AQP3 (AQP2-3E). Equivalents of 0.1 oocyte (lysates) or 8 oocytes (membranes) were separated by SDS-PAGE and immunoblotted. Proteins were visualized by chemiluminescence using AQP2 antibodies.

2B, or AQP0-2E showed a 26 kDa band, of comparable intensities (Fig. 8A). Again, no signal was obtained in lysates of control oocytes. In the fractions enriched for plasma membranes, wt AQP0 and AQP0-2E showed a similar expression, whereas AQP0-2B could hardly be detected (Fig. 8B). Immunoblots of lysates of oocytes expressing AQP2 proteins showed a 29 kDa band present in all lanes, representing the size of the native AQP2 protein (Fig. 9A). However, in lanes loaded with oocytes expressing AQP2-0E, AQP2-3B, or AQP2-3E, an additional band of ~32 kDa was present, representing the ER-retarded form of AQP2. In lysates of oocytes expressing AQP2-0B no ER-retarded band was present. The bands representing AQP2-3B were slightly, and AQP2-3E clearly less intense than that of wt AQP2, which indicates that these proteins are less stable than wt AQP2 (Fig. 9A). Immunoblotting of the plasma membrane fraction revealed only a signal in the lanes loaded with samples from oocytes expressing wt AQP2 or AQP2-0B (Fig. 9B). Sections of oocytes injected with wt AQP0 or wt AQP2 showed an intense staining of the plasma membrane (Fig. 6). A similar staining was observed in oocytes expressing AQP0-2E or AQP2-0B. Sections of oocytes expressing AQP0-2B, AQP2-0E, AQP2-3B or AQP2-3E all showed a diffuse staining of the cytoplasm, without staining of the plasma membrane.

Discussion

Since the discovery of the first water channel, AQP1, the structure-function relationship of AQP1 has been an important issue in aquaporin research. Mutagenesis experiments led to a functional model called the hourglass model, which proposes that loops B and E are of critical importance for the formation of the water pore [75]. We, therefore, undertook a study in which loops B and E of three aquaporins with different features were exchanged, and assessed the effects on aquaporin function.

To be able to exchange loops B and E between AQP0, AQP2 and AQP3, restriction sites were introduced at the start and end of loops B and E with primers designed to introduce the least number of amino acid substitutions (Fig. 1). These mutations caused no change of amino acids for AQP0, whereas in AQP2 only a conserved amino acid substitution (Leu209Val) was introduced (Table 1). Therefore, it was not surprising that these 'mutants' resulted in wild-type water permeability. In AQP3, which is at a greater evolutionary distance from the other aquaporins and is consequently less homologous to AQP0 and AQP2, six amino acid changes were introduced of which four were conserved. Therefore, it is likely that the switch of the Pro to Gly and Ile to Pro at the second *Age*I site caused the inability of mutant AQP3 to confer water permeability (Fig. 2).

When loops B and E of AQP2 were introduced into AQP0 (AQP0-2BE), loops B and E of AQP0 into AQP2 (AQP2-0BE), or loops B and E of AQP3 into AQP2 (AQP2-3BE), no increase in water permeability (P_f) was observed upon expression in *Xenopus* oocytes (Fig. 3). For AQP2-0BE and AQP2-3BE this is explained by misrouting of these proteins, because immunoblots showed that these proteins were retarded in the ER, and were consequently not expressed in the plasma mem-

brane. These results were confirmed by immunocytochemistry, since the distribution was similar to ER-retarded AQP2 proteins encoded in NDI [28,116] (Fig. 6). For AQP0-2BE, no ER-retarded band was present in the lane loaded with oocyte lysates expressing this protein. The band of 32 kDa which is detected with misrouted AQP2 proteins is a high mannose glycosylation form of AQP2 which is generated in the ER. For high mannose glycosylation, an N-glycosylation site is essential. With immunoblotting, ER-retarded AQP0 proteins can not be discriminated from native AQP0 molecules, because AQP0 does not contain an N-glycosylation site. Immunoblots of plasma membrane fractions showed, however, that AQP0-2BE was only expressed at low levels at the plasma membrane (Fig. 5B). Sections of oocytes expressing AQP0-2BE confirmed that a major fraction of the protein was present in the cytoplasm (Fig. 6). In a previous study, we have shown that very low plasma membrane expression levels of misrouted, but functional AQP2 mutant proteins in NDI, conferred water permeability to oocytes [116]. With immunocytochemistry, these mutants were detected at low levels in the plasma membrane, but they could not be detected with immunoblot analysis of plasma membrane fractions. The low level of plasma membrane expression of AQP0-2BE, which could also be detected by immunoblotting of the plasma membrane fraction, should therefore be sufficient to increase water permeability if loops B and E of AQP2 would confer high AQP2 water transport to AQP0. The absence of water transport therefore precludes that loops B and E of AQP2 confer a high water permeability to AQP0. However, it does not rule out the possibility that AQP0-2BE functions as wt AQP0, because the water permeability of AQP0 is much lower than that of AQP2.

Oocytes expressing aquaporins with one loop of another aquaporin, revealed four mutant proteins that did not confer water permeability (AQP0-2B, AQP2-0E, AQP2-3B, AQP2-3E). Immunoblotting revealed that the AQP2 proteins showed an ER-retarded form, and that all these proteins were not detected in a plasma membrane fraction (Figs. 8, 9). Furthermore, immunocytochemistry on these oocytes revealed the typical distribution of ER-retarded aquaporins [28,116]. The impaired transport of these mutant proteins to the plasma membrane does not allow us to draw conclusions with respect to the functionality of these chimeric proteins.

In two cases, AQP0-2E and AQP2-0B, the water permeability was significantly increased above control oocytes, and was comparable to the P_f obtained for the corresponding wt aquaporins. Immunoblotting and sections of oocytes showed that these proteins were properly routed to the plasma membrane. The finding that AQP2-0B functions like AQP2 (high P_f) and AQP0-2E functions like AQP0 (low P_f) shows that introduction of loop B of AQP0 does not lower the P_f of AQP2, and that loop E of AQP2 does not increase the water permeability of AQP0. Since we are dealing here with the two loops which supposedly form the water pore, the most simple conclusion is that, although loops B and E form the pore, other parts of the protein determine the water permeability features. These other parts of the protein do presumably not include the C-tail, because exchanging the tail of AQP1 for that of AQP0 revealed an AQP1 phenotype [117]. More likely, the arrangement of the transmembrane domains are important, because substitution of a proline for a

valine in the 5th transmembrane domain of AQP0 (V160P) increased the water permeability of AQP0 by 50% [117].

An altogether different view could be that not loops B and E, but other parts of the protein form the water pore. This has been suggested by Bai *et al.* [6], who proposed a functional model for AQP2 that differs substantially from the hourglass model. They showed that participation of loops B and E in the formation of the water pore is not as critical for AQP2 as predicted in the hourglass model for AQP1, because insertional mutations in the very conserved loops B and E did not alter water channel function. Instead, these authors state that loops C and D have a significant contribution to the formation of the water pore. In contrast to the model proposed by Bai *et al.* we have shown that results of NDI-related AQP2 mutant proteins are in support with the hourglass model, since amino acid substitutions in loops B and E abolished water channel function completely, whereas mutations in the C and D loop resulted in functional but misrouted water channels [28,31,116, 178]. Furthermore, we have shown that AQP2-C181S, which played an important role in the functional model for AQP2, is severely disturbed in its routing to the plasma membrane [118].

In conclusion, our exchange experiments mostly resulted in chimeric proteins that were impaired in their routing to the plasma membrane, from which no conclusions concerning functionality can be obtained. It rather shows that even the highly conserved loops B and E are not sole entities, but that these loops have aquaporin-specific interactions with other parts of the protein in the maturation process. The three chimeric proteins that were expressed at the plasma membrane, AQP0-2E, AQP2-0B, and AQP0-2BE, revealed the striking finding that neither one nor both loops influenced the water permeability of the aquaporin in which it was inserted, which indicates that, if the pore is formed by loops B and E, other parts of AQP0 and AQP2 determine the extent of water permeability.

Both site-directed mutagenesis and the exchange of loops have been shown to be very useful to solve unanswered questions about the structure-function relationship of ion channels [17,83]. For aquaporins, site directed mutagenesis has been frequently applied and yielded important information, but we have shown now that the exchange of complete loops seems to be less successful due to improper folding and consequent misrouting of the chimeric proteins.

In the near future, we can expect more definite insights into the structure of aquaporin 1 from a different approach. Projection maps of AQP1 determined by electron crystallography show that the AQP1 monomer can be interpreted as a cylinder consisting of six alpha helices, representing the six transmembrane domains [91,112,188]. Within this cylinder, a trapezoidal substructure is located which is probably formed by the hydrophobic loops B and E [9,19,91], confirming the hourglass theory that loops B and E fold back into the membrane. Merging functional data from mutant aquaporins with high resolution 3D maps can lead to a detailed structure-function model which will solve the yet unproven value of the hourglass model.

Chapter 4

New mutations in the AQP2 gene in nephrogenic diabetes insipidus resulting in functional but misrouted water channels

Sabine M. Mulders •
Nine V.A.M. Knoers ••
Angenita F. van Lieburg •••
Leo A.H. Monnens •••
Ernst Leumann ••••
Elke Wühl •••••
Edith Schober ••••••
Johan P.L. Rijss •
Carel H. van Os •
Peter M.T. Deen •

• Department of Cell Physiology,
•• Department of Human Genetics,
••• Department of Pediatrics,
University of Nijmegen, The Netherlands
•••• Universitäts-Kinderklinik Zürich, Switzerland
••••• Department of Pediatrics,
University of Heidelberg, Germany
•••••• Universitäts-Kinderklinik Wien, Austria

J Am Soc Nephrol 8, 242-248 (1997)

Summary

Nephrogenic diabetes insipidus (NDI) is characterized by the inability of the kidney to concentrate urine in response to vasopressin. The autosomal recessive form of NDI is caused by mutations in the AQP2 gene, encoding the vasopressin-regulated water channel of the kidney collecting duct. In this report we present three new mutations in the AQP2 gene that cause NDI, resulting in A147T-, T126M- or N68S-substituted AQP2 proteins. Expression of the A147T and T126M mutant AQP2 proteins in *Xenopus* oocytes revealed a relatively small, but significant increase in water permeability, whereas the water permeability of N68S expressing oocytes was not increased. cRNAs encoding missense and wild-type AQP2 were equally stable in oocytes. Immunoblots of oocyte lysates showed that only the A147T mutant protein was less stable than wild-type AQP2. The mutant AQP2 proteins showed, in addition to the wild-type 29 kDa band, an endoplasmic reticulum-retarded form of AQP2 of ~32 kDa. Immunoblotting and immunocytochemistry demonstrated only intense labeling of the plasma membranes of oocytes expressing wild-type AQP2. In summary, two mutant AQP2 proteins encoded in NDI are functional water channels. Therefore, the major cause underlying autosomal recessive NDI is the misrouting of AQP2 mutant proteins.

Introduction

Aquaporins are selective water channels and form a subset of the MIP family of intrinsic membrane proteins. In the kidney, four aquaporins (AQP 1 through 4) [44,55,68,74,98,140] have been identified and are postulated to be involved in reabsorption and concentration of the glomerular filtrate. AQP1 is constitutively expressed in the proximal tubule and descending limb of Henle, and is localized to apical and basolateral membranes [126]. AQP2 is the vasopressin-regulated water channel of principal cells of the collecting duct [55]. In the absence of vasopressin, AQP2 is localized in vesicles in the subapical region of the cell. Upon binding of vasopressin to its V_2 receptor, AQP2 water channels are inserted into the apical membrane, conferring a high water permeability to this membrane. Upon removal of vasopressin, the channels are retrieved by endocytosis [79,106,122,149,191]. AQP3 and AQP4 are localized to the basolateral membrane of principal cells of the collecting duct, and are suggested to function as an exit pathway for water [50].

So far, only AQP2 has been shown to be involved in diseases. Individuals who lack functional AQP1 do not exhibit clinical symptoms, which raised questions about the physiological significance of AQP1 [143]. Mutations in AQP3 and AQP4 have not been identified so far. Mutations in the AQP2 gene, however, have been shown to be the cause of the autosomal recessive form of nephrogenic diabetes insipidus (NDI), a severe disease that is characterized by the inability of the kidney to concentrate urine in response to vasopressin [31,178]. In the majority of patients, NDI is caused by a mutation in the V_2 receptor gene, and is inherited as a X-linked recessive trait. In approximately 10% of the families, NDI has shown a non-X-linked pattern of inheritance. So far, a one-nucleotide deletion and three mutations coding for missense mutations in AQP2 have been reported as a cause of NDI in some of these families [31,178]. Upon expression in *Xenopus* oocytes, the missense AQP2 proteins with a G64R, R187C, or S216P substitution were unable to increase the water permeability (P_f) of oocytes, whereas expression of wild-type AQP2 increased P_f values more than 10 fold. Further studies revealed that the mutant AQP2 proteins were impaired in their cellular routing [28]. Consequently, it remained undecided whether these mutations resulted in non-functional water channels, since they did not reach the plasma membrane.

In the study presented here, we report three additional NDI patients who are homozygous for mutations in the AQP2 gene. In addition, we performed functional analyses of the mutant AQP2 proteins in oocytes and concluded that two mutations result in functional but misrouted water channels.

Methods

Patients

The three patients investigated in this study come from three separate families from different ethnic origin. In all three families, the parents of the patients are consanguineous.

Family 1 is of Austrian descent. The male proband (patient 1) was admitted to the

hospital at the age of 3 months with signs of dehydration, including recurrent fever and hypernatremia (serum sodium 164 mmol/liter). On admission, urinary osmolality was very low (50 mosmol/kg) and did not increase after a water-deprivation test or after the administration of arginine vasopressin. At present, at the age of 18 years, he has a polyuria and polydipsia of approximately 13 liters/d (no medication). In his older sister, a diagnosis of diabetes insipidus was made at the age of a few months. Data on a water deprivation test or a dDAVP (Minrin®) test were not available in her medical record. She has been treated, however, with Minrin® without a reduction in urinary volume. Now, as an adult, she has a fluid intake of approximately 13 liters/d (no medication).

Family 2 comes from Sri Lanka. The male proband (patient 2) was referred at the age of 5 months because of intermittent high fever, weakness, irritability and weight loss. The diagnosis of NDI was based on the presence of a high serum sodium (186 mmol/liter), a low urinary osmolality (173 mosmol/kg), and unresponsiveness to dDAVP. Therapy with hydrochlorothiazide proved very difficult despite tube feeding and was complicated by intermittent bulging fontanel, fever and vomiting. The boy failed to thrive and showed muscular hypotonia and delayed psychomotor development. At the age of 13 months he was readmitted with high fever, seizures and hypernatremia (173 mmol/liter), followed by coma. He succumbed two weeks later. MRI and necropsy revealed severe brain lesions with necrosis of basal ganglia. Eight months later NDI was diagnosed in the younger brother at the age of 1 week based on elevated serum sodium (147 mmol/liter) and low urinary osmolality (107 mosmol/kg). At present, at the age of two years, his psychomotor development is adequate but there is slight muscular hypotonia. Fluid intake is 2 liters/d.

Family 3 is Turkish by descent. In the female proband (patient 3) the diagnosis diabetes insipidus was made at the age of 6 weeks when she was admitted to the children's hospital with failure to thrive and signs of dehydration, including fever, and hypernatremia (serum sodium 162 mmol/liter). Urinary osmolality was low (82 mosmol/kg) but increased to 236 mosmol/kg after water-deprivation and to 450 mosmol/kg after administration of arginine vasopressin, suggesting a diagnosis of NDI with partial resistance to vasopressin. However, at the age of 18 months a control vasopressin test showed a rise of urine osmolality to only 239 mosmol/kg. According to the parents, two sons of the sister of the paternal grandmother, at that time 7 and 8 years old, both suffered from a similar disease. Further investigation revealed that they both had NDI with total resistance to vasopressin. All three patients have been treated with the combination indomethacin-hydrochlorothiazide, which was replaced for amiloride and Minrin® in the proband at the age of 4 years. Despite treatment she still had a fluid intake of approximately 4 liters/d.

• *DNA amplification and sequence analysis of patients*

Genomic DNA was isolated by the salt-extraction technique. Primers used for amplification of the AQP2 coding regions and for cycle sequencing were as described elsewhere [31]. PCR conditions were 1 min at 92°C, 1.5 min at 60°C and 1.5 min at 72°C for 30 cycles. Cycle sequencing reactions were performed on both DNA strands, and sequences were analyzed on an automated fluorescence-based Applied Biosystems model 373A DNA sequencing system.

• *DNA constructs and transcription*

To introduce the A147T mutation in our AQP2 expression construct (pT7TsAQP2), exon 2 of the AQP2 gene was amplified from genomic DNA of patient 1. A 66 bp *Sac*I-*Sma*I fragment containing the G to A transition at position 533 was isolated by gel electrophoresis. For the T126M mutation, genomic DNA of patient 2 was amplified using primers flanking the coding region of exon 2, and a 43 bp *Dde*I-*Sac*I fragment was isolated, containing the C to T transition at position 471. For the N68S mutation, exon 1 of the AQP2 gene was amplified from genomic DNA of patient 3, and a 144 bp *Apa*I-*Sac*II fragment containing the A to G transition at position 297 was isolated. These fragments were inserted into the corresponding sites of pT7TsAQP2 and clones that were identical to the wild-type (wt) AQP2 cDNA sequence, except for the described mutations, were selected by sequence analysis [63]. These constructs were linearized by *Sal*I and capped RNA transcripts were synthesized *in vitro* using T7 RNA polymerase according to Promega's (1991) Protocols and Principles guide, except that 1 mM final concentrations of nucleotide triphosphates and 7-methyl-di-guanosine triphosphate were used. The cRNAs were purified and dissolved in DEPC-treated water. The integrity of the RNA was checked by agarose gel electrophoresis and the concentration was determined spectrophotometrically.

• *Water permeability*

Xenopus laevis oocytes were isolated, injected with 10 ng of cRNA and analyzed after three days in a swelling assay as described before [31]. Oocyte swelling was performed at 22°C following transfer from 200 mosM to 70 mosM (wt AQP2 expressing oocytes) or 200 mosM to 20 mosM (water-injected control oocytes and mutant AQP2 expressing oocytes).

• *Northern blot analysis*

At the day of injection and three days after injection, RNA was isolated from 6 oocytes according to Chomczynski and Sacchi [21]. RNA equivalents of three oocytes were loaded onto a 2.2 M formaldehyde, 1% (wt/vol) agarose gel. Electrophoresis, blotting and hybridization conditions were as described [29]. A 850 bp *Eco*RI cDNA fragment encoding human AQP2 [31] was labeled with [α-^{32}P] dCTP by random priming [46] and was used as a probe. The relative amount of mRNA loaded onto the gel was assessed by hybridization of the same blot with a probe of a 780 bp *Eco*RI-*Bam*HI cDNA fragment coding for *Xenopus laevis* Histon H3 [39] and subsequent scanning of the autoradiographic signals with an LKB Ultrascan XL laser densitometer.

• *Immunoblotting*

To determine the stability of mutant and wt AQP2 proteins, 8 oocytes were homogenized in 20 µl buffer A per oocyte (20 mM Tris (pH 7.4), 5 mM $MgCl_2$, 5 mM $NaHPO_4$, 1 mM EDTA, 1 mM DTT, 1 mM PMSF, 5 µg/ml leupeptin and pepstatin, 80 mM sucrose) at 4°C at 1, 2 and 3 days after injection. Subsequently, the lysates were centrifuged twice for 10 min at 125 g to remove yolk proteins. At the third day after injection, a fraction enriched for plasma membranes was isolated from 25 oocytes according to Wall and Patel [184].

Lysates or plasma membranes equivalent to 0.1 oocyte or 8 oocytes, respectively,

were denatured for 30 min at 37°C in sample buffer (2% SDS, 50 mM Tris (pH 6.8), 12% glycerol, 0.01% Coomassie Brilliant Blue, 100 mM DTT), electrophoresed through a 12% SDS-polyacrylamide gel [86] and transferred to a nitrocellulose membrane as described [31]. Efficiency of protein transfer was checked by staining the membrane with Ponceau Red. For immunodetection, the membrane was incubated with a 1:10,000 dilution of an affinity-purified polyclonal antibody directed against the 15 C-terminal amino acids of rat AQP2 (17). As a secondary antibody, a 1:5,000 dilution of affinity-purified goat-anti-rabbit IgG conjugated to horse radish peroxidase (Sigma Immuno Chemicals, St. Louis, MO) was used. Proteins were visualized using enhanced chemiluminescence (Boehringer Mannheim). When appropriate, the 29 and 32 kDa AQP2 bands of the third day were scanned as described above.

Immunocytochemistry

At 3 days after injection, remaining vitelline membranes were removed and oocytes were incubated for 1 hour in 1% (wt/vol) paraformaldehyde fixative (PLP) [110], dehydrated, and embedded in paraffin. After blocking with 10% goat serum in Tris-buffered saline (TBS), the sections were incubated O/N at 4°C with the polyclonal AQP2 antibody diluted 1:500 in 10% goat serum in TBS. After three washes for 10 min in TBS, the sections were incubated for 1 hour in a 1:100 dilution of goat-anti-rabbit IgG coupled to fluorescein isothiocyanate (Sigma Immuno Chemicals). The sections were again washed three times for 10 min, dehydrated by washing in 70% to 100% ethanol and mounted in mowiol 4-88, containing 2.5% NaN_3. Photographs were taken with a Zeiss Axioskop with epifluorescent illumination with an automatic camera using Kodak EPH P1600X films.

Results

From three NDI patients, in whom a V_2 receptor defect was either excluded or unlikely, we amplified and sequenced the four exons of the AQP2 gene. All patients were found to be homozygous for three different missense mutations. In patient 1, a G533A transition was found in exon 2, leading to a substitution of an alanine for threonine (A147T). In patient 2, a C471T transition in exon 2 leads to a threonine to methionine substitution (T126M). The AQP2 gene of patient 3 showed a A297G transition in exon 1, which results in a substitution of an asparagine for a serine (N68S) in one of the most conserved regions of the MIP family proteins [145] (Fig. 1).

The asymptomatic parents and a healthy brother and sister of patient 1 were shown to be heterozygous for the A147T mutation; another asymptomatic sister appeared to be homozygous for the normal allele. As expected, the affected brother of patient 2 appeared homozygous for the T126M mutation as well, whereas their asymptomatic parents were both shown to heterozygous for that mutation. DNA of an elder healthy brother was not available for testing. Sequencing of exon 1 in the two affected male family members of patient 3 revealed that they both were homozygous for the N68S mutation. The asymptomatic parents, an asymptomatic sister of the father and the paternal grandparents of patient 3, as well as the mother of the

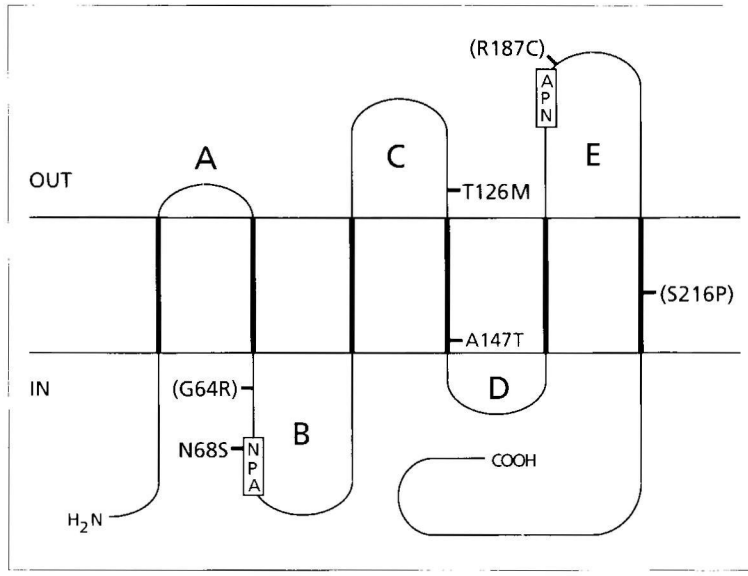

Fig. 1 Proposed membrane topology of AQP2. The three amino acid substitutions as coded for by the AQP2 genes of the three NDI patients and the conserved NPA boxes are indicated. The previously reported amino acid substitutions in NDI patients (15,16) are shown between brackets.

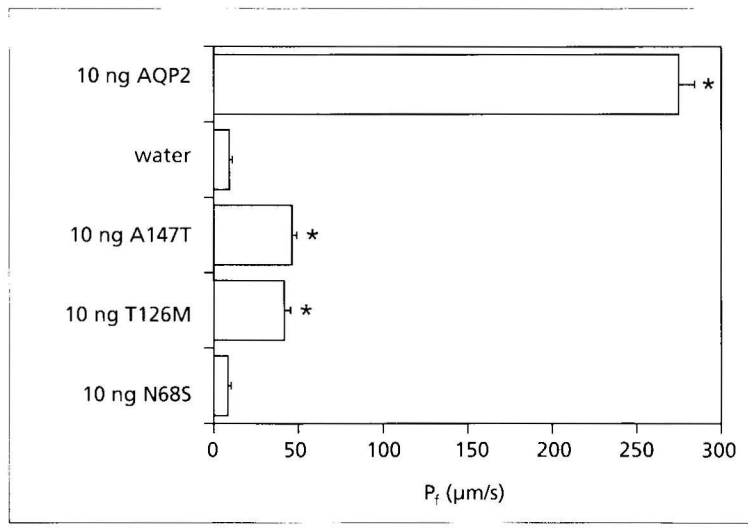

Fig. 2 Osmotic water permeability (P_f) of oocytes three days after injection of water or 10 ng of cRNA encoding wt, A147T, T126M or N68S AQP2. Mean and SE of at least 45 oocytes from 6 different experiments are shown (*, significantly increased above water-injected control oocytes, $p<0.01$).

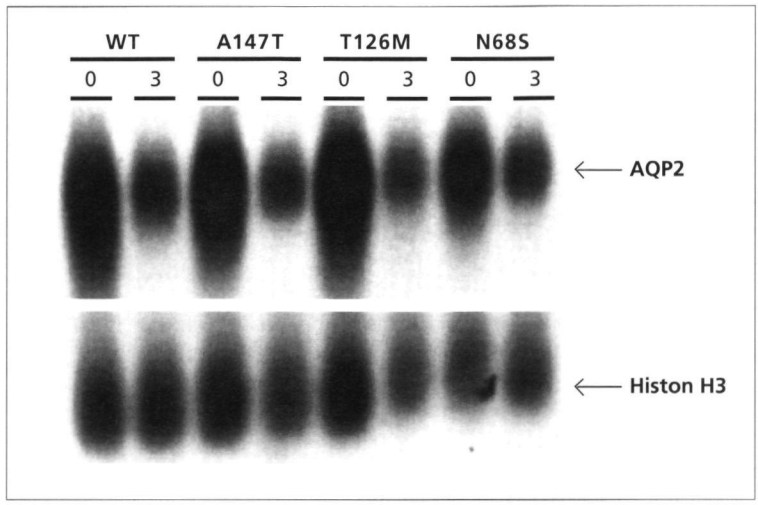

Fig. 3 Northern blot analysis of the stabilities of cRNAs encoding wt, A147T, T126M or N68S AQP2 in *Xenopus* oocytes. At the day of injection and three days after injection, RNA was isolated from six oocytes. An equivalent of three oocytes was blotted and RNA was visualized using a human AQP2 cDNA probe (upper panel). For normalization of the amount of RNA loaded, the blot was hybridized with a *Xenopus* histon H3 probe (lower panel).

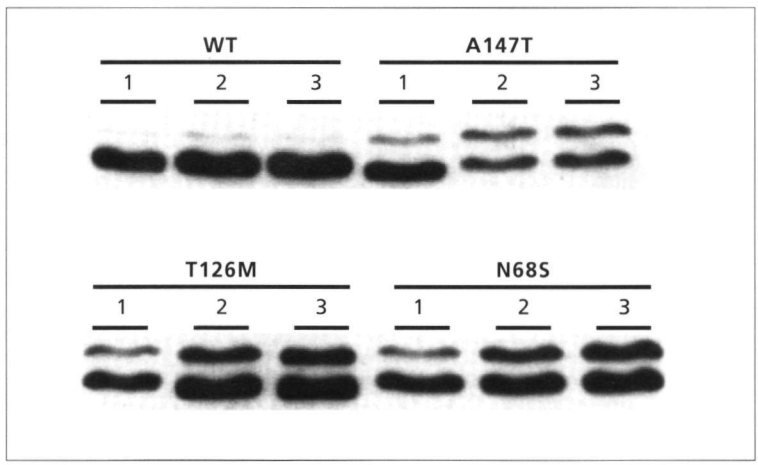

Fig. 4 Immunoblot analysis of AQP2 proteins. At 1, 2 and 3 days after injection, lysates were prepared from 8 oocytes injected with cRNA encoding wt, A147T, T126M or N68S AQP2. Equivalents of 0.1 oocyte were separated by SDS-PAGE and blotted. AQP2 proteins were visualized by chemiluminescence using AQP2 antibodies as a first antibody and anti-rabbit IgG, conjugated to peroxidase, as a second antibody.

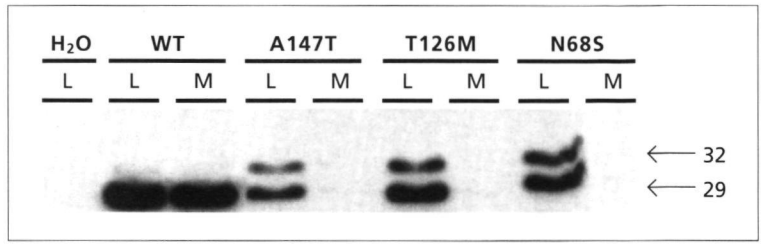

Fig. 5 Immunoblot analysis of lysates and a fraction enriched for plasma membranes of oocytes. Lysates (L) and plasma membranes (M) were prepared 3 days after injection of water or cRNA encoding wt, A147T, T126M or N68S AQP2. Equivalents of 0.1 oocyte (L) or 8 oocytes (M) were separated by SDS-PAGE and immunoblotted as described in the legend of Fig. 4.

two other patients in family 3 were all shown to be heterozygous for the N68S mutation. The data are consistent with co-segregation of the mutant AQP2 allele with the disease and with autosomal recessive inheritance of NDI in these families.

To test whether these mutant AQP2 proteins are functional water channels, PCR fragments containing the mutations were cloned into the AQP2 expression vector and transcripts were injected into *Xenopus* oocytes. Three days later, water permeability measurements revealed that the water permeability ($P_f \pm SE$) of oocytes expressing the N68S mutant (8.3 ± 1.9 μm/s) was not different from water-injected control oocytes (8.9 ± 2.2 μm/s), whereas oocytes expressing the T126M (41.4 ± 3.8 μm/s) or A147T (46.2 ± 2.7 μm/s) AQP2 proteins showed a significantly increased water permeability when compared to water-injected control oocytes. The water permeability of wild-type (wt) AQP2 injected oocytes was 275 ± 9.7 μm/s (Fig. 2).

The low or absent water permeability of mutant AQP2 proteins in *Xenopus* oocytes could be caused by 1) a low stability of the mutant cRNAs in *Xenopus* oocytes; 2) a low stability of the mutant AQP2 proteins in oocytes; 3) an impairment of the routing of the mutant AQP2 proteins to the plasma membrane; and/or 4) a mutant AQP2 protein that is a non-functional water channel.

To test for differences in stability of wt and mutant cRNAs, RNA isolated from oocytes directly after, and three days after injection was subjected to Northern blot analysis. A specific signal with our human AQP2 cDNA probe was only obtained in lanes loaded with RNA isolated from AQP2 cRNA injected oocytes (Fig. 3). After normalization for the amounts of RNA loaded by hybridization with a *Xenopus* Histon H3 probe, the amounts of wt and mutant AQP2 cRNAs were comparable.

To compare the size and stability of mutant and wt AQP2 proteins, oocyte lysates were prepared 1, 2 and 3 days after injection and were subjected to immunoblotting using AQP2 antibodies (Fig. 4). Ponceau Red staining of the immunoblot showed that equal amounts of protein were loaded (not shown). Chemiluminescence detection revealed a band of 29 kDa present in all lanes loaded with AQP2 protein, except in the lane loaded with water-injected control oocytes. In the lanes loaded with mutant AQP2 protein an additional band of ~32 kDa was present. Densitometric scanning of the bands from the third day samples revealed that the stability

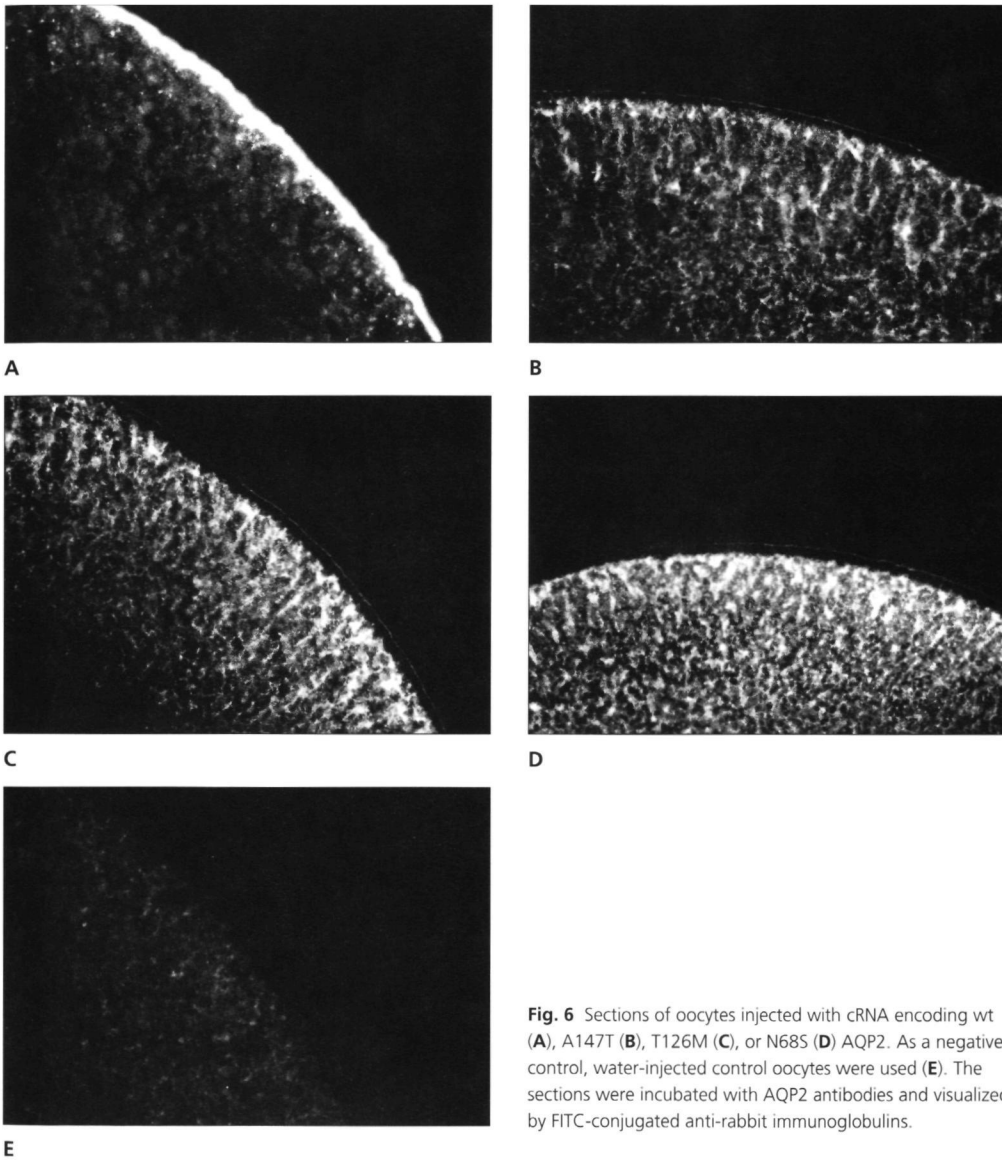

Fig. 6 Sections of oocytes injected with cRNA encoding wt (**A**), A147T (**B**), T126M (**C**), or N68S (**D**) AQP2. As a negative control, water-injected control oocytes were used (**E**). The sections were incubated with AQP2 antibodies and visualized by FITC-conjugated anti-rabbit immunoglobulins.

of the T126M and N68S mutants and wt AQP2 were equal, whereas the stability of the A147T mutant was less than 10% of wt AQP2.

To determine the plasma membrane expression of wt and mutant AQP2 proteins, a fraction enriched for plasma membranes was subjected to immunoblotting (Fig. 5). Only in the membrane fraction of oocytes expressing wt AQP2, a clear 29 kDa band was visible, whereas no AQP2 protein could be detected in the membrane fractions of AQP2 mutants. To visualize the location of AQP2 proteins, immunocytochemistry was performed on injected oocytes (Fig. 6). Staining with the AQP2 antibody revealed a clear, intense staining of the plasma membrane of oocytes expressing wt AQP2 (Fig. 6A), whereas oocytes expressing mutant AQP2 proteins showed a very weak staining of the plasma membrane, with a more pronounced labeling of the cytoplasm (Fig. 6B-D). The water-injected control oocytes showed no staining (Fig. 6E).

Discussion

The discovery of mutations in the V_2 receptor gene, located on the X-chromosome, explained the cause of NDI in a majority of the patients [82], but not in all. Some of these unexplained NDI cases appeared to segregate as an autosomal recessive trait, and mutations in the V_2 receptor coding region could often be excluded in these cases. Therefore, the involvement of a second gene causing NDI was likely. In search for proteins involved in the cascade of events between the binding of vasopressin to the V_2 receptor at the basolateral membrane and the reabsorption of water at the apical membrane of the collecting duct cell, the cloning of the rat AQP2 water channel, which is exclusively expressed in the collecting duct [55], attracted attention. The AQP2 gene was assigned to chromosome 12, region q12-q13, and was therefore a likely candidate [33]. The subsequent identification of mutations in the AQP2 gene in some of these NDI patients provided a definitive proof for a second gene defect in NDI [31,178].

Here we report three new missense mutations in the AQP2 gene of three NDI patients coding for a A147T-, T126M-, or N68S-substituted AQP2 protein. Expressed in *Xenopus* oocytes, the N68S mutant AQP2 was non-functional (Fig. 2). This could be anticipated, because the substituted amino acid is part of the NPA box in loop B, which forms, together with a second NPA box in loop E, the most conserved amino acid sequence of the MIP-family [145]. Unlike the N68S-substituted protein and previously reported AQP2 mutants (G64R, R187C and S216P) [31,178], the A147T and T126M AQP2 mutant proteins were functional. The alanine at position 147 is also well-conserved among the MIP family members [145]. The observed water permeability of the oocytes expressing the A147T and T126M AQP2 proteins was, however, much lower than that of oocytes expressing wt AQP2. To find an explanation for the reduced P_f of oocytes expressing NDI-related AQP2 proteins, these oocytes were analyzed in detail and were compared with wt AQP2 expressing oocytes. The stability of injected cRNA was equal for mutant and wt AQP2 (Fig. 3). In contrast, differences with wt AQP2 were observed on the protein level. Immunoblot analysis revealed that wt AQP2 was only expressed as a 29 kDa

protein, while the three mutants showed an additional 32 kDa form (Fig. 4). In a previous study on mutant AQP2 proteins similar 32 kDa bands were detected, and they were shown to be endoglycosidase H-sensitive [28]. Because endoglycosidase H hydrolyses endoplasmic reticulum-specific high-mannose glycosylation groups, the 32 kDa bands presumably represent ER-retarded forms of mutant AQP2 proteins. The mutant AQP2 proteins are apparently retained in the endoplasmic reticulum and thus impaired in their routing to the plasma membrane. The indication that the A147T-, T126M- and N68S-substituted AQP2 proteins were impaired in their transport was further substantiated by the absence of these proteins in an immunoblotted oocyte fraction enriched for plasma membranes, whereas the wt AQP2 protein was clearly present (Fig. 5). In addition, immunocytochemistry showed a clear AQP2 labeling in the plasma membrane of oocytes expressing wt AQP2, whereas the mutant AQP2 proteins were abundantly expressed in the cytoplasm, but were hardly detectable in the plasma membrane, which confirms the impaired transport of the mutant AQPs (Fig. 6). In the ER, newly-synthesized proteins undergo various posttranslational modifications including folding, oligomerization and glycosylation [14,59]. Proteins that are not properly processed do not pass the 'quality control' of the ER and are usually retained. The processing of the new protein depends in part on the structural motifs displayed during folding and assembly, and on the molecular interactions with chaperones and folding factors. The quality control of the ER recognizes certain conformational features of the misfolded protein, such as hydrophobic peptide elements exposed on the surface of the molecule, and in most cases, misprocessed proteins are subsequently degraded [14,59,60]. In *Xenopus* oocytes, the stability of the T126M and N68S mutants was comparable with that of wt AQP2, but the A147T mutant was considerably less stable, a phenomenon previously shown for the S216P mutant also [28]. Because the A147T and S216P mutations are both located in a transmembrane domain, misfolding may cause the exposure of hydrophobic regions on the surface of the molecule, which could make these mutants more accessible to ER-resident proteases. The other mutations (G64R, N68S, T126M, R187C) are located in the more hydrophilic extramembraneous loops, which may explain their stability in oocytes. In summary, all six NDI-related missense AQP2 proteins (G64R, N68S, T126M, A147T, R187C, S216P) are impaired in their transport to the plasma membrane when expressed in *Xenopus* oocytes ([28]; this study). Despite the impairment in routing, the A147T and T126M mutants significantly increased the P_f of oocytes. In view of the fact that the A147T mutant is very instable in oocytes, the mutants that are stable in oocytes (G64R, N68S, R187C) should also confer water permeability to oocytes, if they were functional water channels. Therefore, it is likely that the G64R, N68S and R187C AQP2 mutants are non-functional.

All our data regarding AQP2 are in line with the hourglass model, which is a structural-functional model proposed for AQP1. In this model, loops B and E are essential for the formation of the pore through which water transport takes place [75]. The hourglass model is based on site-directed mutagenesis studies in which mutations in the B and E loops of AQP1, containing the conserved NPA boxes, resulted in loss of water permeability. Mutations in the A, C and D loops and the N- and C-

terminal regions, however, affected the water transporting properties of AQP1 to a lesser degree [142]. All AQP2 proteins in NDI with mutations in the B loop (G64R, N68S) or E loop (R187C) are non-functional, whereas AQP2 proteins with mutations in the C loop (T126M) or near the D loop (A147T) are functional. Recently, Bai *et al.* [6] proposed that in AQP2 loops C and D are closely located to the aqueous pathway, instead of loops B and E. This is not in line with our data from NDI-related mutant AQP2 proteins. Bai *et al.* [6] reported that mutations near the NPA boxes in loops B and E did not alter water channel function, which contrasts sharply with our data.

In conclusion, two mutant AQP2 proteins, encoded by AQP2 genes of patients suffering from autosomal recessive NDI, appeared to be functional water channels. Therefore, the major cause underlying this disease is the misrouting of the mutant AQP2 proteins, and not the dysfunctioning of the water channels. As shown for the most common mutant form of the cystic fibrosis transmembrane conductance regulator (CFTR), which has a deletion of the phenylalanine at position 508, the primary effect is not a functional impairment, but rather an impairment in the routing of the mutant protein to the plasma membrane. In CFTRΔF508-expressing cells it has been shown that culturing these cells at lower temperatures relieved the impairment in routing of the ΔF508 mutant, which resulted in the appearance of functional Cl^- channels in the plasma membrane [38]. Furthermore, elevated levels of molecular chaperones appeared to increase proper folding of the K304E mutant of the medium chain acyl-CoA dehydrogenase (MCAD) [15] and the Y393N mutation of the E1α subunit of the mitochondrial branched chain α-ketoacid dehydrogenase complex [169]. In future studies, attempts should be undertaken to overcome the biosynthetic arrest and to promote trafficking of the T126M and A147T AQP2 mutants to subapical vesicles or the plasma membrane. This will require knowledge of the mechanism that causes retention. The opportunity to manipulate the cellular machinery associated with protein folding and trafficking may provide the tools for novel pharmaco-therapeutic strategies that may be used in the treatment of this form of nephrogenic diabetes insipidus.

Acknowledgments

We thank A. Hartog for performing immunocytochemistry on oocytes and Dr. R.J.M. Bindels for valuable suggestions.

Chapter 5

Importance of the mercury sensitive cysteine on function and routing of AQP1 and AQP2 in oocytes

Sabine M. Mulders
Johan P.L. Rijss
Anita Hartog
Rene J.M. Bindels
Carel H. van Os
Peter M.T. Deen.

Am J Physiol 273: Renal Physiol 42 (1997)
(in press)

Summary

To discriminate between water transport of AQP2 mutants in nephrogenic diabetes insipidus and that of an AQP2 molecule used to drag them to the oolemma, we investigated the mercury sensitivity of wild-type and AQP2 C181S proteins in oocytes. Incubation with $HgCl_2$ inhibited the water permeability (P_f) of human (h) AQP2 for 40%, whereas inhibition of hAQP1 was 75%. Oocytes expressing hAQP1 C189S revealed a P_f comparable to wild-type hAQP1, but mercury sensitivity was lost. In contrast, no increase in P_f was obtained when hAQP2 C181S was expressed. Also, expression of rat AQP2 C181A and C181S mutants did not increase the P_f, which contrasts with published observations. Immunocytochemistry and immunoblotting revealed that only AQP1, AQP1 C189S and AQP2 were targeted to the plasma membrane, and that AQP2 mutant proteins are retarded in the endoplasmic reticulum.

In conclusion, water transport through AQP2 is less sensitive to mercury inhibition than through AQP1. Furthermore, substitution of the mercury-sensitive cysteine for a serine results in an impaired routing of human and rat AQP2, whereas similar mutations have no effect on AQP1 function.

Introduction

The cloning of the first discovered water channel, aquaporin 1 (AQP1), opened an exciting new field of research, and at the moment, 6 different mammalian aquaporins are known (AQP0-AQP5) [44,55,62,68,74,98,139,144]. Aquaporins are members of the MIP family of intrinsic proteins, traverse the membrane six times and have intracellular amino- and carboxyl termini [121]. A characteristic amino acid stretch present in every member of the MIP family is the NPA box, found in the first intracellular loop (loop B) and in the third extracellular loop (loop E) (Fig. 1). So far, the best studied water channels are AQP1 and AQP2. AQP1 is constitutively expressed in erythrocytes, renal proximal tubules and descending limb of Henle, and in several other epithelia [125]. AQP2 has been shown to be the vasopressin-regulated water channel that is exclusively expressed in renal collecting duct principal cells and inner medullary collecting duct cells [55].

Water permeation through AQP1 can be inhibited by binding of mercury to cysteine 189 [141,197]. When this cysteine is replaced by a serine, the water permeability remains unaffected, but mercury-sensitivity is lost. Recent reports show that mercury binding to cysteine 181 in AQP2 also results in inhibition of the water permeability and substitution of cysteine 181 for serine or alanine results in loss of mercury sensitivity, together with a 20-50% reduction of water permeability compared with wild-type (wt) AQP2 [6,7].

Recently, we have reported mutations in the AQP2 gene, which are the cause of the autosomal recessive form of nephrogenic diabetes insipidus (NDI) [31,178]. All missense AQP2 proteins in NDI were found to be impaired in their routing to the oolemma [28]. Jung *et al.* reported that co-expression of AQP1 missense mutants and an AQP1 truncation mutant (D237Z) in oocytes overcomes the impaired routing to the plasma membrane [75]. To apply a similar strategy as used by Jung *et al.* in the study of AQP2 missense mutants, we must be able to discriminate between water movement through the missense mutant and through a truncated AQP2 protein. Co-expression in oocytes of mercury-insensitive AQP2 missense proteins together with a truncated wild-type AQP2 should result in mercury insensitive water flow when the missense mutant is still a functional water channel. Therefore, the usefulness of mercury (in)sensitivity of AQP2 proteins as a tool to discriminate between water permeation conferred by the truncated or the mutant AQP2 proteins was investigated.

Materials and methods

Expression constructs

The human AQP2 C181S clone was obtained by introducing a C to G transition at position 634 and a G to C transition at position 636 in the human AQP2 cDNA using the Altered Sites II *in vitro* mutagenesis kit (Promega, Madison, WI). The clone that was identical to wt AQP2 except for the above mentioned transitions was selected by sequence analysis [63]. After digestion with *Bam*HI and *Kpn*I, a 282 bp fragment was isolated by gel electrophoresis and inserted into the corresponding

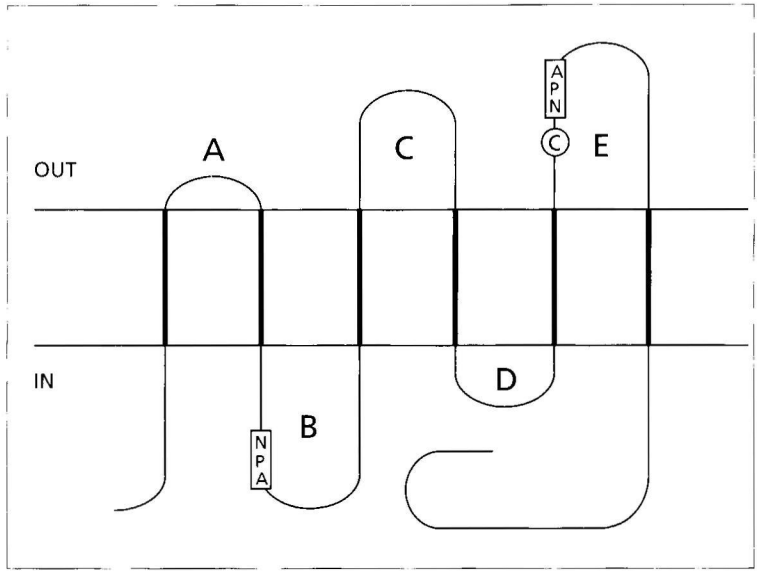

Fig. 1 Proposed topology model of AQP1 and AQP2. The highly conserved NPA boxes in loops B and E and the mercury sensitive cysteine (C189 in AQP1, C181 in AQP2) in loop E are indicated.

sites of pT7TsAQP2 [31]. In this vector, a *Xba*I-*Nde*I fragment had been removed from the polylinker in order to have a unique *BamH*I site in the AQP2 cDNA. The rat AQP2 C181S and C181A cDNAs [6] in the pXBGev1 expression vector were kindly provided by Drs. K. Fushimi and S. Sasaki (Tokyo, Japan). These constructs were checked by restriction analysis. The human AQP1 and the AQP1 C189S cDNAs [141] in the pXBGev1 expression vector were kindly provided by Drs. G.M. Preston and P. Agre (Baltimore, MD).

• *Transcription*

The constructs were linearized with *Sal*I (pT7Ts) or *Xba*I (pXBGevI) and *in vitro* transcribed using T7 RNA polymerase (pT7Ts) or T3 RNA polymerase (pXBGev1), according to Promega's (1991) Protocols and Principles guide, except that nucleotide triphosphates and 7-methyl-diguanosine triphosphate were used at a final concentration of 1 mM. The cRNAs were purified and dissolved in diethyl pyrocarbonate-treated milliQ water. The integrity of the cRNA was checked by agarose gel electrophoresis and the concentration was determined spectrophotometrically.

• *Water permeability*

Stage V and VI oocytes of *Xenopus laevis* were isolated and injected with water or 10 ng of cRNA. After incubation for three days in modified Barth's solution (MBS) at 18°C, oocytes were analyzed in a swelling assay as described previously [31]. Oocyte swelling was performed at 22°C following transfer from 200 mosM to 70 mosM. For the mercury inhibition studies, oocytes that exhibited a high P_f were selected and incubated for 5 min in MBS containing 1 or 3 mM $HgCl_2$. During the swelling assay, the same concentration of $HgCl_2$ was present in the diluted buffer. After this assay,

the same oocytes were incubated for 15 min in buffer containing 5 mM ß-mercaptoethanol, and assayed again in diluted buffer containing 5 mM ß-mercaptoethanol.

Oocyte lysate and membrane isolation

To determine the stability and size of the AQP1 and AQP2 proteins, 8 oocytes were homogenized in 160 µl homogenization buffer A (HbA: 20 mM Tris (pH 7.4), 5 mM $MgCl_2$, 5 mM NaH_2PO_4, 80 mM sucrose, 1 mM EDTA, 1 mM DTT, 1 mM PMSF, 5 µg/ml leupeptin and pepstatin) at 4°C at 1, 2 and 3 days after injection. Subsequently, the lysates were centrifuged twice for 10 min at 125 g to remove yolk proteins. At the third day after injection, plasma membranes were isolated from 25 oocytes according to Wall and Patel [184]. Oocyte lysates of an equivalent of one oocyte were digested with recombinant endoglycosidase H_f (endo H) (New England Biolabs, Beverly, MA) according to the manufacturer, except that protein samples were digested for 18 h after denaturation for 30 min at 37°C.

Immunoblotting

Lysates or plasma membranes equivalent to 0.1 oocyte or 8 oocytes, respectively, were denatured for 30 min at 37°C in sample buffer (2% (wt/vol) SDS, 50 mM Tris (pH 6.8), 12% (vol/vol) glycerol, 0.01% (wt/vol) Coomassie Brilliant Blue, 100 mM DTT), electrophoresed through a 13% SDS-polyacrylamide gel [86] and transferred to a nitrocellulose membrane (Schleicher & Schuell, Dassel, Germany) as described previously [28]. Efficiency of protein transfer was checked by reversible staining of the membrane with Ponceau Red. For immunodetection, the membrane was incubated with a 1:10,000 dilution of affinity-purified rabbit polyclonal antibodies directed against the 15 COOH-terminal amino acids of rat AQP2 [28] or a 1:200 dilution of a mouse monoclonal antibody directed against dog AQP1 (gift from M.L. Jennings, Galveston, TX). As a secondary antibody, a 1:5,000 dilution of affinity-purified anti-rabbit or anti-mouse IgG conjugated to horseradish peroxidase (Sigma, St. Louis, MO) was used. Proteins were visualized using enhanced chemiluminescence (Boehringer Mannheim, Germany).

Immunocytochemistry

Three days after injection, oocytes were stripped from remaining vitelline membranes and were incubated for 1 h in 1% (wt/vol) paraformaldehyde fixative (PLP) [110], dehydrated and embedded in paraffin. After blocking with 10% (vol/vol) goat serum in Tris-buffered saline (TBS), sections of oocytes expressing AQP2 proteins were incubated O/N at 4°C with affinity-purified polyclonal AQP2 antibodies diluted 1:500 in 10% (vol/vol) goat serum in TBS. The sections of oocytes expressing AQP1 proteins were incubated with a 1:100 dilution of a rabbit polyclonal AQP1 antibody. This antibody was prepared by immunization of rabbits with a synthetic peptide representing the last 15 COOH-terminal amino acids of rat AQP1 coupled to rabbit serum albumine. After three washes for 10 min in TBS, the sections were incubated for 1 h in a 1:100 dilution of anti-rabbit IgG coupled to fluorescein isothiocyanate (FITC) (Sigma). The sections were again washed three times for 10 min, dehydrated by washing in 70-100% (vol/vol) ethanol and mounted in mowiol 4-88, 2.5% (wt/vol) NaN_3. Photographs were taken with a Zeiss Axioskop microscope equipped with epifluorescent illumination and Kodak EPH P1600X films were used.

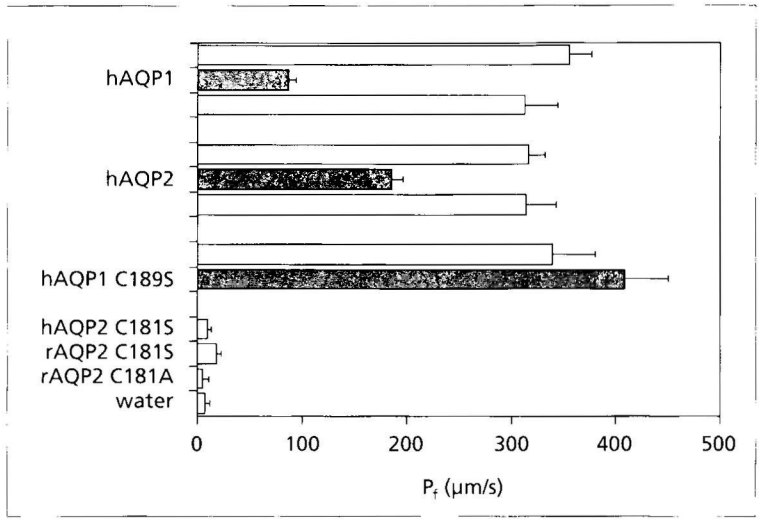

Fig. 2 Osmotic water permeability (P_f) of oocytes three days after injection of water or 10 ng of the following cRNAs: hAQP1, hAQP2, hAQP1 C189S, hAQP2 C181S, rAQP2 C181S or rAQP2 C181A. Identical oocytes were subjected to the standard osmotic swelling assay (light bars), after incubation with 1 mM $HgCl_2$ (dark bars), and after subsequent incubation with 5 mM ß-mercaptoethanol (open bars). Shown are means ± SE of 15-40 oocytes.

Results

To determine the water permeability of wt human (h)AQP2 and hAQP2 C181S, in comparison with wt hAQP1 and hAQP1 C189S, cRNAs encoding these proteins were injected into *Xenopus* oocytes. Water permeability measurements revealed that the water transport mediated by hAQP2 and hAQP1 was comparable (Fig. 2). After incubation of the same oocytes in 1 mM $HgCl_2$, the percentage inhibition of water transport was 40 ± 8% (mean ± SE) for AQP2, while the inhibition of water transport was 75 ± 5% for AQP1. Incubation of the same oocytes in 5 mM ß-mercaptoethanol fully restored the water permeability of hAQP2 and hAQP1. Stronger inhibition was observed after incubation for 5 min in 3 mM $HgCl_2$, with the same relative difference in P_f between AQP2 and AQP1 (data not shown). Expression of hAQP1 C189S resulted in a high water permeability, which was unchanged in the presence of 1 mM $HgCl_2$. In contrast, oocytes injected with cRNA coding for hAQP2 C181S revealed a water permeability that was not different from water-injected control oocytes. Because the latter result is totally in contrast to similar studies with rat AQP2 [6,7], cRNAs encoding rat AQP2 C181S or AQP2 C181A were also injected into oocytes. Swelling tests on these oocytes also revealed P_f values that were not different from water-injected control oocytes (Fig. 2).

The absence of water permeability in oocytes injected with cRNA encoding the AQP2 C181 mutants could be caused by the absence of the protein or a disturbed trafficking to the plasma membrane. To confirm the presence of AQP2 and to

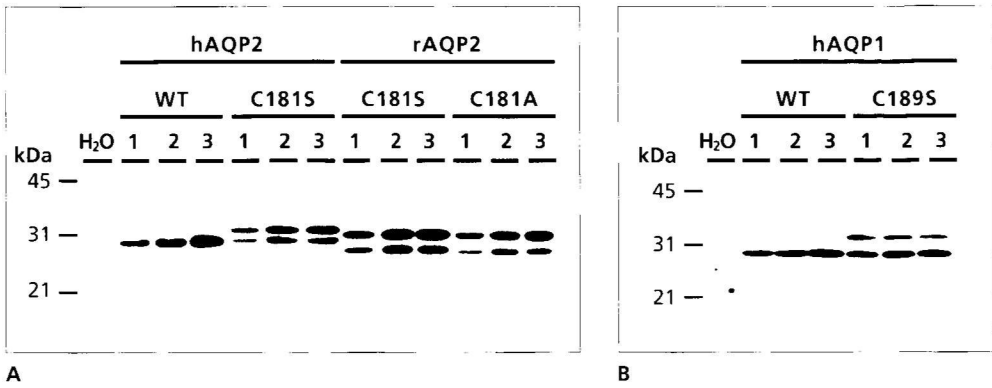

Fig. 3 Immunoblot analysis of oocyte lysates. At 1, 2 and 3 days after injection, lysates were prepared from 8 oocytes injected with water or 10 ng of cRNAs encoding hAQP2, hAQP2 C181S, rAQP2 C181S, rAQP2 C181A, hAQP1 or hAQP1 C189S. Equivalents of 0.1 oocyte were separated by SDS-PAGE and visualized by chemiluminescence. **A** AQP2 proteins were visualized using affinity-purified rabbit polyclonal AQP2 antibodies and anti-rabbit IgG coupled to peroxidase. **B** AQP1 proteins were visualized using monoclonal AQP1 antibodies and anti-mouse IgG coupled to peroxidase.

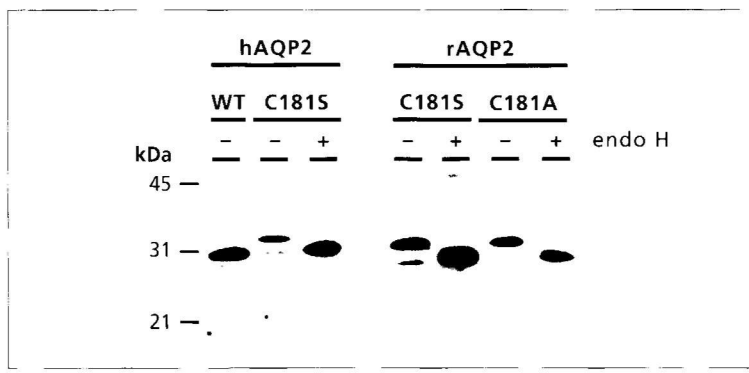

Fig. 4 Immunoblot analysis of oocyte lysates after endoglycosidase H digestion. Lysates of oocytes expressing wt AQP2, hAQP2 C181S, rAQP2 C181S or rAQP2 C181A were incubated in the presence (+) or absence (-) of endoglycosidase H (endo H). Equivalents of 0.1 oocyte were separated by SDS-PAGE and immunoblotted. AQP2 proteins were detected as described in fig. 3.

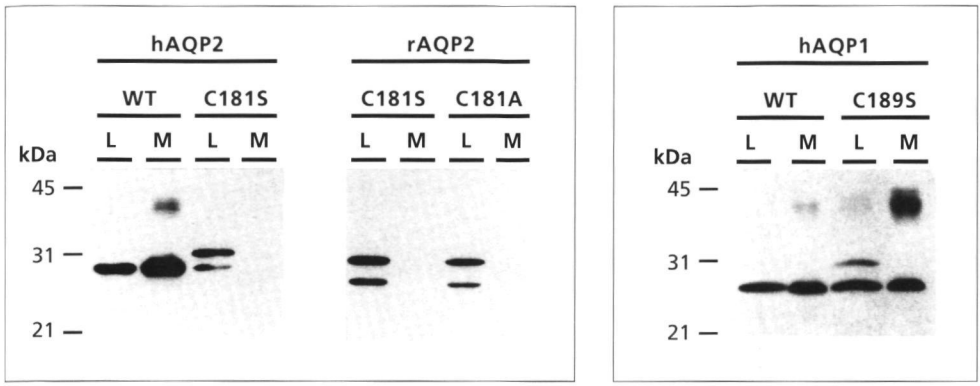

Fig. 5 Immunoblot analysis of oocyte lysates (L) and plasma membranes (M) of AQP2 (**A**) or AQP1 (**B**) expressing oocytes. Three days after injection of 10 ng of cRNAs encoding hAQP2, hAQP2 C181S, rAQP2 C181S, rAQP2 C181A, hAQP1 or hAQP1 C189S, oocyte lysates and plasma membranes were prepared. Equivalents of 0.1 oocyte (L) or 8 oocytes (M) were separated by SDS-PAGE and visualized as described in fig. 3.

determine the stability, oocyte lysates were prepared at 1, 2 and 3 days after injection, and subjected to immunoblotting. Reversible Ponceau red staining showed that comparable amounts of oocyte lysates were loaded (data not shown). Chemiluminescence revealed a band of ~29 kDa in all lanes of oocytes injected with cRNA encoding AQP2, representing the native, unglycosylated form of AQP2 (Fig. 3A). The hAQP2 C181S mutant protein showed, besides the native 29 kDa band, a strong additional band of ~32 kDa. Oocytes expressing rAQP2 C181S or rAQP2 C181A mutants also showed unglycosylated AQP2 and a larger AQP2-specific band, but these bands migrated somewhat faster than the human AQP2 protein (~27 and ~31 kDa) (Fig. 3A).

Immunoblots of oocytes expressing hAQP1 revealed one band of 28 kDa representing the native unglycosylated form of AQP1. Oocytes expressing hAQP1 C189S showed the same native band, and a minor additional band of ~31 kDa (Fig. 3B). Endoglycosidase H (endo H) digestion of oocyte lysates expressing AQP2 proteins and subsequent immunoblotting revealed that the additional bands of hAQP1 C189S (not shown), hAQP2 C181S, rAQP2 C181S and rAQP2 C181A were not detectable anymore (Fig. 4). No AQP1 or AQP2 signals were obtained in lanes loaded with lysates from water-injected oocytes.

To determine the plasma membrane expression of wild-type and mutant aquaporins, a fraction enriched for plasma membranes was subjected to immunoblotting (Fig. 5). Chemiluminescence revealed that wt hAQP2 was clearly present in the plasma membrane, while hC181S, rC181S or rC181A mutant proteins could not be detected in this fraction (Fig. 5A). Wild-type AQP1 and AQP1 C189S were expressed in the plasma membrane to the same extent (Fig. 5B). In the plasma membrane fraction of oocytes expressing AQP1 C189S, a relatively higher amount

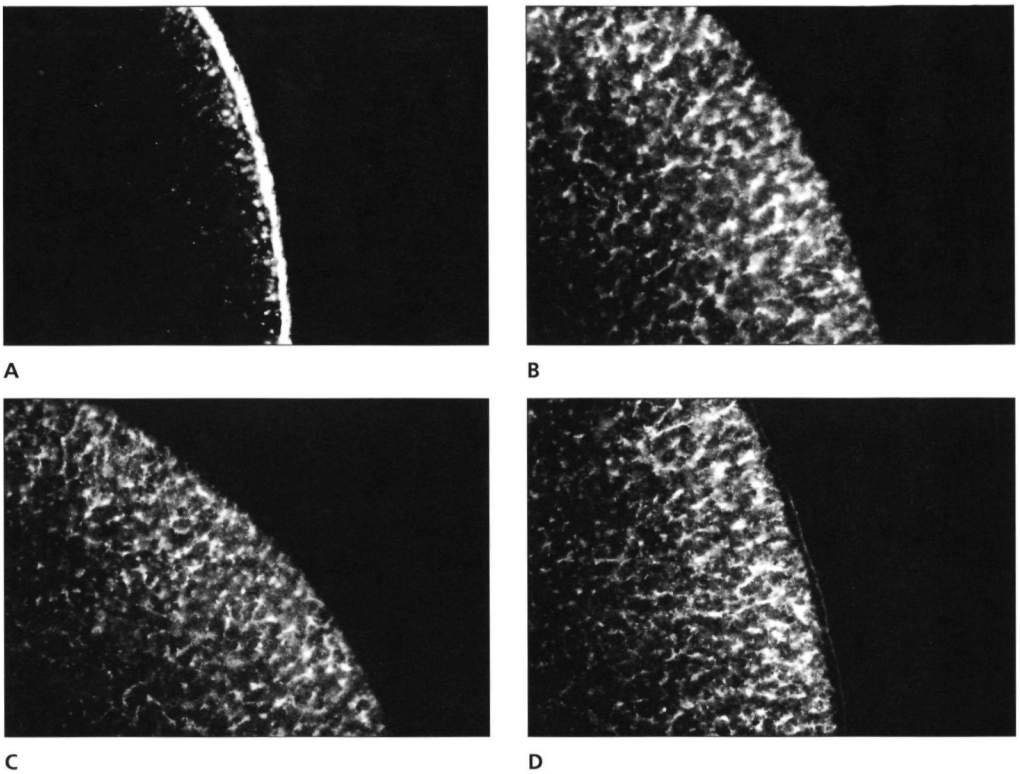

Fig. 6 Sections of oocytes expressing hAQP2 (**A**), hAQP2 C181S (**B**), rAQP2 C181S (**C**) or rAQP2 C181A (**D**). AQP2 proteins were visualized with affinity-purified polyclonal AQP2 antibodies and anti-rabbit IgG conjugated with FITC.

of glycosylated AQP1 (40-45 kDa) was present than in the plasma membrane fraction of wt AQP1.

Immunocytochemical analysis of oocytes expressing wt hAQP2 (Fig. 6A), wt AQP1 (data not shown) or AQP1 C189S (not shown) showed a clear, intense staining of the plasma membrane with a weak staining of the cytoplasm. In contrast, oocytes expressing hAQP2 C181S, rAQP2 C181S or rAQP2 C181A showed an intense staining of the cytoplasm and only a very faint staining of the plasma membrane (Fig. 6B-D). No AQP2 or AQP1 labeling was found in water-injected control oocytes (not shown).

To check the expression system, the water permeability measurements and immunoblots were repeated with oocytes isolated from *Xenopus laevis* from an unrelated source. These experiments yielded identical results (data not shown).

Discussion

To drag NDI-related AQP2 mutants to the plasma membrane of *Xenopus* oocytes to obtain information on the structure-function relationship of AQP2, two requirements had to be fulfilled: 1) Oocytes expressing wt AQP2 should reveal a large decrease in P_f on incubation with mercurials, and 2) The mutation of cysteine 181 to serine in hAQP2 should not affect the expression and function of the protein.

To address the first issue, mercury sensitivity of AQP2 was compared to that of AQP1. Water permeability studies revealed that the P_f values of oocytes expressing hAQP1 or hAQP2 were comparable (Fig. 2), but that the mercury-sensitivity of AQP2 was less than of AQP1 (40% and 70% inhibition, respectively). A full recovery of the water permeability after incubation in ß-mercaptoethanol was found for both AQP1 and AQP2 expressing oocytes indicative of specific mercury inhibition of AQPs rather than toxic effects of mercury chloride.

To address the second requirement, a C181S mutation was introduced into hAQP2. Expression of hAQP2 C181S, however, revealed no increase in P_f, whereas oocytes expressing wt hAQP2, wt hAQP1 or hAQP1 C189S revealed normal, high P_f values. The absence of functional expression for hAQP2 C181S was in complete contrast to the results reported for rat AQP2 C181S [6,7]. To rule out the possibility that a structural difference between human and rat AQP2 causes the discrepancy in functionality, hAQP2 C181S was expressed in parallel with rat AQP2 C181S and C181A mutants. Like hAQP2 C181S, however, both rat mutants did not confer water permeability to oocytes. To address the absence of expression in great detail, the sizes, stability and cellular localization of these mutants were determined (Figs. 3-6).

Immunoblots revealed that hAQP2 C181S, rAQP2 C181S and rAQP2 C181A proteins were as stable as wt AQP2, but were, besides a wt AQP2 protein form, also detected as an endo H-sensitive form (Fig. 3, 4). In the endoplasmic reticulum (ER), chaperones guide the folding of proteins, and misfolding often leads to degradation and/or piling up of intermediates. The presence of endo H-sensitive, high-mannose AQP2 glycoproteins is a clear indication that the proteins are retarded in

the ER, as has been shown for all missense AQP2 proteins involved in NDI [28]. For all three AQP2 mutants, the signal of the ER-retarded form is more intense than the signal of the non-glycosylated form. In contrast, an ER-retarded band is hardly visible on immunoblots of oocytes expressing the functional hAQP1 C189S mutant. This indicates that the severity of the impairment of routing of AQPs is reflected by the relative expression levels of the ER-form and the non-glycosylated form. Immunoblotting of fractions enriched for plasma membranes and immunocytochemistry confirmed the impaired routing of hAQP2 C181S, rAQP2 C181S and rAQP2 C181A to the plasma membrane (Fig. 5, 6). Identical results were obtained in oocytes isolated from *Xenopus laevis* of an unrelated source. Therefore, it is very unlikely that our results are a consequence of the batch of *Xenopi* used. Immunoblots of plasma membranes showed that wt AQP1 and AQP1 C189S are expressed at the plasma membrane at comparable levels. However, the amount of glycosylated AQP1 is higher for the mutated protein. A possible explanation can be that, because AQP1 C189S is somewhat retarded in the ER, more molecules are high-mannose glycosylated in the ER compared with wt AQP1. Since ER-glycosylation is essential for a change to complex glycosylation in the Golgi, a larger portion of the mutant AQP1 is consequently glycosylated.

Our results clearly show that in oocytes, human AQP2 C181S, rat AQP2 C181S and rat AQP2 C181A are not functional because they are severely disturbed in their routing to the oolemma. The misrouting of hAQP2 C181S precluded our goal to use this mutation in AQP2 to discriminate between water permeability conferred by a truncation mutant and NDI-related AQP2 mutants. In addition, the water permeability obtained for rat C181S and C181A by Bai *et al.* [6,7], was of critical importance for their conclusion that the water pore in AQP2 is different from the one in AQP1. They concluded that loops C and D are located near the pore in AQP2 and loops B and E are not of critical importance in AQP2 as in AQP1. Our results with their clones and human AQP2 C181S makes this conclusion at least doubtful.

In conclusion, our results show that water transport through AQP2 is less sensitive to mercury inhibition than through AQP1 and that substitution of the cysteine residue in loop E for a serine completely disturbs proper folding, assembling and/or routing of human and rat AQP2, whereas the same mutation has no effect on AQP1. This suggests that mutations in AQP1 are better tolerated than in AQP2, and thus that AQP1 and AQP2 might differ in their tertiary structure.

Acknowledgments

We thank M. de Jong for the isolation of oocytes.

Chapter 6

Dominant autosomal nephrogenic diabetes insipidus caused by a mutation in the C-terminus of AQP2.

Sabine M. Mulders •
Daniel G. Bichet ••
Johan P.L. Rijss •
Erik-Jan Kamsteeg •
Marie-Françoise Arthus ••
Michele Lonergan ••
Mary Fujiwara •••
Kenneth Morgan ••••
Carel H. van Os •
Peter M.T. Deen •

• Department of Cell Physiology, University of Nijmegen, The Netherlands.
•• Unité de Recherche Clinique, Centre de Recherche et Service de Nephrologie, Université de Montréal, Québec, Canada.
••• Departments of Human Genetics, Medicine and Pediatrics, and
•••• Departments of Human Genetics and Medicine, McGill University, Montreal, Quebec, Canada.

submitted

Summary

Mutations in the gene coding for AQP2 are known to cause autosomal recessive NDI. Here, we report for the first time a patient of a family with an autosomal dominant form of NDI which is also caused by a mutation in the AQP2 gene. A point mutation (G866A) in only one allele causes a substitution of a lysine for a glutamic acid in the C-terminal tail of AQP2 at position 258 (E258K), which is 2 amino acids downstream of the protein kinase A phosphorylation site S256 of AQP2. To address the molecular cause of dominant NDI in this patient, we studied the function and routing of AQP2-E258K in *Xenopus* oocytes in parallel with AQP2-S256A and a truncated AQP2 protein (AQP2-R253*). Compared to wild-type (wt) AQP2, AQP2-E258K conferred a small, but significant increase in water permeability (P_f) to oocytes, whereas the P_f of AQP2-S256A or AQP2-R253* expressing oocytes was similar to wt AQP2. With co-expression, AQP2-E258K did not affect the P_f generated by wt AQP2. Immunoblots of oocyte lysates and plasma membranes revealed that all three mutants were not retarded in the endoplasmic reticulum (ER) and were as stable as wt AQP2, but the plasma membrane expression of AQP2-E258K was reduced. Immunocytochemistry showed some AQP2-E258K expression in the plasma membrane, but the majority was located just underneath the plasma membrane, presumably in a golgi or post-golgi compartment. The E258K mutant protein was phosphorylated as wt AQP2, whereas AQP2-S256A was not phosphorylated. AQP2-S256A and AQP2-R253* expressing oocytes showed strong signals in the plasma membrane, but also some staining below this membrane. These differences in localization were supported by subcellular fractionation of oocytes. Because AQP2-R253* lacks the region where the E258K mutation is found, but is hardly impaired in its routing, the E258K mutation presumably does not change an existing AQP2 routing signal, but rather introduces a retention signal. In conclusion, AQP2-E258K does not impair phosphorylation of S256, but is retarded in the golgi or a post-golgi compartment. Since AQPs are thought to tetramerize in the ER or golgi, the retention of AQP2-E258K and the consequent retardation of wt AQP2 proteins in a post-ER compartment, provides a good explanation for the dominant inheritance of NDI in this family.

Introduction

In kidney, water transport through specialized channels, called aquaporins, plays an important role in reabsorption of water and in concentration of urine. At least four different aquaporins participate in these processes (AQP1 through 4) [44,55,68,74,98,140], but so far, only one water channel, AQP2, has been shown to be essential [31]. AQP2 is uniquely localized to subapical vesicles in principal cells of the collecting duct [55]. Upon binding of vasopressin (AVP) to the V_2 receptor at the basolateral side of the cell, intracellular cAMP levels increase, resulting in phosphorylation of AQP2 by protein kinase A (PKA). Subsequently, vesicles containing the AQP2 water channels fuse with the apical membrane. Upon removal of AVP, AQP2 is internalized by endocytosis [79,106,122,149,191].

Nephrogenic diabetes insipidus (NDI) is a disease that is characterized by the inability of the kidney to concentrate urine in response to AVP. Until recently, two inheritance patterns for this disease had been described. The X-linked form of NDI has been shown to be caused by mutations in the AVPR2 gene, coding for the V_2 receptor [147,173]. We have shown that the autosomal recessive form of NDI is caused by mutations in the AQP2 gene [31]. In *Xenopus* oocytes, mutant AQP2 proteins as encoded in this form of NDI were shown to be retarded in the endoplasmic reticulum (ER) and therefore impaired in their routing to the plasma membrane [28,116].

Recently, it has been described that NDI can also segregate in an autosomal dominant trait [10]. In this paper, we report that in NDI patients from a family, in which NDI segregates in a dominant fashion, the disease is caused by a missense mutation in the C-tail of AQP2. This surprising finding implies interference of a mutant AQP2 protein with proper functioning of unaffected AQP2 proteins. In order to delineate the molecular cause of NDI in these patients, we investigated the expression and routing of this mutant AQP2 protein in *Xenopus* oocytes.

Methods

Patients

The proband (436) is a 37 year old female patient with congenital nephrogenic diabetes insipidus and a 24-hour urinary output of 10 to 12 liters (164 ml/kg of body weight/24 hours). She had a documented lifelong history of polyuria and polydipsia and normal or elevated plasma concentrations of arginine-vasopressin. Her daughter (724), born in 1985, progressively showed increased polyuric-polydipsic symptoms and her 24 hours urinary output was recently measured at 6 liters (136 ml/kg of body weight/24 hours). dDAVP infusion studies were carried out as described before (0.3 μg/kg of body weight infused in 20 min)[13] (Table 1).

Genetic analysis

The AVPR2 gene of the proband and her daughter was sequenced with methods previously described [11,12]. The AQP2 gene of all the family members was amplified and sequenced using a primer 5' to the coding region of exon 1 (forward primer 5'-GCGAGAGCGAGTGCCCG-3') and a reverse primer flanking the cod-

ing region of exon 4 except for the terminal three codons (reverse primer 5'-GCG-GCCCTCAGGCCT-3'), followed by a second amplification, using the reverse primer flanking exon 4 and a forward primer flanking exon 4 (5'-GATTAAT-GTCGGGGAGGAGG-3'). Manual sequencing was done as previously described [11]. A G866A transition was identified, resulting in a E258K substitution, which correlated perfectly with the polyuric phenotype. Haplotype analysis was carried out using AQP2 flanking markers [89].

* *DNA constructs and transcription*

To introduce the E258K mutation in an AQP2 expression construct (pT7TsAQP2) [31], the G866A transition was introduced in the human AQP2 cDNA using the Altered sites II *in vitro* mutagenesis kit (Promega, Madison. WI), with the following forward primer: 5'-CGGCAGTCGGTGAAGCTTCACTCGCCGCAG-3'. Besides the G866A transition, this primer introduces a G to T transition at position 871. In this way, a *Hin*dIII restriction site is created close to the mutation, without changing the amino acid sequence. A *Nar*I- *Kpn*I fragment of 174 bp, containing the transitions, was isolated by gel electrophoresis and inserted into the corresponding sites of pT7TsAQP2.

Using the same technique, an AQP2-S256A mutant was made by introduction of a T860G transition in the AQP2 cDNA (forward primer 5'-GACGGCGGCAGGCG-GTGGAGCTGC-3'). Next, a 282 bp *Bam*HI-*Kpn*I fragment was isolated by gel electrophoresis and inserted into the corresponding sites of pT7TsAQP2.

A truncated AQP2, AQP2-R253*, was created by digestion of pT7TsAQP2 with *Bsg*I and *Kpn*I. Subsequently, the sites were blunt ended with T4 DNA polymerase, and ligated. In this way, the nucleotide sequence coding for all amino acids of AQP2 following R253 was deleted, except for the final amino acids K270 and A271. The AQP2-R187C construct was as described previously [31]. Clones that were identical to the wt AQP2 nucleotide sequence except for the transitions or deletions were selected by restriction analysis and subsequent sequence analysis [63].

The obtained pT7TsAQP2 constructs were linearized by *Sal*I and capped RNA transcripts were synthesized *in vitro* using T7 RNA polymerase according to Promega's (1991) Protocols and Principles guide, except that 1 mM final concentrations of nucleotidetriphosphates and 7-methyl-di-guanosine triphosphate were used. The cRNAs were purified and dissolved in DEPC-treated water. The integrity of the cRNAs was checked by agarose gel electrophoresis and their concentrations were determined spectrophotometrically.

* *Water permeability*

Oocytes were isolated from *Xenopus laevis*, and defolliculated by digestion at room temperature for 2 hours with collagenase A (2 mg/ml, Boehringer, Mannheim, Germany). Stage V and VI oocytes were selected and incubated at 18°C in modified Barth's solution (MBS) supplemented with gentamycine (50 μg/ml) [31]. The day after isolation, oocytes were injected with 5 ng to 10 ng of cRNA, and analyzed after two or three days in a swelling assay as described before [31]. Oocyte swelling was performed at 22°C following transfer from 200 mosM to 20 mosM (for the AQP2-E258K mutant) or 200 mosM to 70 mosM (for other AQP2 proteins).

• *Immunoblotting*

At three days after injection, oocyte lysates were prepared by homogenization of 8 oocytes in 160 µl homogenization buffer A (HbA: 20 mM Tris (pH 7.4), 5 mM $MgCl_2$, 5 mM $NaHPO_4$, 1 mM EDTA, 1 mM DTT, 1 mM phenylmethylsulfonylfluoride, 5 µg/ml leupeptin and pepstatin, 80 mM sucrose) at 4°C. Subsequently, the lysates were centrifugated twice for 10 min at 125g to remove yolk proteins. At the same day, a fraction enriched for plasma membranes was isolated from 25 oocytes according to Wall and Patel [184].

Lysates or plasma membranes equivalent to 0.1 oocyte or 8 oocytes, respectively, were denatured for 30 min at 37°C in sample buffer (2% SDS, 50 mM Tris (pH 6.8), 12% glycerol, 0.01% Coomassie Brilliant Blue, 100 mM DTT), subjected to 12% SDS-PAGE electrophoresis [86] and transferred to a nitrocellulose membrane as described [31]. Efficiency of protein transfer was checked by staining the membrane with Ponceau Red. For immunodetection, the membrane was incubated with a 1:10,000 dilution of an affinity-purified polyclonal antibody directed against the 15 C-terminal amino acids of rat AQP2 [28] (AQP2:257-271), or with affinity-purified antibodies directed against the E loop and C-terminal tail of AQP2 (AQP2:175-269). This antibody was obtained in the following way: a 282 bp *Bam*HI-*Kpn*I fragment of AQP2 was cloned in frame behind the cDNA for glutathion S-transferase (GST) in the expression vector pGEX-3X (Pharmacia Biotech, Uppsala, Sweden) and transfected to DH5α bacteria. Expression from this construct was induced by IPTG and the resulting fusion-protein was isolated. Rabbits were primed with 400 µg of the fusion protein in Freund's adjuvant. After 3 weeks, rabbits were boosted with 200 µg of fusion protein in incomplete Freund's adjuvant, which was repeated until the titer of the rabbit serum was sufficiently high. Antibodies were affinity-purified by passing the serum through an Affi-gel 15 column (Pharmacia Biotech) of a lysate of DH5α bacteria expressing GST followed by a column on which the fusion protein was immobilized. Antibodies were eluted with 0.1 M glycine (pH 2.8) and directly neutralized. As a secondary antibody, a 1:5,000 dilution of affinity-purified goat-anti-rabbit IgG conjugated to horse radish peroxidase (Sigma Immuno Chemicals, St. Louis, MO) was used. Proteins were visualized using enhanced chemiluminescence (Boehringer Mannheim, Germany).

• *Immunocytochemistry*

At 3 days after injection, remaining vitelline membranes were removed and oocytes were incubated for 1 hour in 1% (wt/vol) paraformaldehyde fixative (PLP) [110], dehydrated, and embedded in paraffin. After blocking with 10% goat serum in Tris-buffered saline (TBS), the sections were incubated O/N at 4°C with the affinity-purified polyclonal antibody AQP2:175-269, diluted 1:500 in 10% goat serum in TBS. After three washes for 10 min in TBS, the sections were incubated for 1 hour in a 1:100 dilution of goat-anti-rabbit IgG coupled to fluorescein isothiocyanate (FITC) (Sigma Immuno Chemicals). The sections were again washed three times for 10 min in TBS, dehydrated by washing in 70% to 100% ethanol and mounted in mowiol 4-88, containing 2.5% NaN_3. Photographs were taken with a Zeiss Axioskop with epifluorescent illumination with an automatic camera using Kodak EPH P1600X films.

- *^{35}S labeling of AQP2 in oocytes*

Directly after injection of 10 ng cRNA encoding wt AQP2, AQP2-E258K, AQP2-S256A or a co-injection of 5 ng wt AQP2 and 5 ng AQP2-E258K cRNA, 12 oocytes were incubated in 0.5 ml MBS containing 45 µCi TRAN^{35}S label (specific activity 1380 Ci/mmol; ICN Pharmaceuticals, Irvine, CA). The day after injection, the medium was replaced. Two days after injection, 10 oocytes were homogenized in 100 µl HbA and oocyte lysates were prepared (see above).

- *Phosphorylation and immunoprecipitation of AQP2*

Two days after injection, 10 oocytes were homogenized in 100 µl HbA, and 10 oocytes were homogenized in 100 µl HbA without $NaHPO_4$. Of this latter homogenate, proteins were phosphorylated for 30 minutes at room temperature in the presence of 5 mU of the catalytic subunit of protein kinase A (Boehringer Mannheim, Germany), $5x10^{-5}$ M forskolin, $1x10^{-6}$ M cAMP and 20 µCi [γ^{32}P]-ATP (Amersham Life Sciences, Buckinghamshire, UK). Of both batches, oocyte lysates were prepared as described above.

For immunoprecipitation, 10 µl of 10% sodium dodecyl sulphate (SDS) was added to both these lysates and that of oocytes labelled with ^{35}S methionine, and samples were incubated for 30 minutes at 37°C. Next, the lysates were centrifugated at 14.000 rpm for one minute at 4°C, and the supernatant was diluted 10x with IPP100 (10 mM Tris pH 8.0, 100 mM NaCl, 0.1% NP-40, 0.1% Tween-20).

10 µl protein A agarose beads (Kem-En Tec, Copenhagen, Denmark) was washed three times with IPP500 (10 mM Tris pH 8.0, 500 mM NaCl, 0.1% NP-40, 0.1% Tween-20) and rotated O/N at 4°C in 500 µl IPP500 containing 3 µl of the polyclonal antibody AQP2:257-271 [28]. The beads were washed by rotation for 30 minutes at 4°C with fresh IPP500, followed by three short washes in IPP500 and one wash with IPP100. Lysate samples, equivalent to 2 oocytes for ^{35}S methionine- or non-labelled oocytes, or 4 oocytes for the ^{32}P labelled oocyte homogenates, were added to the beads and rotated for 2 hours at 4°C. Subsequently, the beads were washed three times with IPP100. After the last wash, the beads incubated with the labelled proteins were resuspended in sample buffer (see above). The beads incubated with the untreated proteins were resuspended in 100 µl HbA without $NaHPO_4$ and phosphorylated as described above. Next, these beads were also washed three times with IPP100 and resuspended in sample buffer. All samples were incubated for 30 minutes at 37°C, loaded on a 12% acrylamide gel and electrophoresed. The gel was stained (0.25% (wt/vol) Coomassie Brilliant Blue, 50% (vol/vol) methanol, 10% (vol/vol) acetic acid), destained (25% (vol/vol) methanol, 7% (vol/vol) acetic acid), dried, and exposed to a film with an intensifying screen at -80°C.

- *Fractionation*

The fractionation of oocytes was performed according to Pralong-Zamofing *et al.* [138]. Three days after injection of 10 ng cRNA encoding wt AQP2, AQP2-E258K, AQP2-S256A or AQP2-R187C, 80-100 oocytes were homogenized in 1 ml of cold buffer A (250 mM sucrose, 1 mM EDTA, and 10 mM Tris-HCl pH 7.5, supplemented with 10 mM PMSF and 5 µg/ml pepstatin and leupeptin). The homogenate was centrifugated twice at 1,000 g for 10 minutes to remove yolk proteins. The

Time (minutes)	-60	-30	0*	30	60	90	120	150	180
Patient 436 (proband)	113	132	76	92	–	366	351	355	180
Patient 724 (daughter)	112	99	92	156	–	375	222	–	158
nine patients with AVPR2 mutations	–	–	96 ±12	–	117 ±12	–	116 ±10	–	110 ±11
three patients homozygous for AQP2 mutations	94 ±4	92 ±6	93 ±6	94 ±6	100 ±6	96 ±6	94 ±6	92 ±6	100 ±6

Table 1 Urinary osmolality measurements (in mmol/kg H_2O) before and after dDAVP infusion in patients with nephrogenic diabetes insipidus. (* dDAVP was infused from 0 to 20 minutes)

supernatant was layered on a 9 ml linear 12-50% sucrose gradient and centrifuged in a Beckmann SW40 Ti rotor for 4 hours at 165,000 g at 4°C. After centrifugation, the top 1.4 ml of the gradient was removed and 12 fractions of 0.7 ml were collected. These fractions were diluted with buffer A to 10 ml and membranes were collected by centrifugation for 3 hours at 228,000 g in a Beckmann Ti70 rotor at 4°C. The membrane pellets were taken up in 40 µl buffer A without sucrose and 10 µl of each sample was prepared for immunoblotting. After blotting, immunodetection was performed using the affinity-purified polyclonal antibody AQP2:257-271.

Results

From the proband (436) and her affected daughter (724) (Fig. 1), whose family history of NDI indicated an autosomal dominant form of inheritance, the V_2 receptor gene (AVPR2) was sequenced, since mutations in AVPR2 are frequent and AQP2 mutations are rare, and since their NDI could be caused by skewed inactivation of the normal AVPR2 allele. However, no mutations in AVPR2 were found. Subsequently, the AQP2 gene of all family members was sequenced. In one allele of the AQP2 gene of the proband, a point mutation in exon 4 was found. This G866A transition in exon 4 leads to a substitution of a lysine for a glutamic acid at position 258 (E258K). The same mutation was found in one allele of the AQP2 gene of the affected daughter. The other members of the family appeared to be homozygous for the normal allele. During dDAVP infusion studies both patients transiently increased their urinary osmolalities to ~350 mmol/kg H_2O (Table 1). In patients with X-linked nephrogenic diabetes insipidus (AVPR2 mutations) or patients with autosomal recessive nephrogenic diabetes insipidus (AQP2 mutations), the urine osmolality stayed below 150 mmol/kg H_2O (Table 1). All the members of the family presented here were examined and tested and no other patients demon-

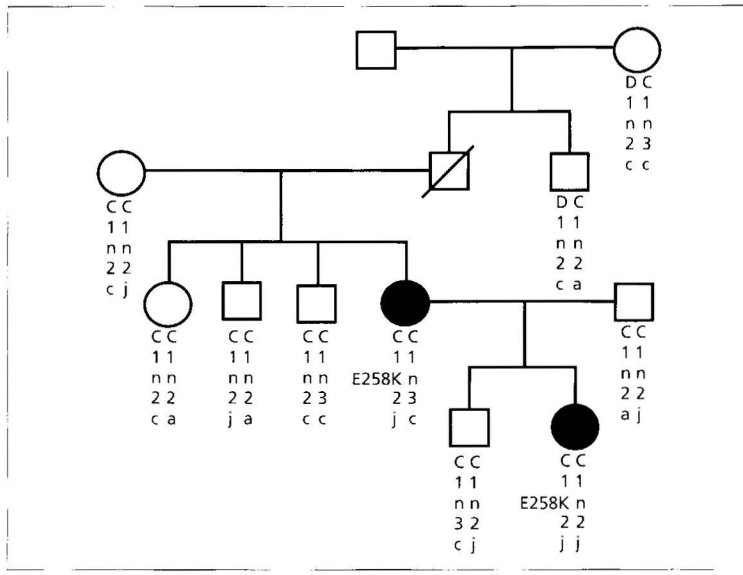

Fig. 1 Pedigree with an autosomal dominant inheritance of nephrogenic diabetes insipidus. The two solid symbols indicate the two affected patients heterozygote for the E258K mutation. The 12q13 haplotype is represented and the marker order: centromere-Col2A1-AFM259vf9-AQP2-D12S131-AFMb007yg5-telomere has been determined in Dr. Kucherlapati's laboratory [89].

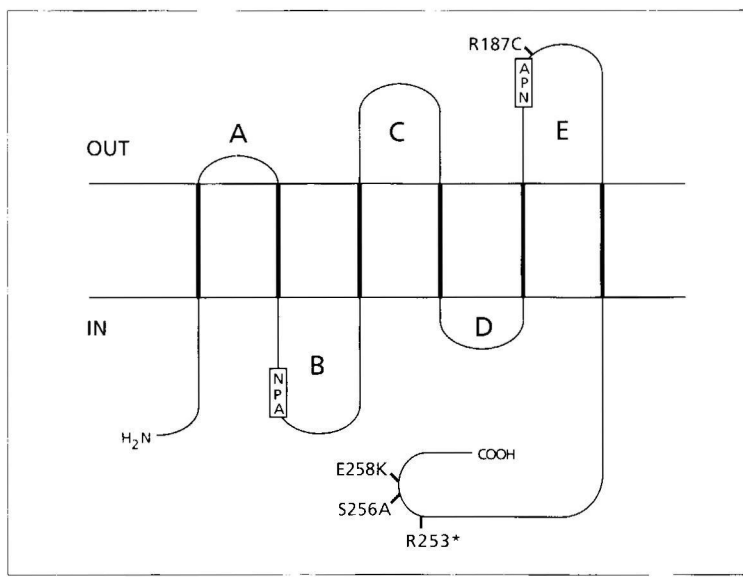

Fig. 2 Proposed membrane topology of AQP2. Indicated are the amino acid substitution causing the dominant form of NDI (E258K), the phosphorylation mutant S256A, the truncation mutant R253*, and the mutant R187C found in recessive NDI.

strated polyuric-polydipsic symptoms. Haplotype analysis using AQP2 flanking markers revealed that G866A was a *de novo* mutation which occurred on the maternal haplotype (mother of the proband) (Fig. 1).

We next tried to address the molecular cause of NDI in these patients. The E258K mutation is located 2 residues downstream from serine 256, the residue which is phosphorylated upon stimulation of collecting duct cells by AVP [85]. In an LLCPK-1 cell model, it was shown that phosphorylation of this serine is critical for vesicles containing AQP2 to fuse with the plasma membrane upon activation by forskolin [54,78]. To find out whether distorted phosphorylation of S256 in the AQP2-E258K mutant might explain the NDI phenotype in these patients, three mutant AQP2 proteins (Fig. 2) were analyzed in *Xenopus* oocytes: 1) AQP2-E258K, the AQP2 mutant encoded in the NDI patient; 2) AQP2-S256A, in which the protein kinase A phosphorylation site S256 was changed into an alanine; 3) AQP2-R253*, which lacks the C-terminus of AQP2 following arginine 253, except for the last two amino acids. cRNA transcripts from corresponding expression constructs were injected into *Xenopus* oocytes. Three days after injection, water permeabilities of wt AQP2, AQP2-S256A and AQP2-R253* were not significantly different from each other (Fig. 3). However, the P_f of oocytes expressing the E258K mutant was low, but still significantly higher than of water-injected control oocytes (Fig. 3).

Co-injection of 10 ng of wt AQP2 cRNA and 10 ng of AQP2-E258K cRNA (WT+EK 10+10) revealed that the P_f of oocytes expressing both proteins was higher than the P_f of oocytes injected with 10 ng of wt cRNA alone, indicating that a dominant negative effect of the AQP2-E258K protein on the function of wt AQP2 is not observed in oocytes (Fig. 4). To rule out the possibility that the dominant negative effect of the E258K mutant is obscured due to the high expression levels of these proteins, oocytes were co-injected with smaller amounts of cRNA. However, even in oocytes which were injected with 10 ng of cRNA encoding AQP2-E258K and only 1 ng of cRNA encoding wt AQP2, or with 1 ng of cRNA from both constructs, no dominant negative effect was observed, because water permeabilities of these oocytes were higher or similar compared to those of oocytes injected with 1 ng of wt AQP2 cRNA only (Fig. 4).

Immunoblotting of lysates from oocytes injected with 10 ng of cRNA encoding wt AQP2, AQP2E258K, AQP2-S256A, AQP2-R253*, or 5 ng of both wt AQP2 cRNA and AQP2-E258K cRNA, revealed that equal amounts of protein were expressed (Fig. 5A). The wt and missense AQP2 proteins run at a size of 29 kDa, whereas AQP2-R253* is ~2 kDa smaller because this protein lacks 16 amino acids of the C-terminal tail. No signal was obtained in the lane loaded with lysates from non-injected control oocytes. To determine the plasma membrane expression of wild-type and mutant AQP2 proteins, plasma membranes were isolated from oocytes and subjected to immunoblotting (Fig. 5B). AQP2-S256A, AQP2-R253*, and wt AQP2 expressing oocytes showed a comparable level of expression at the plasma membrane, but the expression of the E258K mutant was much lower. Control oocytes were negative for AQP2.

To determine the subcellular localization of the mutant AQP2 proteins, immunocytochemistry was performed on paraformaldehyde-fixed oocytes (Fig. 6). Oocytes

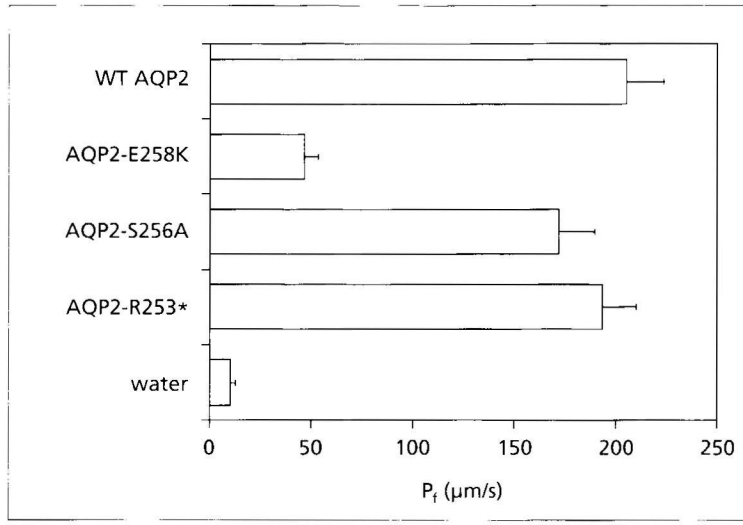

Fig. 3 Osmotic water permeability (P_f) of oocytes. Three days after injection of water or 10 ng of cRNA encoding wt AQP2, AQP2-E258K, AQP2-S256A or AQP2-R253*, water permeabilities were measured in a standard swelling assay. Mean and SE of at least 40 oocytes from 4 different experiments are shown.

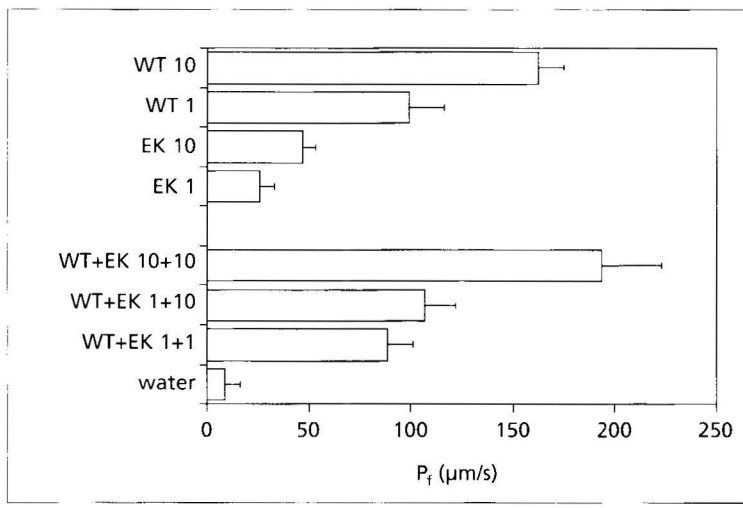

Fig. 4 Osmotic water permeability (P_f) of oocytes. Three days after injection of water or the indicated amounts of cRNA encoding wt AQP2 and/or AQP2-E258K (10 ng, 1 ng, 10+10 ng, 1+10 ng or 1+1 ng) water permeabilities were measured in a standard swelling assay. Shown are mean ± SE of at least 10 oocytes.

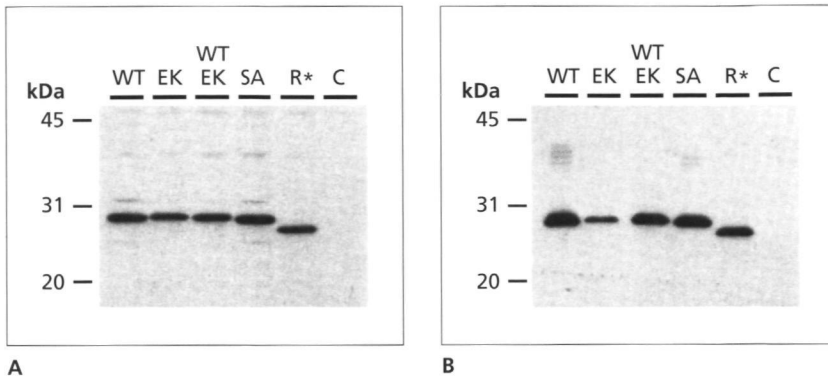

Fig. 5 Immunoblot analysis of AQP2 proteins from oocyte lysates (A) or plasma membranes (B). **A** At three days after injection, lysates were prepared from 8 oocytes injected with water (c) or 10 ng of cRNA encoding wt, E258K, wt+E258K (5 ng each), S256A, or R253* AQP2. Equivalents of 0.1 oocyte were separated by SDS-PAGE and blotted. **B** Plasma membranes were prepared three days after injection of oocytes injected with water or cRNA encoding wt, E258K, wt+E258K (5 ng each), S256A, or R253* AQP2. Equivalents of 8 oocytes were separated by SDS-PAGE and immunoblotted. AQP2 proteins were visualized by chemiluminescence using AQP2 antibodies as a first antibody and anti-rabbit IgG, conjugated to peroxidase, as a second antibody.

expressing wt AQP2 showed a clear, intense staining of the plasma membrane. In contrast, in oocytes expressing the AQP2-E258K mutant protein only a very faint plasma membrane staining was detectable, whereas most of the protein was confined to a cytoplasmic region just underneath the plasma membrane. Oocytes expressing AQP2-S256A or AQP2-R253*, show a distinct staining of the plasma membrane, but it is clear that part of these mutant proteins is also expressed just below the plasma membrane. Non-injected oocytes showed no staining with the AQP2 antibody.

To investigate whether phosphorylation of S256 was affected by the E258K mutation, phosphorylation experiments were performed with oocytes injected with 10 ng of cRNA encoding wt AQP2, AQP2-E258K, or AQP2-S256A, and in oocytes injected with both 5 ng of wt AQP2 cRNA and 5 ng of AQP2-E258K cRNA (wt+EK). First, the efficiency of immunoprecipitation of these AQP2 proteins was tested. To this end, oocytes were incubated in MBS containing ^{35}S-labeled methionine directly after cRNA injection, to radiolabel all newly synthesized proteins. After two days of incubation, AQP2 proteins were immunoprecipitated and separated on an acrylamide gel. Fig. 7A shows that the efficiency of immunoprecipitation of wt AQP2, AQP2-E258K, AQP2 wt+EK, and AQP2-S256A was similar. To determine whether the E258K mutation interferes with phosphorylation of S256 and to exclude possible differences in extent of phosphorylation because of differences in compartimentalisation of the AQP2 proteins in oocytes, AQP2 proteins from oocytes of one batch were phosphorylated directly after homogenization, or after immunoprecipitation. Fig. 7B shows that phosphorylation of wt AQP2,

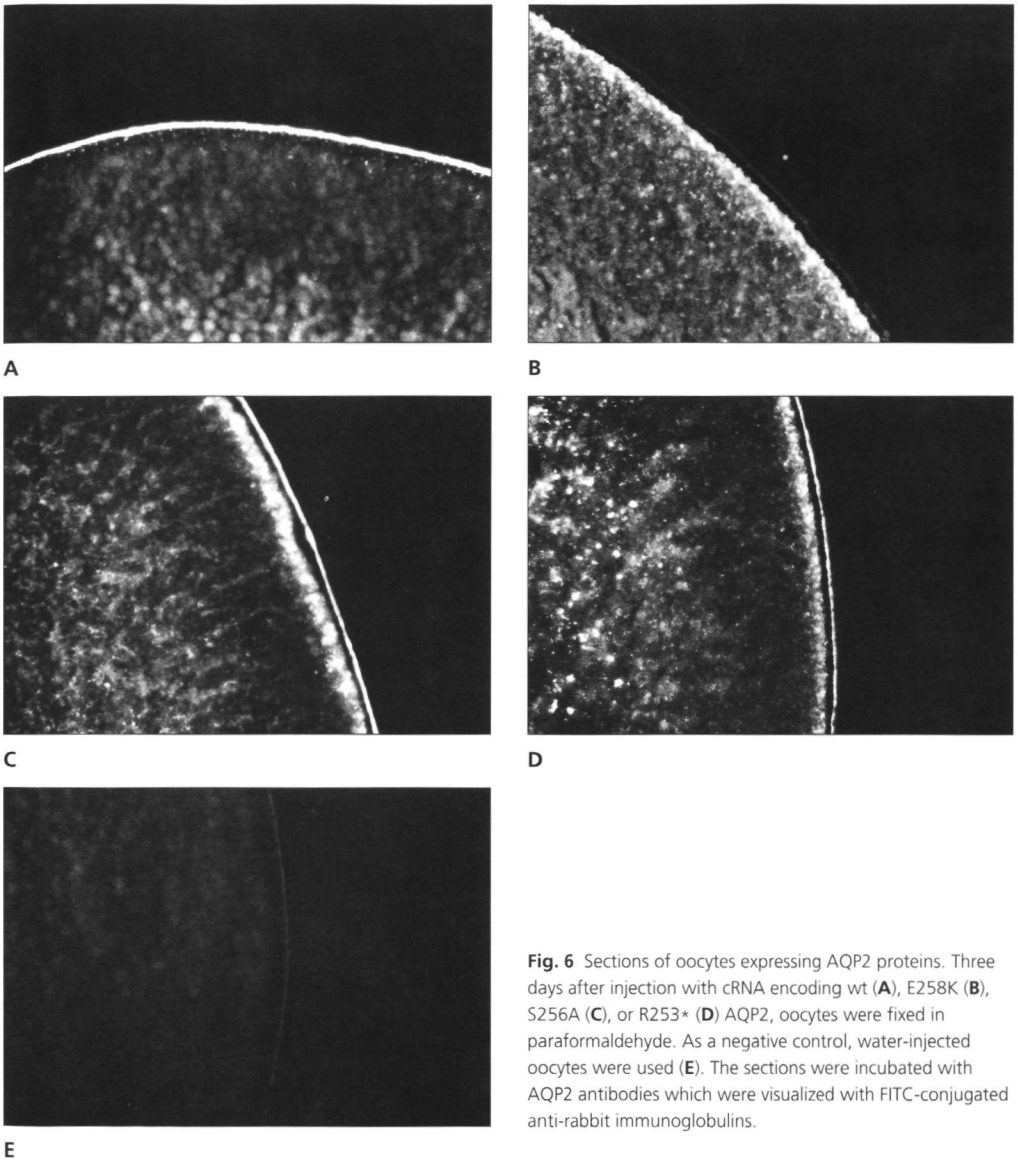

Fig. 6 Sections of oocytes expressing AQP2 proteins. Three days after injection with cRNA encoding wt (**A**), E258K (**B**), S256A (**C**), or R253* (**D**) AQP2, oocytes were fixed in paraformaldehyde. As a negative control, water-injected oocytes were used (**E**). The sections were incubated with AQP2 antibodies which were visualized with FITC-conjugated anti-rabbit immunoglobulins.

AQP2-E258K, and AQP2 wt+EK in the oocyte homogenate was identical, and as expected, AQP2-S256A was not phosphorylated. Fig. 7C shows that phosphorylation of wt AQP2, AQP2 wt+EK, and AQP2-E258K after immunoprecipitation yields similar results. The radioactive band around 45 kDa is visible in all lanes and most likely reflects phosphorylated immunoglobulins.

To further corroborate the different subcellular localization of wt AQP2, AQP2-S256A, AQP2-E258K, and AQP2-R187C, a mutant AQP2 reported previously in a patient with autosomal recessive NDI [28,31], oocytes expressing these proteins were fractionated in a 12-50% sucrose gradient. Fig. 8 shows the distribution of AQP2 over 12 fractions of the sucrose gradient. Wild-type AQP2 protein was not present in the first 3 fractions. In fraction 4 a small amount of protein was detectable, the amount of AQP2 peaked in fraction 7 and 8, and decreased towards the higher density fractions. AQP2-E258K and AQP2-S256A are present in all fractions of the gradient, except for fraction 1 and 12 for the S256A mutant. The amount of AQP2-E258K protein, but not AQP2-S256A, is highest in fractions 5 through 8. AQP2-R187C, which has been shown to be ER-retarded [28], is only present in fractions 6, 7 and 8 (Fig. 8). The middle band constitutes the 29 kDa AQP2 band, the upper band represents the ER-retarded form of AQP2 [28].

Discussion

Recently, we have shown that mutations in the AQP2 gene cause the autosomal recessive form of NDI [31,116,178]. Here, we report for the first time that the autosomal dominant form of inheritance of NDI is also caused by a mutation in the AQP2 gene. Sequence analysis of the AQP2 genes of the family of the patient showed that the affected patient and her daughter carried one mutated allele, coding for a E258K-substituted AQP2 protein, whereas non-affected family members were homozygous for the wild-type allele (Fig. 1). Interestingly, all mutations in AQP2 reported in recessive NDI are located in between the first and last transmembrane domain. In contrast, the new mutation in dominant NDI is located in the C-terminal tail. This suggests a relationship between the site of mutation and the inheritance pattern. As shown for other diseases, a dominant form of inheritance occurs when a mutant protein oligomerizes with other subunits of a functional complex and disturbs the routing or just the function of the complex. Aquaporins are known to oligomerize and are present in the plasma membrane as homotetramers [161,180] and it has been shown that the monomeric form acts as the functional unit [174]. Therefore, the dominant action of AQP2 mutants in NDI can only be explained if 1) the mutant is able to oligomerize with wild-type AQP2 and 2) the complex is disturbed in its routing after oligomerization.

Swelling tests of oocytes expressing AQP2-E258K revealed a low water permeability, which was higher than that of water-injected control oocytes (Fig. 3). Immunoblots of lysates of oocytes revealed that AQP2-E258K was as stable as wt AQP2, and that this mutant was present as a single band of 29 kDa, representing the native form of AQP2 (Fig. 5A). The immunoblots of plasma membranes, however, showed that the reduced P_f of this mutant was caused by an impaired routing,

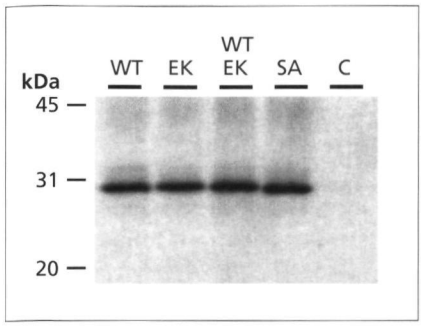

A

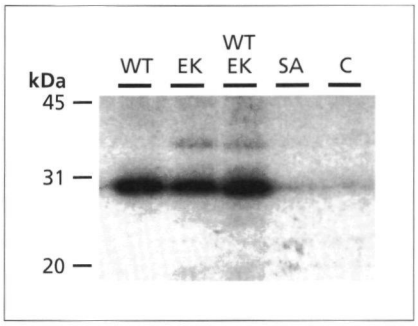

B

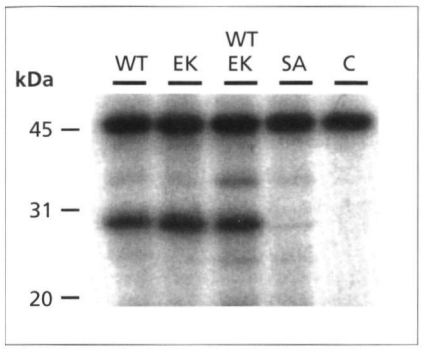

C

Fig. 7 Immunoprecipitation and phosphorylation of AQP2 proteins. Oocytes were injected with water (c), or 10 ng of cRNA encoding wt, E258K, or S256A AQP2, or 5 ng of both wt AQP2 and AQP2-E258K cRNA. **A** After injection, newly synthesized proteins were metabolically labeled with ^{35}S-labeled methionine for two days. Next, oocytes were homogenized and ^{35}S labeled AQP2 proteins were immunoprecipitated with an AQP2 antibody and subjected to SDS-PAGE. **B** Two days after injection, oocytes were homogenized and proteins were labeled with [γ^{32}P]-ATP and PKA. AQP2 proteins were immunoprecipitated and samples were separated by SDS-PAGE. **C** Two days after injection, oocytes were homogenized and AQP2 proteins were immunoprecipitated. After immunoprecipitation, AQP2 proteins were phosphorylated using [γ^{32}P]-ATP and PKA, and separated by SDS-PAGE.

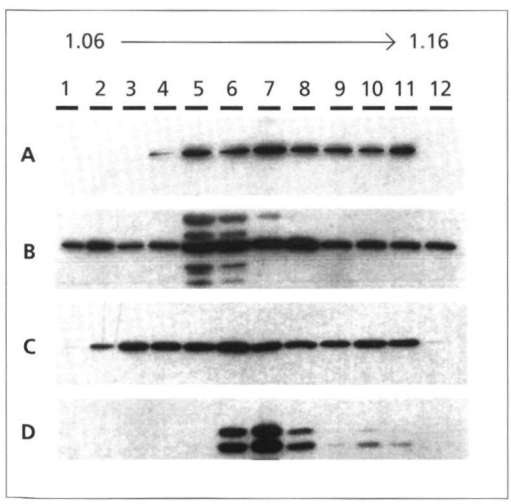

Fig. 8 Fractionation of oocytes. Oocytes were injected with 10 ng of cRNA encoding wt (**A**), E258K (**B**), S256A (**C**), or R187C (**D**) AQP2. After three days, oocytes were homogenized and fractionated by centrifugation over a linear 12-50% sucrose gradient. From 12 fractions of 0.7 ml, membranes were collected and subjected to immunoblotting and AQP2 proteins were visualized by chemiluminescence. The density (g/ml) of these fractions is indicated at the top of the figure (1.06-1.16 g/ml).

because significantly less AQP2-E258K was found in the oolemma compared to wt AQP2 (Fig 5B). This was corroborated by the immunocytochemical analysis, which revealed that a major fraction of AQP2-E258K was present just underneath the plasma membrane, and only some expression was found at the plasma membrane, whereas wt AQP2 was only detected in the plasma membrane (Fig 6).

The fact that some AQP2-E258K is expressed at the plasma membrane, is in line with results from dDAVP infusion studies, in which both patients transiently increased their urinary osmolalities (Table 1). These results are contrasting with those obtained in patients with X-linked nephrogenic diabetes insipidus (AVPR2 mutations) or in patients with autosomal recessive nephrogenic diabetes insipidus (AQP2 mutations), where a full phenotype, with urinary osmolalities less than 150 mmol/kg H_2O, is regularly observed (Table 1).

The appearance of AQP2-E258K on immunoblot is remarkably different from AQP2 mutants in recessive NDI, because these mutants always showed an additional band of ~32 kDa, which appeared to be an endoplasmic reticulum-retarded form of AQP2 [28]. In addition, the subcellular localization of AQP2-E258K differs greatly from previously-reported ER-retarded mutant AQP2 proteins, which were evenly distributed in the cytoplasm [28,116]. The difference in subcellular distribution between AQP2-E258K and AQP2-R187C (a mutant AQP2 found in recessive NDI) was underscored by their difference in sedimentation velocity in a sucrose gradient (Fig. 8).

The folding and maturation of proteins in the ER is thought to be subjected to a stringent 'quality control'. Consequently, misfolded proteins, which are often recognized on immunoblots as ER-retarded forms, are usually degraded. Oligomerization usually takes place in the ER [23,27] or golgi [120]. The E258K mutant is apparently properly folded in the ER, is routed to the golgi and is presumably able, in contrast to AQP2 mutants in recessive NDI, to oligomerize with wt AQP2. A functional oligomerization, however, could not be shown in oocytes, because a dominant-negative action of AQP2-E258K on wt AQP2 function was not observed (Fig. 4). In aquaporins, the monomer is the functional unit, and oligomerization might not be essential for functionality in oocytes. Possibly, a dominant-negative effect might be obtained upon co-expression of these proteins in MDCK type 1 cells, because MDCK cells stably-transfected with an AQP2 expression construct have been shown to route and regulate AQP2 in a way which closely resembles the vasopressin-regulated AQP2 shuttling in kidney collecting duct cells [34].

To identify the cause of the impaired transport of AQP2-E258K, we compared its function and routing with wt AQP2, AQP2-S256A and AQP2-R253*. In renal collecting duct cells, phosphorylation of AQP2 at S256 by protein kinase A (PKA) is thought to be essential for vesicles containing AQP2 to fuse with the apical membrane and become water permeable. This hypothesis has been corroborated by the recent finding that in stably-transfected $LLCPK_1$ cells, AQP2-S256A mutants are not inserted into the plasma membrane after AVP stimulation, whereas wt AQP2 is [54,78]. Since the E258K mutation is located closely to S256, it was hypothesized that the dominant mutation might interfere with S256 phosphorylation. When tested, however, it appeared that the E258K mutation did not interfere with phos-

phorylation of S256. AQP2-S256A could not be phosphorylated by PKA, which is in line with experiments from others [85] (Fig. 7).

In contrast to the dominant mutant, the water permeability of oocytes expressing AQP2-S256A or AQP2-R253* was not significantly different from wt AQP2 expressing oocytes (Fig. 3), which was in line with the immunocytochemistry, which showed a considerable amount of expression of these mutants in the plasma membrane (Fig. 6). The high water permeability of oocytes expressing AQP2-S256A and the high level of expression in the plasma membrane is in contrast to results obtained with the same mutant transfected to $LLCPK_1$ cells [54,78]. This might be partly due to a shuttling machinery of oocytes, which is not so tightly controlled as in mammalian cells. In oocytes, for example, the most common mutant in the cystic fibrosis transmembrane conductance regulator, CFTRΔF508, is retarded in its transport, but a small portion of the mutant protein is found at the plasma membrane [41]. Expressed in mammalian cells, however, this mutant is never found at the plasma membrane [20]. Sections of oocytes expressing AQP2-S256A or AQP2-R253* showed, besides a considerable amount of expression in the plasma membrane, some protein in the region just below the plasma membrane (Fig. 6). This suggests that phosphorylation triggers some endocytotic vesicles containing AQP2 to fuse with the plasma membrane, which might explain the increase in AQP2-mediated water transport in oocytes after treatment with cAMP [85]. This shuttling response to phosphorylation in oocytes has also been shown for the Na^+/glucose cotransporter [65]. Since the water permeabilities of oocytes expressing wt AQP2, AQP2-S256A, or AQP2-R253* were not different, we have to conclude that in oocytes the C-terminal tail of AQP2, and phosphorylation of S256 in particular, is not of critical importance for AQP2 to reach its final destination, the plasma membrane. More importantly, however, the finding that AQP2-R253* is hardly impaired in its routing to the plasma membrane shows that the absence of 16 amino acids of the C-tail, including the region of the E258K mutation, does not cause a severe impairment of the routing. Therefore, it very likely that the change from a negative into a positive charge in the E258K mutant introduces a golgi retention/routing signal instead of a rupture of an genuine AQP2 routing signal.

In conclusion, we reported that autosomal dominant NDI is caused by a mutation in the AQP2 gene. This mutation caused the substitution of a lysine for a glutamic acid in the C-terminal tail of AQP2, which did not interfere with phosphorylation of S256. In contrast to AQP2 mutants in recessive NDI, which are all impaired in their transport from the ER, the E258K mutant was piled up in the golgi, presumably because the substitution introduced a golgi retention/routing signal. In mixed tetramers of wild-type AQP2 and AQP2-E258K, retention of the AQP2-E258K mutant in such a cell compartment offers an explanation for the dominant form of inheritance of NDI in the described family.

Chapter 7

General discussion

In 1992, a red cell membrane protein of 28 kDa, of which the function was still unknown, was shown to be a molecular water channel by expression in *Xenopus* oocytes [140]. This breakthrough opened a new field of research, which yielded an avalanche of information about water channel proteins or aquaporins, which existence had both been questioned and searched for for many decades. One year after the discovery of AQP1, this Ph.D. project was started. At that time, a second water channel, AQP2, had just been cloned [55] and little information was available about the structure-function relationship of water channels. In the past four years, several other mammalian aquaporins and homologs from other species were cloned. In the same period, two functional models were proposed, the hourglass model for AQP1 by Jung *et al.* [75], and a model for AQP2 by Bai *et al.* [6] which is substantially different from the hourglass model. In this thesis, studies on the structure and function of aquaporins in health and disease are described using *in vitro* mutagenesis and expression of the derived mutant aquaporins in *Xenopus* oocytes. The emphasis in this thesis is on AQP2, since naturally occurring mutations in AQP2, as found in patients suffering from nephrogenic diabetes insipidus (NDI) [28,31,178], offered a unique opportunity to study the effect of mutations on the function of the AQP2 water channel.

The first water channel appeared to be a member of the MIP family of transmembraneous proteins. MIP, the major intrinsic protein of lens fiber cells, was cloned in 1984 [57] and is thought to play a role in the maintenance of lens transparency, but the function of this protein was not yet understood. When purified MIP was reconstituted into planar lipid bilayers, it behaved as a voltage-dependent ion channel with large conductances [45]. However, results from reconstitution experiments in planar lipid bilayers have to be interpreted with extreme caution, since also AQP1, which is certainly not an ion channel, induces MIP-like conductances upon reconstitution into planar lipid bilayers (personal communication, J. Hall). The main conclusion in chapter 2 is that when MIP is expressed in *Xenopus* oocytes, no additional ion conductances are induced, but a small water permeability is observed which is characterized by a low activation energy, indicative of channel-mediated water transport. Therefore, MIP was renamed AQP0. Two distinct mutations in MIP have been shown to cause cataract in mice, confirming the role of MIP in the maintenance of lens transparency [158]. The question is, however, whether this is caused by malfunctioning of the water channel aspect, or of another, yet unidentified function of this abundant lens protein. The two mutations in MIP that cause cataract in mice are a point mutation resulting in an amino acid substitution that inhibits targeting of MIP to the cell membrane, and a splicing error that substitutes the C-terminus of MIP by a divergent sequence, resulting in a non-functional protein [158]. In chapter 2, it was shown that the C-terminus of MIP is essential for the water transport function, because a chimeric MIP protein with the C-tail of AQP1 did not confer water permeability to oocytes. This suggests that cataract is caused by a loss of water channel function of MIP. However, MIP comprises over 60% of the total membrane protein in lens fiber cells, and if the only function of MIP

would be that of a water channel, then there would be no need for such a high expression level. Therefore, MIP is likely to have, besides a water channel function, another function which requires high expression levels, for example in cell-cell adhesion [111]. Experiments with lenses from mice bearing these MIP mutations might shed light on the other physiological role of MIP.

Mutagenesis studies with AQP1 resulted in a functional model which was called the hourglass model [75]. In this model, it is proposed that the very conserved loops B and E fold back into the membrane and form together the pore through which water transport takes place. We used this model as a starting point for mutagenesis studies to investigate the importance of the conserved loops B and E for water channel function, by exchanging loops B and E among three aquaporins with different transport characteristics: AQP0, AQP2 and AQP3 (chapter 3). Unfortunately, most chimeric proteins in which one or both loops were exchanged, were impaired in their routing to the plasma membrane. The major fraction of AQP0 with loops B and E of AQP2 was also misrouted, although part of it was expressed at the plasma membrane. No increase in water permeability was measured in oocytes expressing this chimeric protein. The low plasma membrane expression should be sufficient to increase water permeability of oocytes if loops B and E of AQP2 would confer high AQP2 water permeability to AQP0 [116]. Therefore, it was concluded that loops B and E of AQP2 do not increase water transport through AQP0, but this chimeric protein might still function like AQP0, for which the low water permeability in combination with low plasma membrane expression might not be sufficient to increase water permeability of oocytes. Two chimeric proteins were routed properly, and these proteins, AQP0 with loop E of AQP2 and AQP2 with loop B of AQP0, showed exactly the same functional characteristics as the unmutated water channels. Loop B of AQP0 did not restrict water permeability of AQP2, and loop E of AQP2 did not confer high water permeability to AQP0. Therefore, we concluded that loops B and E might form the water pore, but that other parts of the molecule are also important and determine the transport characteristics of the pore. For AQP0, for example, it was shown that substitution of one amino acid in the fifth transmembrane domain (V160P), increased the water permeability by 50% (chapter 2). The C-tail does not seem to play an important role for AQP1, because AQP1 with the C-tail of AQP0 still functions like AQP1 (chapter 2).

More evidence that the hourglass model also holds for AQP2 was obtained from three new mutations in the AQP2 gene found in patients suffering from autosomal recessive nephrogenic diabetes insipidus (NDI). These mutations encoded for N68S, T126M, or A147T mutant AQP2 proteins (chapter 4). All mutations in the AQP2 gene in NDI that were reported previously [31,178], resulted in mutant AQP2 proteins that did not increase the water permeability upon expression in *Xenopus* oocytes, and these mutant proteins were shown to be retarded in the endoplasmic reticulum (ER) [28]. The mutant AQP2 proteins resulting from these three new mutations were also shown to be ER-retarded, but in spite of this misrouting, AQP2-T126M and AQP2-A147T yielded a small increase in P_f when expressed in oocytes, indicating that they are functional water channels. The location of these mutations provided important information on the structure-function relation of

AQP2. The T126M and A147T substitutions are located in loop C and at the cytoplasmic end of the transmembrane domain between loops C and D. The substitutions which resulted in non-functional mutants are all located in loops B and E and in the middle of other transmembraneous domains. This underscores the importance of loops B and E for water transport. The tolerance for mutations in the C and D loop indicates that loops C and D are less important for water transport, which is in line with the hourglass model.
For AQP2, a different functional model was proposed by Bai *et al.* suggesting that loops B and E are not as critical as in the hourglass model, but loops C and D play a more important role in the formation of the water pore [6]. Considering the high homology between AQP1 and AQP2, it is unlikely that water transport through both molecules occurs through totally different pathways. Results from the exchange of loops B and E among aquaporins as described in chapter 3 do not exclude the probability of this model, but functional results from AQP2 mutants in NDI suggest that loops B and E, and not loops C and D are essential for water transport (chapter 4). Furthermore, an AQP2-C181S mutant played an important role in postulating this divergent functional model for AQP2 [6], whereas this same mutant AQP2 protein proved to be nonfunctional when expressed in our laboratory (chapter 5). Bai *et al.* [6] had reported that in AQP2, like in AQP1 [141,197], substitution of the mercury-sensitive cysteine by a serine results in a normally functional AQP2 protein of which the water transport is no longer inhibitable by mercury. We originally wanted to use this fact in studies to drag routing-impaired AQP2 proteins as found in NDI to the plasma membrane with the help of a truncated AQP2 protein, a protocol which has been successfully used in studies with mutant AQP1 proteins [75]. To be able to discriminate between the water permeability of the mutant AQP2 and the truncated AQP2, we wanted to create mutant AQP2 proteins of which the water transport was mercury-insensitive, by changing the mercury-sensitive cysteine 181 into a serine. In chapter 5, however, it is described how this approach ended prematurely, because introduction of a C181S substitution in AQP2 resulted in a non-functional, severely ER-retarded AQP2 protein. All possible controls that were carried out to solve this discrepancy with results from Bai *et al.* yielded only one conclusion: substitution of the mercury-sensitive cysteine by a serine in AQP1 did not affect the P_f, whereas this substitution in AQP2 caused a misrouting of the protein, making this mutation unuseful for the proposed studies. The difference in effect of mutagenesis of AQP1 and AQP2 is now explained by the more general conclusion that AQP2 is much more susceptible to disturbances in the structure and the resulting effect on routing than AQP1. This does not per se implicate a difference in structure. AQP2 in the collecting duct is routed in a more complex way, under the control of the hormone vasopressin, and this could result in more strict structural requirements.

Additional support for the hourglass model stems from 3 dimensional (3D) projection maps of AQP1. AQP1 forms well-ordered 2-dimensional (2D) crystals upon reconstitution of solubilized tetramers in the presence of phospholipids [186]. Projection maps of AQP1 crystals determined by electron crystallography showed that

the AQP1 monomer can be interpreted in six to eight alpha helices, which are oriented perpendicular or slightly tilted to the bilayer [91,112,188]. Within each monomer, an aqueous domain was observed [112]. The high resolution 3D projection map of Li *et al.* [92] revealed that the basic structure of AQP1 may be described as a cylinder with a trapezoidal cross section. The cylinder is formed by six alpha helices, which can be interpreted as the six transmembrane domains. The trapezoidal cross section is likely to be an additional short alpha helix, which is part of a branched rod-like substructure within the cylinder. This substructure is assumed to be formed by the other two hydrophobic regions: loops B and E. These results were confirmed by others [9,19]. So the 3D maps shows that the water channel is formed by six alpha helices surrounding a pore in which a substructure is found, which is formed by loops B and E. This is a further improvement of the hourglass model which predicts that loops B and E are folding back into the membrane but form a water pore outside the six helices.
A more detailed 3D map at higher resolution will be needed to reveal all structural details necessary to determine the pore structure of AQP1. Merging structural data with results from mutagenesis studies will finally solve the structure-function relationship of AQP1. Understanding the structure of AQP1 will also lead to predictions for the structure of other aquaporins. From our mutagenesis studies, we can conclude that the hourglass model also provides a good description of the water pore in AQP2. In view of the high homology between the aquaporins, the hourglass model might as well predict the structure of the water pore in AQP4 and AQP5. However, AQP3, which is also permeable for small solutes, originates from a different ancestor which is a glycerol facilitator rather than an aquaporin [133]. It is still debated whether water and solutes use the same pore through AQP3 [43,152]. For this aquaporin it might be anticipated that the water pore, and consequently the functional model describing this pore, is different from the other aquaporins.

For NDI, three different inheritance patterns have been described. The X-linked form and the autosomal recessive form are caused by mutations in the V_2 receptor gene and mutations in the AQP2 gene, respectively. Mutations in the AQP2 gene in autosomal recessive NDI have been shown to cause retardation of AQP2 proteins in the ER [28]. However, in spite of misrouting, oocytes expressing AQP2-T126M and AQP2-A147T yielded a small, but significant increase in P_f, indicating that they are functional water channels. Therefore, it was concluded that the major cause underlying autosomal recessive NDI is the misrouting of AQP2 mutants (chapter 4). The reason why these mutant AQP2 proteins are retarded in the ER is not exactly known. Mutant AQP2 proteins probably don't fold properly, and are retained by the 'ER quality control'. Attempts should be undertaken to find ways to overcome the ER retention of the functional AQP2 mutants, and to promote trafficking of these proteins to the plasma membrane. The use of molecular chaperones, for example, may provide tools for treatment of this form of NDI.
Recently, a third inheritance pattern of NDI, the autosomal dominant form, has been reported in two independent families [10]. Two different mutations were identified in only one allele of the AQP2 gene of the patients [10]. In contrast to

AQP2 mutants in recessive NDI, in which the mutations are located in the transmembraneous regions or the connecting loops, these mutations in dominant NDI are located in the C-terminal tail of AQP2. In chapter 6, the function and routing in oocytes of one of these mutant AQP2 proteins in autosomal dominant NDI, AQP2-E258K, is described. The AQP2-E258K mutant was shown to be retarded, not like the mutant AQP2 proteins in recessive NDI in the ER, but in the golgi or a post-golgi compartment. The reason for this retardation may be that the substitution in the C-tail introduces a golgi retention signal, which might change AQP2 from an endosomally recycling protein to a protein that is targeted to the trans golgi network. In AQP2, the E258K substitution causes a change from the sequence SVEL to SVKL, replacing a negative charge (E) by a positive charge (K). A database search did not identify this sequence as a known routing signal, indicating that this mutation might reveal a not yet identified routing signal. Studies of truncated AQP2-E258K proteins will reveal the importance of this putative routing signal. The introduction of a retention signal could also explain the dominant character of this AQP2 mutant. In mammalian cells, aquaporins are expressed at the plasma membrane as tetramers, and if wild-type AQP2 and the dominant AQP2 mutant form mixed tetramers, the routing of the whole tetramer could be changed. Tetramerization of aquaporins presumably takes place in the ER [23,27] or in the golgi [120]. In oocytes, however, the dominant effect of the E258K mutant could not be shown. This raises the question where, and if, tetramerization of aquaporins takes place in oocytes.

Not all mutations in the C-tail of AQP2 lead to a dominant inheritance pattern, as was shown for a patient with an autosomal recessive form of NDI who was found to be a compound heterozygote for two mutations in the AQP2 gene, leading to A190T- and P262L-substituted AQP2 proteins. The P262L substitution is located 4 amino acids downstream from the E258K substitution in the C-tail of AQP2. However, the reason for dysfunctioning of AQP2-P262L is still unknown because in oocytes the function and routing of this protein was identical to wt AQP2 [76].

The putative existence of routing signals in the C-tail of AQP2 opens new possibilities for research on regulation of AQP2. Evidence for the shuttle hypothesis of vesicles containing AQP2 has been shown, but the molecular machinery needed for the shuttling of vesicles is still largely unknown. It has been shown that phosphorylation of AQP2 at the C-tail plays a key-role in the targeting of AQP2 from intracellular vesicles to the plasma membrane [54,78], and presumably there are more, yet unidentified targeting signals or binding motifs in the C-tail of AQP2 that are essential for proper routing of the protein. To identify the small binding proteins which are involved in the targeting of AQP2 to the plasma membrane, protein-protein interactions can be unraveled using the yeast-two-hybrid system.

So far, only dysfunction of AQP0 and AQP2 has been related to a disease [31,158], and therefore the physiological importance of the other aquaporins is still unknown. The physiological importance of AQP1 is still a matter of debate. Its wide tissue distribution suggests an important physiological role, but people who lack a functional AQP1 do not have any apparent clinical symptoms [143]. However, thorough assessment of kidney function, eye function and liquor production has not yet taken place, and could unmask subclinical manifestations. It could be

that the role of AQP1 in these people is taken over by upregulation of other water channels, or even by cotransporters. Recently it was shown that water transport is directly linked to solute cotransport proteins such as the small intestine brush border Na^+/glucose cotransporter. It was demonstrated that 260 water molecules are directly coupled to each sugar molecule transported, suggesting that cotransporters play an important role in water homeostasis [94].
Transgenic mice deficient for distinct aquaporins will yield valuable information about the physiological importance of these aquaporins. Recently, a transgenic knock-out mouse lacking AQP4 has been generated [100]. Preliminary studies revealed that AQP4 deletion has no effect on development, survival, growth and neuromuscular function, but produced a small defect in urinary concentrating ability. Interestingly, no other aquaporins were upregulated. Although this phenotypic analysis is preliminary, it is obvious that lack of AQP4 in these mice is, like AQP1 deficiency in humans, not of critical importance. It might be that AQP0 and AQP2 will remain the only water channels whose dysfunction is linked to a clinical manifestation. Strikingly, these two aquaporins are the only water channels whose expression is limited to only one specialized cell type.

In this thesis, *Xenopus* oocytes were used as an expression system for water channels. This system has many advantages, such as the simplicity of isolation and culturing of these cells, the enormous translational capacity of these oocytes, and a relatively easy method to inject and measure the water permeability of oocytes in a standard swelling assay using video-microscopy. However, the disadvantage of *Xenopus* oocytes is that it is an unpolarized cell, and the routing machinery of these cells is far from as advanced as of mammalian polarized epithelial cells as for example kidney collecting duct cells. When mutations are studied that cause a routing problem, care should be taken in the interpretation of results, and transfection of mammalian cells should be the next step to confirm results as revealed by the oocyte expression system. The polarized MDCK cell line which has been used for stable transfection with AQP2 (WT10) not only possesses the required routing machinery comparable with collecting duct principal cells, but also contains a V_2 receptor [34].
An example for different results in oocytes and cultured mammalian cells is the AQP2 mutant in which the phosphorylation site has been replaced by an alanine, which is hardly impaired in its routing to the oolemma (chapter 6), but in $LLCPK_1$ cells phosphorylation at this site appears to be critical for the AQP2 protein to be inserted into the plasma membrane [54,78]. Although oocytes have been very useful to demonstrate the routing problem of the AQP2-E258K mutant protein (chapter 6), and will be useful to show the importance of the targeting motif introduced by the E258K mutation, the dominant behaviour of the AQP2-E258K mutant could not be demonstrated in oocytes, which demands expression in mammalian cells. In addition, oocytes might not be the best system to measure ion conductances upon expression of channel proteins. Yool *et al.* published that AQP1 induces cationic conductances in oocytes after forskolin stimulation [194], which could not be reproduced by other groups [2,30,48,134,153,182].

The search for new aquaporins will continue and more surprises can be anticipated. So far, the discovery of aquaporins has greatly enhanced our insight in the physiology of water transport. However, the picture is far from complete. Why are several aquaporins expressed in the same tissue, and what is the physiological importance of these aquaporins? The growing family of AQPs may harbour causes for other hereditary diseases. The absence of clinical symptoms in persons with AQP1 knock-out mutations is still puzzling and asks for further studies. Experiments with transgenic knockout mice will probably answer many questions. High resolution structural analysis of AQP1 crystals will be needed to finally visualize the structure of the water pore. Understanding of this structure might provide new AQP-inhibitors which can be used as aquaretics. For AQP2, the emphasis will be on unravelling the molecular machinery involved in vesicle targeting, and solving the routing problem of misrouted water channels, which might eventually lead to therapeutic strategies in the autosomal form of NDI.

Chapter 8

Summary / Samenvatting

In certain cell types, the water permeability is much higher than can be explained by diffusion of water through the lipid bilayer alone. The discovery of molecular water channels, called aquaporins, has provided insight into the mechanism of this rapid water transport across biological membranes. Aquaporins are involved in many physiological processes in the human body that demand rapid water transport, like the concentration of urine in the kidney, the production and reabsorption of cerebrospinal fluid, fluid secretion in salivary and lacrimal glands, and lung water homeostasis. Several mammalian aquaporins have been cloned, and more aquaporins are expected to be discovered.

In this thesis, studies on the structure and function of aquaporins in health and disease are described, using mutagenesis and expression of the resulting mutant water channels in *Xenopus* oocytes. **Chapter 1** gives an overview of the cellular and tissue distributions, genetics, functional characteristics and structural features of the mammalian aquaporins cloned until now. All aquaporins share common structural features, characteristic for members of the MIP family of transmembrane proteins. The proteins are predicted to contain six transmembrane regions, connected by loops A through E, with intracellular amino- and carboxy termini. The intracellular loop B and the extracellular loop E contain a stretch of amino acids, called the NPA box, which is conserved among all aquaporins. The water transport through most aquaporins can be blocked by binding of mercury to a cysteine located close to the second NPA box in loop E. Aquaporins are selective for water, although some, in particular AQP3, are also permeable for small polar solutes like urea and glycerol.

The prototype of the MIP family, the major intrinsic protein of lens (MIP), is thought to play a role in the maintenance of lens transparency. This protein was cloned more than a decade ago [57], but the function of MIP was not yet understood, although it behaved as a voltage-dependent ion channel upon reconstitution in planar lipid bilayers [45]. In view of the high homology between MIP and AQP1, previously called CHIP, we decided to study the water channel characteristics of MIP in oocytes, in comparison to AQP1. In **chapter 2** it is described that MIP does not induce ion conductances in oocytes, but instead functions as a water channel with a low water permeability, compared to the high water permeability conferred by AQP1. To identify structures or amino acids responsible for the difference in water permeability between MIP and AQP1, recombinant MIP proteins and MIP proteins with single amino acid substitutions were expressed in oocytes. Introduction of a proline in the 5th transmembrane domain yielded a 50% increase in water permeability, suggesting that simple alterations can make MIP a more efficient water channel. It was concluded that MIP functions as a water channel in lens and MIP was rebaptized as AQP0. However, in view of the abundant expression of MIP, which comprises over 60% of the total membrane proteins in lens fibers, it may also have another essential function.

For AQP1, mutagenesis studies led to the proposal of a functional model, called the hourglass model [75]. This model predicts that the conserved loops B and E fold

back into the membrane and form together the pore through which water transport takes place. This hourglass model was used as a starting point in a study in which the importance of loops B and E for water channel function was investigated, by exchanging loops B and E among three aquaporins with different transport characteristics: AQP0, AQP2 and AQP3 (**chapter 3**). Unfortunately, most proteins in which loops had been exchanged were not expressed at the plasma membrane, due to misrouting. However, oocytes expressing AQP0 with loop E of AQP2 and AQP2 with loop B of AQP0 yielded water permeabilities which were equal to the water permeabilities of oocytes expressing the unmutated proteins. AQP0 with both loops B and E of AQP2 did not increase water permeability in oocytes and was partly misrouted, but the plasma membrane expression was high enough to conclude that loops B and E of AQP2 did not confer high AQP2 water permeability to AQP0, but it might still function like AQP0. These results show that the water permeability of one aquaporin is not influenced by loops B and/or E of another aquaporin and suggest that if loops B and E form the water pore, other parts of the protein are important for the tertiary structure that determines the magnitude of water permeability.

Recently, it has been reported that mutations in the gene for AQP2 are the cause for the autosomal recessive form of nephrogenic diabetes insipidus (NDI) [31], a disease that is characterized by the inability of the kidney to concentrate urine in response to vasopressin. Upon expression of the NDI-related mutant AQP2 water channels in oocytes, it was shown that these proteins were retarded in the endoplasmic reticulum (ER) [28]. In **chapter 4**, three new mutations in the AQP2 gene causing autosomal recessive nephrogenic diabetes insipidus are reported, resulting in N68S-, T126M-, or A147T-substituted AQP2 proteins. All three AQP2 mutants were retarded in the ER. In spite of this misrouting, AQP2-T126M and AQP2-A147T yielded a relatively small, but significant increase in water permeability in oocytes, indicating that they are functional water channels. Therefore, it was concluded that the major cause underlying autosomal recessive NDI is the misrouting of AQP2 mutant proteins. The location of NDI-related mutations in AQP2 provided important information on the structure-function relationship of AQP2. The A147T and T126M mutations are located in loop C and in the transmembrane region between loop C and D. The mutations resulting in non-functional water channels are located in loops B and E and in the other transmembrane regions. This suggests a critical importance of loops B and E in water transport, and a relatively minor importance of loops C and D, which is in line with the hourglass model as a functional model for AQP2.

For AQP1, it has been described how a truncated AQP1 was used to drag routing-impaired AQP1 mutant proteins to the plasma membrane [75]. We wanted to use the same approach for misrouted AQP2 proteins as found in NDI. To be able to discriminate between truncated and mutant AQP2 proteins, we wanted to create differences in mercury sensitivity of water transport. In **chapter 5**, however, it is described how an attempt to drag misrouted AQP2 proteins to the plasma membrane failed, because of unanticipated differences between AQP1 and AQP2 in the effect of mutagenesis of the mercury sensitive cysteine. For both AQP1 and AQP2 it

has been reported that replacement of the mercury sensitive cysteine (C189 and C181, respectively), by a serine resulted in a functional, but mercury insensitive water channel [6,141]. In this chapter, however, we show that this holds for AQP1, but the same mutation in AQP2 causes a severe routing problem.
For AQP2, a different functional model was proposed suggesting that loops B and E are not as critical as proposed in the hourglass model, but that loops C and D are located close to the water pore [6]. However, the AQP2-C181S mutant, which we showed is severely disturbed in its routing (chapter 5), played an important role in postulating this model. Additionally, functional results from NDI-related AQP2 mutants are not in line with this model, but corroborate the hourglass model (chapter 4).
In **chapter 6** it is described that also the autosomal dominant form of NDI is caused by a mutation in the AQP2 gene. This mutation, leading to a E258K-substituted AQP2 protein, is located in the C-terminal tail of AQP2, close to the protein kinase A phosphorylation site. However, phosphorylation of AQP2 was not affected by the mutation. Expression of AQP2-E258K in oocytes yielded a low water permeability in combination with a low plasma membrane expression. The dominant behaviour of the mutant protein could not be demonstrated in oocytes. In contrast to the AQP2 mutants as encoded in autosomal recessive NDI, the AQP2-E258K mutant was not retarded in the ER but in a golgi or post-golgi compartment, presumably because the E258K substitution introduces a golgi retention signal. This could also explain the dominant behaviour of this protein, if the mutant protein forms mixed tetramers with wild-type AQP2 and when the mixed tetramer is consequently misrouted.
Finally, the results obtained are evaluated in **chapter 7**, and a summary is provided in **chapter 8.**

This thesis has generated new facts about the structure-function relationship of aquaporins. However, there are still many questions to be answered. It can be anticipated that new aquaporins will be discovered, and the physiological importance of most aquaporins still has to be shown. More detailed knowledge about the structure-function relationship of aquaporins will provide tools for stimulation or inhibition of water transport in clinical situations in which water transport is either inappropriate low or high.

In een aantal celtypen is de waterpermeabiliteit veel hoger dan op grond van diffusie door de lipide bilaag verklaard kan worden. De ontdekking van moleculaire waterkanalen, genaamd aquaporines, heeft inzicht verschaft in het mechanisme van dit snelle watertransport over biologische membranen. Aquaporines zijn betrokken bij veel fysiologische processen in het menselijk lichaam die snel watertransport vereisen, zoals de concentrering van urine in de nier, het produceren en reabsorberen van cerebrospinale vloeistof, de productie van speeksel en traanvocht, en het handhaven van de waterhomeostase in de long. Een aantal humane aquaporines is gekloneerd en naar verwachting zullen er nog meer aquaporines ontdekt worden.
In dit proefschrift worden studies beschreven naar de structuur en functie van aquaporines in gezondheid en ziekte, uitgevoerd met behulp van mutagenese en expressie van de resulterende mutante waterkanalen in *Xenopus* oöcyten. **Hoofdstuk 1** geeft een overzicht van de cellulaire- en weefseldistributie, genetica, functionele karakteristieken en structurele kenmerken van de waterkanalen van zoogdieren die tot nu toe zijn gekloneerd. Alle aquaporines hebben overeenkomstige structurele kenmerken, die karakteristiek zijn voor leden van de MIP familie van transmembraaneiwitten. Deze eiwitten bevatten zes transmembraandomeinen, die met elkaar verbonden zijn door lus A tot en met E, met intracellulaire amino- en carboxytermini. De intracellulaire lus B en de extracellulaire lus E bevatten een reeks van aminozuren, die het NPA motief wordt genoemd en die geconserveerd is tussen alle aquaporines. Het watertransport door de meeste aquaporines kan worden geremd door binding van kwik aan een cysteïne die zich vlakbij het tweede NPA motief bevindt. De meeste aquaporines zijn selectief voor water, hoewel enkele, met name AQP3, behalve water ook kleine verbindingen als ureum en glycerol transporteren.
Het prototype van de MIP familie, het 'major intrinsic protein' (MIP) van de lens, speelt waarschijnlijk een rol in het handhaven van de transparantheid van de lens. Dit eiwit werd al meer dan tien jaar geleden gekloneerd [57], maar de functie van MIP is nog niet opgehelderd, hoewel MIP functioneert als een voltage-afhankelijk ionkanaal na reconstitutie in planaire lipide bilagen [45]. Gezien de grote homologie tussen MIP en AQP1, die voorheen CHIP werd genoemd, besloten we de waterkanaaleigenschappen van MIP te bestuderen in oöcyten en die te vergelijken met AQP1. In **hoofdstuk 2** wordt beschreven dat MIP geen ionconductanties induceert in oöcyten, maar juist functioneert als een waterkanaal met een lage waterpermeabiliteit, vergeleken met de hoge waterpermeabiliteit van AQP1. Om de structuren of aminozuren te identificeren die verantwoordelijk zijn voor het verschil in waterpermeabiliteit tussen MIP en AQP1, werden recombinante MIP eiwitten en MIP eiwitten waarin enkele aminozuren waren vervangen, tot expressie gebracht in oöcyten. De introductie van een proline in het vijfde transmembraan segment resulteerde in een toename in waterpermeabiliteit van 50%, wat suggereert dat kleine veranderingen in MIP het een efficiënter waterkanaal kunnen maken. Er werd geconcludeerd dat MIP functioneert als een waterkanaal in de lens en MIP werd omgedoopt tot AQP0. Gezien de hoge expressie van MIP, die meer dan 60% van de

totale membraaneiwitten in lensvezels vormt, kan MIP echter ook nog een andere essentiële functie hebben.
Resultaten van mutagenesestudies hebben voor AQP1 geleid tot een functioneel model dat het zandlopermodel wordt genoemd. Dit model voorspelt dat de geconserveerde lussen B en E terugvouwen in de membraan en zo samen de porie vormen waardoor watertransport plaatsvindt. Dit zandlopermodel werd gebruikt als uitgangspunt voor een studie waarin het belang van de lussen B en E voor de waterkanaalfunctie is bestudeerd, door lussen B en E te verwisselen tussen drie aquaporines met verschillende transporteigenschappen: AQP0, AQP2 en AQP3 (**hoofdstuk 3**).
Helaas werden de meeste eiwitten waarin lussen waren verwisseld niet tot expressie gebracht in de plasmamembraan doordat ze gestoord waren in hun transport. Echter, AQP0 met lus E van AQP2 en AQP2 met lus B van AQP0 gaven in oöcyten een watertransport dat vergelijkbaar was met het watertransport van de ongemuteerde eiwitten. AQP0 met zowel lus B als E van AQP2 gaf geen verhoogde waterpermeabiliteit van oöcyten en was merendeels gestoord in het transport, maar de expressie in de plasmamembraan was hoog genoeg om te kunnen concluderen dat door lus B en E van AQP2 de waterpermeabiliteit van AQP0 niet verhoogd wordt. Deze resultaten tonen aan dat de waterpermeabiliteit van de ene aquaporine niet wordt beïnvloed door lus B en/of E van een andere aquaporine, en suggereren daarom dat, indien de lussen B en E de waterporie vormen, andere gedeelten van het eiwit van belang zijn voor de tertiaire structuur die de mate van watertransport bepaalt.
Recent is aangetoond dat mutaties in het AQP2 gen de oorzaak zijn van de autosomaal recessieve vorm van nefrogene diabetes insipidus (NDI) [31], een ziekte die gekarakteriseerd wordt door het onvermogen van de nier om urine te concentreren in respons op vasopressine. Door expressie van de NDI-gerelateerde mutante AQP2 waterkanalen in oöcyten werd aangetoond dat deze eiwitten geretardeerd zijn in het endoplasmatisch reticulum (ER) [28]. In **hoofdstuk 4** worden drie nieuwe mutaties in het AQP2 gen beschreven die autosomaal recessieve NDI veroorzaken en die resulteren in N68S-, T126M-, of A147T-gesubstitueerde AQP2 eiwitten. Alle drie de AQP2 mutanten waren geretardeerd in het ER. Ondanks het verstoorde transport, gaven AQP2-T126M en AQP2-A147T een relatief kleine, maar significante toename in de waterpermeabiliteit van oöcyten, wat aangeeft dat het functionele waterkanalen zijn. Daarom werd geconcludeerd dat het verstoorde transport van mutante AQP2 eiwitten de voornaamste oorzaak is die ten grondslag ligt aan autosomaal recessieve NDI. De lokatie van de NDI-gerelateerde mutaties in AQP2 leverde belangrijke informatie op over de structuur-functie relatie van AQP2. De A147T en T126M mutaties zijn gelokaliseerd in lus C en in het transmembraandomein tussen lus C en lus D. De mutaties die resulteren in niet-functionele waterkanalen zijn gelokaliseerd in de lussen B en E en in de andere transmembraandomeinen. Dit suggereert dat de lussen B en E van kritisch belang zijn voor watertransport en dat de lussen C en D relatief minder belangrijk zijn, wat in overeenstemming is met het zandlopermodel als functioneel model voor AQP2.
Voor AQP1 is beschreven hoe een getrunceerd AQP1 eiwit gebruikt is om AQP1 mutanten, die gestoord zijn in hun transport, naar de membraan te trekken [75]. Wij wilden dezelfde aanpak gebruiken voor transport-gestoorde AQP2 eiwitten,

zoals die gevonden zijn in NDI. Om onderscheid te kunnen maken tussen getrunceerde en mutante AQP2 eiwitten, wilden we verschillen introduceren in kwikgevoeligheid van het watertransport. In **hoofdstuk 5** wordt echter beschreven hoe een poging om deze transport-gestoorde AQP2 eiwitten naar de plasmamembraan te trekken, mislukte door onverwachte verschillen tussen AQP1 en AQP2 in het effect van mutagenese van de kwik-gevoelige cysteïne. Voor zowel AQP1 als AQP2 was beschreven dat vervanging van de kwik-gevoelige cysteïne (C189 en C181, respectievelijk) door een serine resulteerde in een functioneel, maar kwik-ongevoelig waterkanaal [6,141]. In dit hoofdstuk laten we echter zien dat dit wel opgaat voor AQP1, maar dat dezelfde mutatie in AQP2 een ernstige verstoring van het transport veroorzaakt.
Voor AQP2 is een ander functioneel model voorgesteld, dat suggereert dat de lussen B en E niet zo belangrijk zijn als werd voorspeld in het zandlopermodel, maar dat juist de lussen C en D zich dichtbij de waterporie bevinden [6]. De AQP2-C181S mutant speelde echter een belangrijke rol in de totstandkoming van dit model, terwijl wij hebben laten zien dat deze mutant ernstig gestoord is in het transport (hoofdstuk 5). Bovendien zijn functionele resultaten van NDI-gerelateerde AQP2 mutanten niet in overeenstemming met dit model, maar ondersteunen het zandlopermodel (hoofdstuk 4).
In **hoofdstuk 6** is beschreven dat ook de autosomaal dominante vorm van NDI wordt veroorzaakt door een mutatie in het AQP2 gen. De mutatie, die leidt tot een E258K substitutie in AQP2, is gelokaliseerd in de C-terminus van AQP2, vlakbij de proteïne kinase A fosforylatieplaats. Fosforylatie van AQP2 werd echter niet beïnvloed door de mutatie. Expressie van AQP2-E258K in oöcyten resulteerde in een lage water permeabiliteit in combinatie met een lage plasmamembraanexpressie. Het dominante karakter van het mutante eiwit kon niet worden aangetoond in oöcyten. In tegenstelling tot de AQP2 mutanten in autosomaal recessieve NDI, was de AQP2-E258K mutant niet geretardeerd in het ER, maar in een golgi of post-golgi compartiment, wat waarschijnlijk wordt veroorzaakt doordat de E258K substitutie een golgi-retentiesignaal introduceert. Dit zou ook het dominante gedrag van dit eiwit kunnen verklaren als het mutante eiwit gemengde tetrameren vormt met wild-type AQP2, en de hele tetrameer vervolgens gestoord wordt in het transport.
Tot slot worden de verkregen resultaten geëvalueerd in **hoofdstuk 7** en wordt een samenvatting gegeven in **hoofdstuk 8.**

Dit proefschrift heeft nieuwe kennis opgeleverd over de structuur-functie relatie van aquaporines. Er blijven echter nog vele vragen onbeantwoord. Het ligt in de lijn der verwachtingen dat nieuwe aquaporines worden ontdekt en het fysiologische belang van veel aquaporines moet nog worden aangetoond. Gedetailleerde kennis van de structuur-functie relatie van aquaporines kan mogelijkheden verschaffen om watertransport te remmen of te stimuleren in klinische situaties waar watertransport ontregeld is.

References

1

Abrami L, Tacnet F, Ripoche P (1995). Evidence for a glycerol pathway through aquaporin 1 (CHIP28) channels. *Eur J Physiol* 430:447-458

2

Agre P, Lee MD, Devidas S, Guggino WB (1997). Aquaporins and ion conductance (technical comment). *Science* 275:1490

3

Agre P, Sasaki S, Chrispeels MJ (1993). Aquaporins: a family of water channel proteins. *Am J Physiol* 265:F461

4

Apostol EL, Terris J, Ecelbarger CA, Andrews P, Knepper MA (1995). Aquaporin water channel expression in puromycin aminonucleoside (PAN) nephrosis. *J Am Soc Nephrol* 6:1009 (Abstract)

5

Asahina Y, Izumi N, Enomoto N, Sasaki S, Fushimi K, Marumo F, Sato C (1995). Increased gene expression of water channel in cirrhotic rat kidneys. *Hepatology* 21:169-173

6

Bai LQ, Fushimi K, Sasaki S, Marumo F (1996). Structure of aquaporin-2 vasopressin water channel. *J Biol Chem* 271:5171-5176

7

Bai LQ, Fushimi K, Sasaki S, Marumo M (1994). Identification of N-glycosylation and mercury-sensitive site of AQP-CD vasopressin sensitive water channel. *J Am Soc Nephrol* 5:268 (Abstract)

8

Barik S, Galinski MS (1991). 'Megaprimer' method for PCR: increased template concentration improves yield. *Biotechniques* 10:489-490

9

Walz T, Hirai T, Murata K, Heymann JB, Mitsuoka K, Fujiyoshi Y, Smith BL, Agre P, Engel A (1997). The three-dimensional structure of aquaporin-1. *Nature* 387,624-627.

10

Bichet DG, Arthus MF, Lonergan M, Balfe W, Skorechi K, Nivet H, Robertson G, Oksche A, Rosenthal W, Fujiwara M, Morgan K, Sasaki S (1995). Autosomal dominant and autosomal recessive nephrogenic diabetes insipidus: novel mutations in the AQP2 gene. *J Am Soc Nephrol* 6:717 (Abstract)

11

Bichet DG, Arthus MF, Lonergan M, Hendy GN, Paradis AJ, Fujiwara TM, Morgan K, Gregory MC, Rosenthal W, Didwania A, et al (1993). X-linked nephrogenic diabetes insipidus mutations in North America and the Hopewell hypothesis. *J Clin Invest* 92:1262-1268

12

Bichet DG, Birnbaumer M, Lonergan M, Arthus MF, Rosenthal W (1994). Nature and recurrence of AVPR2 mutations in X-linked nephrogenic. *Am J Hum Genet* 55:278-286

13

Bichet DG, Razi M, Lonergan M, Arthus MF, Papukna V, Kortas C, Barjon JN (1988). Hemodynamic and coagulation responses to 1-desamino [8-D-arginine] vasopressin in patients with congenital nephrogenic diabetes insipidus. *N Engl J Med* 318:881-887

14

Bonifacino JS, Lippincott Schwartz J (1991). Degradation of proteins within the endoplasmic reticulum. *Curr Opin Cell Biol* 3:592-600

15

Bross P, Andresen BS, Winter V, Krautle F, Jensen TG, Nandy A, Kolvraa S, Ghisla S, Bolund L, Gregersen N (1993). Co-overexpression of bacterial GroESL chaperonins partly overcomes non-productive folding and tetramer assembly of E. coli-expressed human medium-chain acyl-CoA dehydrogenase (MCAD) carrying the prevalent disease-causing K304E mutation. *Biochim Biophys Acta* 1182:264-274

16

Canfield M, Tamarappoo BK, Moses AM, Verkman AS, Holtzman EJ (1996). Novel AQP2 mutations as a cause of partially dDAVP-responsive post V_2 receptor congenital nephrogenic diabetes insipidus (CNDI). *J Am Soc Nephrol* 7:1611 (Abstract)

17

Catterall WA (1993). Structure and function of voltage-gated ion channels. *Trends Neurosci* 16:500-506

18

Chandy G, Kreman M, Laidlaw DL, Zampighi GA, Hall JE (1995). The water permeability per molecule of MIP is less than that of CHIP. *Biophys J* 68:353 (Abstract)

19

Cheng AC, Van Hoek AN, Yeager M, Verkman AS, Mitra AK (1997). Three-dimensional organization of a human water channel. *Nature* 387:627-630

20

Cheng SH, Gregory RJ, Marshall J, Paul S, Souza DW, White GA (1990). Defective intracellular transport and processing of CFTR is the molecular basis of

most cystic fibrosis. *Cell* 63:827-834

21

Chomczynski P, Sacchi N (1987). Single-step method of RNA isolation by acid guanidinium thiocyanate-phenol-chloroform extraction. *Anal Biochem* 162:156-159

22

Chrispeels MJ, Agre P (1994). Aquaporins: water channel proteins of plant and animal cells. *Trends Biochem Sci* 19:421-425

23

Copeland CS, Zimmer KP, Wagner KR, Healey GA, Mellman I, Helenius A (1988). Folding, trimerization, and transport are sequential events in the biogenesis of influenza virus hemagglutinin. *Cell* 53:197-209

24

Corvera S, Chawla A, Chakrabarti R, Joly M, Buxton J, Czech MP (1994). A double leucine within the GLUT4 glucose transporter COOH-terminal domain functions as an endocytosis signal. *J Cell Biol* 126:979-989

25

Davis JQ, Bennett V (1984). Brain ankyrin, purification of a 72,000 Mr spectrin-binding domain. *J Biol Chem* 259:1874-1881

26

De Jong WW, Lubsen NH, Kraft HJ (1994). Molecular evolution of the eye lens. *Prog Ret Eye Res* 13:391-442

27

De Silva A, Braakman I, Helenius A (1993). Posttranslational folding of vesicular stomatitis virus G protein in the ER: involvement of noncovalent and covalent complexes. *J Cell Biol* 120:647-655

28

Deen PMT, Croes H, van Aubel RA, Ginsel LA, van Os CH (1995). Water channels encoded by mutant aquaporin-2 genes in nephrogenic diabetes insipidus are impaired in their cellular routing. *J Clin Invest* 95:2291-2296

29

Deen PMT, Dempster JA, Wieringa B, van Os CH (1992). Isolation of a cDNA for rat CHIP28 water channel: high mRNA expression in kidney cortex and inner medulla. *Biochem Biophys Res Commun* 188:1267-1273

30

Deen PMT, Mulders SM, Kansen SM, van Os CH (1997). Aquaporins and ion conductance (technical comment). *Science* 275:1491

31

Deen PMT, Verdijk MA, Knoers NVAM, Wieringa B, Monnens LAH, van Os CH, van Oost BA (1994). Requirement of human renal water channel aquaporin-2 for vasopressin-dependent concentration of urine. *Science* 264:92-95

32

Deen PMT, Weghuis DO, Geurs van Kessel A, Wieringa B, van Os CH (1994). The human gene for water channel aquaporin 1 (AQP1) is localized on chromosome 7p15- ->p14. *Cytogenet Cell Genet* 65:243-246

33

Deen PMT, Weghuis DO, Sinke RJ, Geurts van Kessel A, Wieringa B, van Os CH (1994). Assignment of the human gene for the water channel of renal collecting duct aquaporin 2 (AQP2) to chromosome 12 region q12- ->q13. *Cytogenet Cell Genet* 66:260-262

34

Deen PMT, Rijss JPL, Mulders SM, Errington RJ, van Baal J, van Os CH (1997). Aquaporin-2 transfection of MDCK cells reconstitutes vasopressin-regulated transcellular osmotic water transport. *J Am Soc Nephrol* (in press)

35

Deen PMT, van Aubel RAMH, van Lieburg AF, van Os CH (1996). Urinary content of aquaporin 1 and 2 in nephrogenic diabetes insipidus. *J Am Soc Nephrol* 7:836-841

36

Delporte C, O Connell BC, He XJ, Lancaster HE, O Connell AC, Agre P, Baum BJ (1997). Increased fluid secretion after adenoviral mediated transfer of the aquaporin 1 cDNA to irradiated rat salivary glands. *Proc Natl Acad Sci* 94:3268-3273

37

Denker BM, Smith BL, Kuhajda FP, Agre P (1988). Identification, purification, and partial characterization of a novel Mr 28,000 integral membrane protein from erythrocytes and renal tubules. *J Biol Chem* 263:15634-15642

38

Denning GM, Anderson MP, Amara JF, Marshall J, Smith AE, Welsh MJ (1992). Processing of mutant cystic fibrosis transmembrane conductance regulator is temperature-sensitive. *Nature* 358:761-764

39

Destree OH, Bendig MM, De Laaf RT, Koster JG (1984). Organization of Xenopus histone gene variants within clusters and their transcriptional expression. *Biochim Biophys Acta* 782:132-141

40

Digiovanni SR, Nielsen S, Christensen EI, Knepper MA (1994). Regulation of collecting duct water channel expression by vasopressin in Brattleboro rat. *Proc Natl Acad Sci USA* 91:8984-8988

41
Drumm ML, Wilkinson DJ, Smit LS, Worrell RT, Strong TV, Frizzell RA, Dawson DC, Collins FS (1991). Chloride conductance expressed by delta F508 and other mutant CFTRs in Xenopus oocytes. *Science* 254:1797-1799

42
Ecelbarger CA, Terris J, Frindt G, Echevarria M, Marples D, Nielsen S, Knepper MA (1995). Aquaporin-3 water channel localization and regulation in rat kidney. *Am J Physiol* 38:F663-F672

43
Echevarria M, Windhager EE, Frindt G (1996). Selectivity of the renal collecting duct water channel aquaporin-3. *J Biol Chem* 271:25079-25082

44
Echevarria M, Windhager EE, Tate SS, Frindt G (1994). Cloning and expression of AQP3, a water channel from the medullary collecting duct of rat kidney. *Proc Natl Acad Sci USA* 91:10997-11001

45
Ehring GR, Zampighi G, Horwitz J, Bok D, Hall JE (1990). Properties of channels reconstituted from the major intrinsic protein of lens fiber membranes. *J Gen Physiol* 96:631-664

46
Feinberg AP, Vogelstein B (1983). A technique for radiolabeling DNA restriction endonuclease fragments to high specific activity. *Anal Biochem* 132:6-13

47
Finkelstein A (1987). Water movement through lipid bilayers, pores, and plasma membranes. Theory and reality. *New York: John Wiley & Sons*

48
Fischbarg J, Kuang K, Li J, Iserovich P, Wen Q (1997). Aquaporins and ion conductance (technical comment). *Science* 275:1491-1492

49
Franki N, Macaluso F, Schubert W, Gunther L, Hays RM (1995). Water channel-carrying vesicles in the rat IMCD contain cellubrevin. *Am J Physiol* 38:C797-C801

50
Frigeri A, Gropper MA, Turck CW, Verkman AS (1995). Immunolocalization of the mercurial-insensitive water channel and glycerol intrinsic protein in epithelial cell plasma membranes. *Proc Natl Acad Sci USA* 92:4328-4331

51
Frigeri A, Gropper MA, Umenishi F, Kawashima M, Brown D, Verkman AS (1995). Localization of MIWC and GLIP water channel homologs in neuromuscular, epithelial and glandular tissues. *J Cell Science* 108:2993-3002

52
Frokiaer J, Marples D, Knepper MA, Nielsen S (1996). Bilateral ureteral obstruction downregulates expression of vasopressin-sensitive AQP-2 water channel in rat kidney. *Am J Physiol* 39:F657-F668

53
Fujita N, Ishikawa S, Sasaki S, Fujisawa G, Fushimi K, Marumo F, Saito T (1995). Role of water channel AQP-CD in water retention in SIADH and cirrhotic rats. *Am J Physiol* 38:F926-F931

54
Fushimi K, Sasaki S, Marumo F (1997). Phosphorylation of serine 256 is required for cAMP dependent regulatory exocytosis of the aquaporin 2 water channel. *J Biol Chem* 272:14800-14804

55
Fushimi K, Uchida S, Hara Y, Hirata Y, Marumo F, Sasaki S (1993). Cloning and expression of apical membrane water channel of rat kidney collecting tubule. *Nature* 361:549-552

56
Girsch SJ, Peracchia C (1985). Lens cell-to-cell channel protein: II. Conformational change in the presence of calmodulin. *J Membr Biol* 83:227-233

57
Gorin MB, Yancey SB, Cline J, Revel JP, Horwitz J (1984). The major intrinsic protein (MIP) of the bovine lens fiber membrane: characterization and structure based on cDNA cloning. *Cell* 39:49-59

58
Griffin CS, Shiels A (1992). Localisation of the gene for the major intrinsic protein of eye-lens-fiber cell membranes to mouse chromosome 10 by in situ hybridisation. *Cytogenet Cell Genet* 59:300-302

59
Halban PA, Irminger JC (1994). Sorting and processing of secretory proteins. *Biochem J* 299:1-18

60
Hammond C, Helenius A (1995). Quality control in the secretory pathway. *Cur Opin Cell Biol* 7:523-529

61
Hanaoka K, Devuyst O, Schwiebert EM, Wilson PD, Guggino WB (1996). A role for CFTR in human autosomal dominant polycystic kidney disease. *Am J Physiol* 270:C389-99

62
Hasegawa H, Ma T, Skach W, Matthay MA, Verkman AS (1994). Molecular cloning of a mercurial-insensitive water channel expressed in selected water-transporting tissues. *J Biol Chem* 269:5497-5500

63
Hattori M, Sakaki Y (1986). Dideoxy sequencing method using denatured plasmid templates. *Anal Biochem* 152:232-238

64
Hayashi M, Sasaki S, Tsuganezawa H, Monkawa T, Kitajima W, Konishi K, Fushimi K, Marumo F, Saruta T (1994). Expression and distribution of aquaporin of collecting duct are regulated by vasopressin V_2 receptor in rat kidney. *J Clin Invest* 94:1778-1783

65
Hirsch JR, Loo DDF, Wright EM (1996). Regulation of Na+/glucose cotransporter expression by protein kinases in Xenopus laevis oocytes. *J Biol Chem* 271:14740-14746

66
Hochberg Z, Van Lieburg A, Even L, Brenner B, Lanir N, van Oost BA, Knoers NV (1997). Autosomal recessive nephrogenic diabetes insipidus caused by an aquaporin-2 mutation. *J Clin Endocrinol Metab* 82:686-689

67
Inase N, Fushimi K, Ishibashi K, Uchida S, Ichioka M, Sasaki S, Marumo F (1995). Isolation of human aquaporin 3 gene. *J Biol Chem* 270:17913-17916

68
Ishibashi K, Sasaki S, Fushimi K, Uchida S, Kuwahara M, Saito H, Furukawa T, Nakajima K, Yamaguchi Y, Gojobori T, et al (1994). Molecular cloning and expression of a member of the aquaporin family with permeability to glycerol and urea in addition to water expressed at the basolateral membrane of kidney collecting duct cells. *Proc Natl Acad Sci USA* 91:6269-6273

69
Ishibashi K, Sasaki S, Fushimi K, Yamamoto T, Kuwahara M, Marumo F (1997). Immunolocalization and effect of dehydration on AQP3, a basolateral water channel of kidney collecting ducts. *Am J Physiol* 41:F235-F241

70
Ishibashi K, Sasaki S, Kuwahara M, Marumo F (1997). Cloning and expression of a new water channel (AQP7) from rat with a permeability to glycerol and urea. *International Symposium on Molecular Physiology of Water Transport, Paris*:43 (Abstract)

71
Ishibashi K, Sasaki S, Saito F, Ikeuchi T, Marumo F (1995). Structure and chromosomal localization of a human water channel (AQP3) gene. *Genomics* 27:352-354

72
Ishibashi K, Sasaki S, Saito F, Ikeuchi T, Marumo F (1995). Structure and chromosomal localization of a human water channel (AQP3) gene (erratum vol 27, pg 352, 1995). *Genomics* 30:633

73
Jo I, Harris HW, Amendt Raduege AM, Majewski RR, Hammond TG (1995). Rat kidney papilla contains abundant synaptobrevin protein that participates in the fusion of antidiuretic hormone-regulated water channel-containing endosomes in vitro. *Proc Natl Acad Sci USA* 92:1876-1880

74
Jung JS, Bhat RV, Preston GM, Guggino WB, Baraban JM, Agre P (1994). Molecular characterization of an aquaporin cDNA from brain: candidate osmoreceptor and regulator of water balance. *Proc Natl Acad Sci USA* 91:13052-13056

75
Jung JS, Preston GM, Smith BL, Guggino WB, Agre P (1994). Molecular structure of the water channel through aquaporin CHIP. The hourglass model. *J Biol Chem* 269:14648-14654

76
Kamsteeg EJ, Mulders SM, Rijss JPL, Bichet DG, van Os CH, Deen PMT (1997). A new mutant AQP2 protein in recessive nephrogenic diabetes insipidus is not impaired in routing or functioning in Xenopus oocytes. *International Symposium on Molecular Physiology of Water Transport, Paris*:60 (Abstract)

77
Kanno K, Sasaki S, Hirata Y, Ishikawa S, Fushimi K, Nakanishi S, Bichet DG, Marumo F (1995). Urinary excretion of aquaporin-2 in patients with diabetes insipidus. *N Engl J Med* 332:1540-1545

78
Katsura T, Gustafson CE, Ausiello DA, Brown D (1997). Protein kinase A phosphorylation is involved in regulated exocytosis of aquaporin 2 in transfected LLC-PK1 cells. *Am J Physiol* 41:F816-F822

79
Katsura T, Verbavatz JM, Farinas J, Ma T, Ausiello DA, Verkman AS, Brown D (1995). Constitutive and regulated membrane expression of aquaporin 1 and aquaporin 2 water channels in stably transfected LLC-PK1 epithelial cells. *Proc Natl Acad Sci USA* 92:7212-7216

80
King LS, Nielsen S, Agre P (1996). Aquaporin-1 water channel protein in lung – Ontogeny, steroid-induced expression, and distribution in rat. *J Clin Invest* 97:2183-2191

81
Kishore BK, Mandon B, Oza NB, Digiovanni SR, Coleman RA, Ostrowski NL, Wade JB, Knepper MA (1996). Rat renal arcade segment expresses vasopressin-regulated water channel and vasopressin V-2 receptor. *J Clin Invest* 97:2763-2771

82
Knoers NVAM, van Os CH (1996). Molecular and cellular defects in nephrogenic diabetes insipidus. *Curr Opin Nephrol Hypertens* 5:353-358

83
Kukuljan M, Labarca P, Latorre R (1995). Molecular determinants of ion conductance and inactivation in K+ channels. *Am J Physiol* 268:C535-C556

84
Kushmerick C, Rice SJ, Baldo GH, Haspel HC, Mathias RT (1994). Cloning, expression, and functional studies of frog lens MIP. *Biophys J* 66:215 (Abstract)

85
Kuwahara M, Fushimi K, Terada Y, Bai L, Marumo F, Sasaki S (1995). cAMP-dependent phosphorylation stimulates water permeability of aquaporin-collecting duct water channel protein expressed in Xenopus oocytes. *J Biol Chem* 270:10384-10387

86
Laemmli UK (1970) Cleavage of structural proteins during the assembly of the head of bacteriophage T4. *Nature* 227:680-685

87
Lampe PD, Johnson RG (1990). Amino acid sequence of in vivo phosphorylation sites in the main intrinsic protein (MIP) of lens membranes. *Eur J Biochem* 194:541-547

88
Lande MB, Jo I, Zeidel ML, Somers M, Harris HW (1996). Phosphorylation of aquaporin-2 does not alter the membrane water permeability of rat papillary water channel- containing vesicles. *J Biol Chem* 271:5552-5557

89
LeBlanc-Straceski JM, Montgomery KT, Kissel H, Murthaugh L, Tsai P, Ward DC, Krauter KS, Kucherlapati R (1994). Twenty-one polymorphic markers from human chromosome 12 for integration of genetic and physical maps. *Genomics* 19:341-349

90
Lee MD, Bhakta KY, Raina S, Yonescu R, Griffin CA, Copeland NG, Gilbert DJ, Jenkins NA, Preston GM, Agre P (1996). The human aquaporin-5 gene - Molecular characterization and chromosomal localization. *J Biol Chem* 271:8599-8604

91
Li H, Lee S, Jap BK (1997). Molecular design of aquaporin-1 water channel as revealed by electron crystallography. *Nature Struct Biol* 4:263-265

92
Li HL, Lee S, Jap BK (1997). Molecular design of aquaporin-1 water channel as revealed by electron crystallography. *Nature Struct Biol* 4:263-265

93
Liebenhoff U, Rosenthal W (1995). Identification of Rab3-, Rab5a- and synaptobrevin II-like proteins in a preparation of rat kidney vesicles containing the vasopressin-regulated water channel. *FEBS Letters* 365:209-213

94
Loo DD, Zeuthen T, Chandy G, Wright EM (1996). Cotransport of water by the Na+/glucose cotransporter. *Proc Natl Acad Sci USA* 93:13367-13370

95
Low P (1986). Structure and function of the cytoplasmic domain of band 3: center of erythrocyte membrane-peripheral protein interactions. *Biochim Biophys Acta* 864:145-167

96
Lu L, Montrose Rafizadeh C, Hwang TC, Guggino WB (1990). A delayed rectifier potassium current in Xenopus oocytes. *Biophys J* 57:1117-1123

97
Lu MQ, Lee MD, Smith BL, Jung JS, Agre P, Verdijk MAJ, Merkx G, Rijs JPL, Deen PMT (1996). The human AQP4 gene: Definition of the locus encoding two water channel polypeptides in brain. *Proc Natl Acad Sciences USA* 93:10908-10912

98
Ma T, Frigeri A, Hasegawa H, Verkman AS (1994). Cloning of a water channel homolog expressed in brain meningeal cells and kidney collecting duct that functions as a stilbene-sensitive glycerol transporter. *J Biol Chem* 269:21845-21849

99
Ma T, Hasegawa H, Skach WR, Frigeri A, Verkman AS (1994). Expression, functional analysis, and in situ hybridization of a cloned rat kidney collecting duct water channel. *Am J Physiol* 266:C189-C197

100
Ma T, Yang B, Gillespie A, Carlson EJ, Epstein CJ, Verkman AS (1997). Generation and preliminary phenotype analysis of a transgenic knock-out mouse lacking the mercurial-insensitive water channel AQP4. *International Symposium on Molecular Physiology of Water Transport, Paris*:56 (Abstract)

101
Ma TH, Yang BX, Kuo WL, Verkman AS (1996). cDNA cloning and gene structure of a novel water channel expressed exclusively in human kidney: Evidence for a gene cluster of aquaporins at chromosome locus 12q13. *Genomics* 35:543-550

102
Mandon B, Chou CL, Nielsen S, Knepper MA (1996). Syntaxin-4 is localized to the apical plasma membrane of rat renal collecting duct cells: Possible role in aquaporin- 2 trafficking. *J Clin Invest* 98:906-913

103
Marinelli RA, Pham L, Agre P, LaRusso NF (1997). Secretin promotes osmotic water transport in rat cholangiocytes by increasing aquaporin-1 water channels in plasma membrane -Evidence for a secretin-induced vesicular translocation of aquaporin-1. *J Biol Chem* 272:12984-12988

104
Marples D, Christensen S, Christensen EI, Ottosen PD, Nielsen S (1995). Lithium-induced down-regulation of aquaporin-2 water channel expression in rat kidney medulla. *J Clin Invest* 95:1838-1845

105
Marples D, Frokiaer J, Dorup J, Knepper MA, Nielsen S (1996). Hypokalemia-induced downregulation of aquaporin-2 water channel expression in rat kidney medulla and cortex. *J Clin Invest* 97:1960-1968

106
Marples D, Knepper MA, Christensen EI, Nielsen S (1995). Redistribution of aquaporin-2 water channels induced by vasopressin in rat kidney inner medullary collecting duct. *Am J Physiol* 38:C655-C664

107
Mathai JC, Mori S, Smith BL, Preston GM, Mohandas N, Collins M, Vanzijl PCM, Zeidel ML, Agre P (1996). Functional analysis of aquaporin-1 deficient red cells - The Colton-null phenotype. *J Biol Chem* 271:1309-1313

108
Mathias RT, Rae JL, Eisenberg RC (1979) Electrical properties of structural components of the crystalline lens. *Biophys J* 25:181-201

109
Mathias RT, Riquelme G, Rae JL (1991). Cell to cell communication and pH in the frog lens. *J Gen Physiol* 98:1085-1103

110
McLean IW, Nakane PK (1974) Periodate-lysine-paraformaldehyde fixative. A new fixation for immunoelectron microscopy. *J Histochem Cytochem* 22:1077-1083

111
Michea LF, de la Fuente M, Lagos N (1994). Lens major intrinsic protein (MIP) promotes adhesion when reconstituted into large unilamellar liposomes. *Biochemistry* 33:7663-7669

112
Mitra AK, Vanhoek AN, Wiener MC, Verkman AS, Yeager M (1995). The CHIP28 water channel visualized in ice by electron crystallography. *Nature Struct Biol* 2:726-729

113
Modesto E, Lampe PD, Ribeiro MC, Spray DC, Campos de Carvalho AC (1996). Properties of chicken lens MIP channels reconstituted into planar lipid bilayers. *J Membr Biol* 154:239-249

114
Moon C, Preston GM, Griffin CA, Jabs EW, Agre P (1993). The human aquaporin-CHIP gene. Structure, organization, and chromosomal localization. *J Biol Chem* 268:15772-15778

115
Muggleton Harris AL, Festing MF, Hall M (1987). A gene location for the inheritance of the cataract Fraser (CatFr) mouse congenital cataract. *Genet Res* 49:235-238

116
Mulders SM, Knoers NVAM, van Lieburg AF, Monnens LAH, Leumann E, Wuhl E, Schober E, Rijss JPL, van Os CH, Deen PMT (1997). New mutations in the AQP2 gene in nephrogenic diabetes insipidus resulting in functional but misrouted water channels. *J Am Soc Nephrol* 8:242-248

117
Mulders SM, Preston GM, Deen PM, Guggino WB, van Os CH, Agre P (1995). Water channel properties of major intrinsic protein of lens. *J Biol Chem* 270:9010-9016

118
Mulders SM, Rijss JPL, Hartog A, Bindels RJM, van Os CH, Deen PMT (1997). Importance of the mercury sensitive cysteine on the function and routing of AQP1 and AQP2 in oocytes. *Am J Physiol: Renal Physiol* (in press)

119
Mulders SM, Weghuis DO, van Boxtel JAF, van Kessel AG, Echevarria M, van Os CH, Deen PMT (1996). Localization of the human gene for aquaporin 3 (AQP3) to chromosome 9, region p21->p12, using fluorescent in situ hybridization. *Cytogenet Cell Genet* 72:303-305

120
Musil LS, Goodenough DA (1993). Multisubunit assembly of an integral plasma membrane channel protein, gap junction

connexin43, occurs after exit from the ER. *Cell* 74:1065-1077

121

Nadler SP, Zimpelmann JA, Hebert RL (1992). Endothelin inhibits vasopressin-stimulated water permeability in rat terminal inner medullary collecting duct. *J Clin Invest* 90:1458-1466

122

Nielsen S, Chou CL, Marples D, Christensen EI, Kishore BK, Knepper MA (1995). Vasopressin increases water permeability of kidney collecting duct by inducing translocation of aquaporin-CD water channels to plasma membrane. *Proc Natl Acad Sci USA* 92:1013-1017

123

Nielsen S, Digiovanni SR, Christensen EI, Knepper MA, Harris HW (1993). Cellular and subcellular immunolocalization of vasopressin-regulated water channel in rat kidney. *Proc Natl Acad Sci USA* 90:11663-11667

124

Nielsen S, Marples D, Birn H, Mohtashami M, Dalby NO, Trimble W, Knepper M (1995). Expression of VAMP2-like protein in kidney collecting duct intracellular vesicles – Colocalization with Aquaporin-2 water channels. *J Clin Invest* 96:1834-1844

125

Nielsen S, Smith BL, Christensen EI, Agre P (1993). Distribution of the aquaporin CHIP in secretory and resorptive epithelia and capillary endothelia. *Proc Natl Acad Sci USA* 90:7275-7279

126

Nielsen S, Smith BL, Christensen EI, Knepper MA, Agre P (1993). CHIP28 water channels are localized in constitutively water-permeable segments of the nephron. *J Cell Biol* 120:371-383

127

Nielsen S, Terris J, Andersen D, Ecelbarger C, Frokiaer J, Jonassen T, Marples D, Knepper MA, Petersen JS (1997). Congestive heart failure in rats is associated with increased expression and targeting of aquaporin-2 water channel in collecting duct. *Proc Natl Acad Sciences USA* 94:5450-5455

128

Nikaido H, Rosenberg EY (1985). Functional reconstitution of lens gap junction proteins into proteoliposomes. *J Membr Biol* 85:87-92

129

Oksche A, Dickson J, Schulein R, Seyberth HW, Muller M (1994). Two novel mutations in the vasopressin V_2 receptor gene in patients. *Biochem Biophys Res Commun* 205:552-557

130

Oksche A, Moller A, Dickson J, Rosendahl W, Rascher W, Bichet DG, Rosenthal W (1996). Two novel mutations in the aquaporin-2 and the vasopressin V_2 receptor genes in patients with congenital nephrogenic diabetes insipidus. *Human Genetics* 98:587-589

131

Pannekeet MM, Mulder JB, Weening JJ, Struijk DG, Zweers MM, Krediet RT (1996). Demonstration of aquaporin-CHIP in peritoneal tissue of uremic and CAPD patients. *Perit Dial Int* 16 Suppl 1:S54-7

132

Pao GM, Wu LF, Johnson KD, Hofte H, Chrispeels MJ, Sweet G, Sandal NN, Saier MHJ (1991). Evolution of the MIP family of integral membrane transport proteins. *Mol Microbiol* 5:33-37

133

Park JH, Saier MH (1996). Phylogenetic characterization of the MIP family of transmembrane channel proteins. *J Membr Biol* 153:171-180

134

Patil RV, Han Z, Wax MB (1997). Aquaporins and ion conductance (technical comment). *Science* 275:1492

135

Peracchia C, Girsch SJ (1989). Calmodulin site at the C-terminus of the putative lens gap junction protein MIP26. *Lens Eye Toxic Res* 6:613-621

136

Piatigorsky J, Wistow GJ (1989). Enzyme/crystallins: gene sharing as an evolutionary strategy. *Cell* 57:197-199

137

Pisano MM, Chepelinsky AB (1991). Genomic cloning, complete nucleotide sequence, and structure of the human gene encoding the major intrinsic protein (MIP) of the lens. *Genomics* 11:981-990

138

Pralong-Zamofing D, Yi QH, Schmalzing G, Good P, Geering K (1992). Regulation of alpha 1-beta 3-Na+-K+-ATPase isozyme during meiotic maturation of Xenopus laevis oocytes. *Am J Physiol* 262:C1520-C1530

139

Preston GM, Agre P (1991). Isolation of the cDNA for erythrocyte integral membrane protein of 28 kilodaltons: member of an ancient channel family. *Proc Natl Acad Sci USA* 88:11110-11114

140

Preston GM, Carroll TP, Guggino WB, Agre P (1992). Appearance of water channels in Xenopus oocytes expressing red cell

CHIP28 protein. *Science* 256:385-387

141

Preston GM, Jung JS, Guggino WB, Agre P (1993). The mercury-sensitive residue at cysteine 189 in the CHIP28 water channel. *J Biol Chem* 268:17-20

142

Preston GM, Jung JS, Guggino WB, Agre P (1994). Membrane topology of aquaporin CHIP. Analysis of functional epitope-scanning mutants by vectorial proteolysis. *J Biol Chem* 269:1668-1673

143

Preston GM, Smith BL, Zeidel ML, Moulds JJ, Agre P (1994). Mutations in aquaporin-1 in phenotypically normal humans without functional CHIP water channels. *Science* 265:1585-1587

144

Raina S, Preston GM, Guggino WB, Agre P (1995). Molecular cloning and characterization of an aquaporin cDNA from salivary, lacrimal, and respiratory tissues. *J Biol Chem* 270:1908-1912

145

Reizer J, Reizer A, Saier MHJ (1993). The MIP family of integral membrane channel proteins: sequence comparisons, evolutionary relationships, reconstructed pathway of evolution, and proposed functional differentiation of the two repeated halves of the proteins. *Crit Rev Biochem Mol Biol* 28:235-257

146

Roberts SK, Yano M, Ueno Y, Pham L, Alpini G, Agre P, LaRusso NF (1994). Cholangiocytes express the aquaporin CHIP and transport water via a channel-mediated mechanism. *Proc Natl Acad Sci USA* 91:13009-13013

147

Rosenthal W, Seibold A, Antaramian A, Lonergan M, Arthus MF, Hendy GN, Birnbaumer M, Bichet DG (1992). Molecular identification of the gene responsible for congenital nephrogenic diabetes insipidus. *Nature* 359:233-235

148

Sabolic I, Brown D (1995). Water channels in renal and nonrenal tissues. *News Physiol Sci* 10:12-17

149

Sabolic I, Katsura T, Verbavatz JM, Brown D (1995). The AQP2 water channel: effect of vasopressin treatment, microtubule disruption, and distribution in neonatal rats. *J Membr Biol* 143:165-175

150

Saito F, Sasaki S, Chepelinsky AB, Fushimi K, Marumo F, Ikeuchi T (1995). Human AQP2 and MIP genes, two members of the MIP family, map within chromosome band 12q13 on the basis of two-color FISH. *Cytogenet Cell Genet* 68:45-48

151

Sambrook J, Fritsch EF, Maniatis T (1989). Molecular cloning: a laboratory manual. *Cold Spring Harbor Laboratory, Cold Spring Harbor, NY*

152

Sasaki S, Ishibashi K, Fushimi K, Uchida S, Marumo F (1997). Aquaporin 2 and -3: representatives of two subfamilies of the MIP/AQP2 family. *International Symposium on Molecular Physiology of Water Transport, Paris*:40 (Abstract)

153

Sasaki S, Uchida S, Kuwahara M, Fushimi K, Marumo F (1997). Aquaporins and ion conductance (technical comment). *Science* 275:1490-1491

154

Shen L, Shrager P, Girsch SJ, Donaldson PJ, Peracchia C (1991). Channel reconstitution in liposomes and planar bilayers with HPLC purified MIP26 of bovine lens. *J Membr Biol* 124:21-32

155

Shi LB, Skach WR, Ma T, Verkman AS (1995). Distinct biogenesis mechanisms for the water channels MIWC and CHIP28 at the endoplasmic reticulum. *Biochemistry* 34:8250-8256

156

Shi LB, Skach WR, Verkman AS (1994). Functional independence of monomeric CHIP28 water channels revealed by expression of wild-type mutant heterodimers. *J Biol Chem* 269:10417-10422

157

Shi LB, Verkman AS (1996). Selected cysteine point mutations confer mercurial sensitivity to the mercurial-insensitive water channel MIWC/AQP-4. *Biochemistry* 35:538-544

158

Shiels A, Bassnett S (1996). Mutations in the founder of the MIP gene family underlie cataract development in the mouse. *Nature Genet* 12:212-215

159

Shiels A, Griffin CS (1993). Aberrant expression of the gene for lens major intrinsic protein in the CAT mouse. *Curr Eye Res* 12:913-921

160

Skach WR, Shi LB, Calayag MC, Frigeri A, Lingappa VR, Verkman AS (1994). Biogenesis and transmembrane topology of the CHIP28 water channel at the endoplasmic reticulum. *J Cell Biol* 125:803-815

161
Smith BL, Agre P (1991). Erythrocyte Mr 28,000 transmembrane protein exists as a multisubunit oligomer similar to channel proteins. *J Biol Chem* 266:6407-6415

162
Sollner T, Whiteheart SW, Brunner M, Erdjument Bromage H, Geromanos S, Tempst P, Rothman JE (1993). SNAP receptors implicated in vesicle targeting and fusion. *Nature* 362:318-324

163
Stamer WD, Snyder RW, Smith BL, Agre P, Regan JW (1994). Localization of aquaporin CHIP in the human eye: implications in the pathogenesis of glaucoma and other disorders of ocular fluid balance. *Invest Ophthalmol Vis Sci* 35:3867-3872

164
Stankovic KM, Adams JC, Brown D (1995). Immunolocalization of aquaporin CHIP in the guinea pig inner ear. *Am J Physiol* 38:C1450-C1456

165
Swenson KI, Jordan JR, Beyer EC, Paul DL (1989). Formation of gap junctions by expression of connexins in Xenopus oocyte pairs. *Cell* 57:145-155

166
Takahashi H, Hasegawa H, Hayakawa H, Suzuki M, Kawaguchi Y, Imai M, Sakai O (1995). Involvement of kidney water channels in disability of urine concentration in chronic renal failure. *J Am Soc Nephrol* 6:1032 (Abstract)

167
Terris J, Ecelbarger CA, Marples D, Knepper MA, Nielsen S (1995). Distribution of aquaporin-4 water channel expression within rat kidney. *Am J Physiol* 38:F775-F785

168
Terris J, Ecelbarger CA, Nielsen S, Knepper MA (1996). Long-term regulation of four renal aquaporins in rats. *Am J Physiol* 40:F414-F422

169
Thomas PJ, Qu BH, Pedersen PL (1995). Defective protein folding as a basis of human disease. *Trends Biochem Sci* 20:456-459

170
Uchida S, Sasaki S, Fushimi K, Marumo F (1994). Isolation of human aquaporin-CD gene. *J Biol Chem* 269:23451-23455

171
Umenishi F, Carter EP, Yang BX, Oliver B, Matthay MA, Verkman AS (1996). Sharp increase in rat lung water channel expression in the perinatal period. *Am J Resp Cell Mol Biol* 15:673-679

172
Valenti G, Frigeri A, Ronco PM, Dettorre C, Svelto M (1996). Expression and functional analysis of water channels in a stably AQP2-transfected human collecting duct cell line. *J Biol Chem* 271:24365-24370

173
Van den Ouweland AM, Dreesen JC, Verdijk M, Knoers NV (1992). Mutations in the vasopressin type 2 receptor gene (AVPR2) associated with nephrogenic diabetes insipidus. *Nature Genet* 2:99-102

174
Van Hoek AN, Hom ML, Luthjens LH, de Jong MD, Dempster JA, van Os CH (1991). Functional unit of 30 kDa for proximal tubule water channels as revealed by radiation inactivation. *J Biol Chem* 266:16633-16635

175
Van Hoek AN, Luthjens LH, Hom ML, van Os CH, Dempster JA (1992). A 30 kDa functional size for the erythrocyte water channel determined in situ by radiation inactivation. *Biochem Biophys Res Commun* 184:1331-1338

176
Van Hoek AN, Wiener M, Bicknese S, Miercke L, Biwersi J, Verkman AS (1993). Secondary structure analysis of purified functional CHIP28 water channels by CD and FTIR spectroscopy. *Biochemistry* 32:11847-11856

177
Van Hoek AN, Wiener MC, Verbavatz JM, Brown D, Lipniunas PH, Townsend RR, Verkman AS (1995). Purification and structure-function analysis of native, PNGase F-treated, and endo-beta-galactosidase-treated CHIP28 water channels. *Biochemistry* 34:2212-2219

178
Van Lieburg AF, Verdijk MA, Knoers VV, van Essen AJ, Proesmans W, Mallmann R, Monnens LA, van Oost BA, van Os CH, Deen PM (1994). Patients with autosomal nephrogenic diabetes insipidus homozygous for mutations in the aquaporin 2 water-channel gene. *Am J Hum Genet* 55:648-652

179
Van Lieburg AF, Knoers VVAM, Mallmann R, Proesmans W, van den Heuvel LPWJ, Monnens LAH (1996). Normal fibrinolytic responses to 1-desamino-8-D-arginine vasopressin in patients with nephrogenic diabetes insipidus caused by mutations in the aquaporin 2 gene. *Nephron* 72:544-546

180
Verbavatz JM, Brown D, Sabolic I, Valenti G, Ausiello DA, Van Hoek AN, Ma T, Verkman AS (1993). Tetrameric assembly of

CHIP28 water channels in liposomes and cell membranes: a freeze-fracture study. *J Cell Biol* 123:605-618

181

Verbavatz JM, Van Hoek AN, Ma T, Sabolic I, Valenti G, Ellisman MH, Ausiello DA, Verkman AS, Brown D (1994). A 28 kDa sarcolemmal antigen in kidney principal cell basolateral membranes: relationship to orthogonal arrays and MIP26. *J Cell Sci* 107:1083-1094

182

Verkman AS, Yang B (1997). Aquaporins and ion conductance (technical comment). *Science* 275:1491

183

Wade JB, Stetson DL, Lewis SA (1981). ADH action: evidence for a membrane shuttle mechanism. *Ann N Y Acad Sci* 372:106-117

184

Wall DA, Patel S (1989). Isolation of plasma membrane complexes from Xenopus oocytes. *J Membr Biol* 107:189-201

185

Walz T, Smith BL, Agre P, Engel A (1994). The three-dimensional structure of human erythrocyte aquaporin CHIP. *EMBO J* 13:2985-2993

186

Walz T, Smith BL, Zeidel ML, Engel A, Agre P (1994). Biologically active two-dimensional crystals of aquaporin CHIP. *J Biol Chem* 269:1583-1586

187

Walz T, Tittmann P, Fuchs KH, Muller DJ, Smith BL, Agre P, Gross H, Engel A (1996). Surface topographies at subnanometer-resolution reveal asymmetry and sidedness of aquaporin-1. *J Mol Biol* 264:907-918

188

Walz T, Typke D, Smith BL, Agre P, Engel A (1995). Projection map of aquaporin-1 determined by electron crystallography. *Nature Struct Biol* 2:730-732

189

Weaver CD, Shomer NH, Louis CF, Roberts DM (1994). Nodulin 26, a nodule-specific symbiosome membrane protein from soybean, is an ion channel. *J Biol Chem* 269:17858-17862

190

Xu DL, Martin PY, Ohara M, St John J, Pattison T, Meng XZ, Morris K, Kim JK, Schrier RW (1997). Upregulation of AQP2 water channel expression in chronic heart failure rat. *J Clin Invest* 99:1500-1505

191

Yamamoto T, Sasaki S, Fushimi K, Ishibashi K, Yaoita E, Kawasaki K, Marumo F, Kihara I (1995). Vasopressin increases AQP-CD water channel in apical membrane of collecting duct cells in Brattleboro rats. *Am J Physiol* 268:C1546-C1551

192

Yang BX, Ma TH, Verkman AS (1995). cDNA cloning, gene organization, and chromosomal localization of a human mercurial insensitive water channel – Evidence for distinct transcriptional units. *J Biol Chem* 270:22907-22913

193

Yisraeli JK, Melton DA (1989). Synthesis of long, capped transcripts in vitro by SP6 and T7 RNA polymerases. *Methods Enzymol* 180:42-50

194

Yool AJ, Stamer WD, Regan JW (1996). Forskolin stimulation of water and cation permeability in aquaporin1 water channels. *Science* 273:1216-1218

195

Zampighi GA, Hall JE, Ehring GR, Simon SA (1989). The structural organization and protein composition of lens fiber junctions. *J Cell Biol* 108:2255-2275

196

Zeidel ML, Ambudkar SV, Smith BL, Agre P (1992). Reconstitution of functional water channels in liposomes containing purified red cell CHIP28 protein. *Biochemistry* 31:7436-7440

197

Zhang R, Van Hoek AN, Biwersi J, Verkman AS (1993). A point mutation at cysteine 189 blocks the water permeability of rat kidney water channel CHIP28k. *Biochemistry* 32:2938-2941

198

Zhang RB, Logee KA, Verkman AS (1990). Expression of mRNA coding for kidney and red cell water channels in Xenopus oocytes. *J Biol Chem* 265:15375-15378

Abbreviations

AQP	aquaporin
AVP	arginine vasopressin
cAMP	cyclic adenosine monophosphate
bp	basepairs
CFTR	cystic fibrosis transmembrane conductance regulator
CHIP	channel forming integral protein
dDAVP	1-desamino-8-D-arginine vasopressin
DEPC	diethyl pyrocarbonate
DTT	dithiothreitol
E_A	Arrhenius activation energy
EDTA	ethylenediamine tetraacetate
ELISA	enzyme-linked immunosorbent assay
EM	electron microscopy
ER	endoplasmic reticulum
FITC	fluorescein isothiocyanate
IgG	immunoglobulin G
kb	kilobases
kDa	kilodaltons
MBS	modified Barth's solution
MIP	major intrinsic protein
NDI	nephrogenic diabetes insipidus
PAGE	polyacrylamide gel electrophoresis
P_d	diffusional water permeability coefficient
P_f	osmotic water permeability coefficient
PKA	protein kinase A
PMSF	phenylmethylsulfonyl fluoride
RT-PCR	reverse transcriptase polymerase chain reaction
SD	standard deviation
SDS	sodium dodecyl sulphate
SE	standard error of the mean
TBS	tris-buffered saline
TGN	trans golgi network
V_2 receptor	vasopressin type 2 receptor
wt	wild-type

List of amino acids

Amino acid	Three letter code	One letter code	Charge
Alanine	Ala	A	0
Arginine	Arg	R	+
Asparagine	Asn	N	0
Aspartic acid	Asp	D	-
Cysteine	Cys	C	0
Glutamine	Gln	Q	0
Glutamic acid	Glu	E	-
Glycine	Gly	G	0
Histidine	His	H	+
Isoleucine	Ile	I	0
Leucine	Leu	L	0
Lysine	Lys	K	+
Methionine	Met	M	0
Phenylanaline	Phe	F	0
Proline	Pro	P	0
Serine	Ser	S	0
Threonine	Thr	T	0
Tryptophan	Trp	W	0
Tyrosine	Tyr	Y	0
Valine	Val	V	0

Mulders SM, Preston GM, Deen PMT, Guggino WB, van Os CH, and Agre P (1995). Water channel properties of major intrinsic protein of lens. *J Biol Chem* 270:9010-9016.

Mulders SM, Olde Weghuis D, van Boxtel JAF, Geurts van Kessel A, Echevarria M, van Os CH, and Deen PMT (1996). Localization of the human gene for aquaporin 3 (AQP3) to chromosome 9, region p21-p12, using fluorescent in situ hybridization. *Cytogenet Cell Genet* 72:303-305.

Mulders SM, van Lieburg AF, Monnens LAH, Knoers NVAM, Deen PMT, and van Os CH (1996). Physiology and pathophysiology of aquaporins. *Eur J Clin Invest* 26:1041-1050.

Mulders SM, Knoers NVAM, van Lieburg AF, Monnens LAH, Leumann E, Wühl E, Schober E, Rijss JPL, van Os CH, and Deen PMT (1997). New mutations in the AQP2 gene in nephrogenic diabetes insipidus resulting in functional but misrouted water channels. *J Am Soc Nephrol* 8:242-248.

Mulders SM, Rijss JPL, Hartog A, Bindels RJM, van Os CH, and Deen PMT (1997). Importance of the mercury sensitive cysteine on function and routing of AQP1 and AQP2 in oocytes. *Am J Physiol* 273: *Renal Physiol* 42: in press.

Mulders SM, van der Kemp AJ, Terlouw SA, van Boxtel JAF, van Os CH, and Deen PMT. The exchange of functional domains among aquaporins with different transport characteristics; testing the hourglass model. *Submitted.*

Mulders SM, Bichet DG, Rijss JPL, Kamsteeg EJ, Arthus MF, Lonergan M, Fujiwara M, Morgan K, van Os CH, and Deen PMT. Dominant autosomal nephrogenic diabetes insipidus caused by a mutation in the C-terminus of AQP2. *Submitted.*

Deen PMT, Mulders SM, Kansen SM, and van Os CH (1997). Aquaporins and ion-conductance (technical comment). *Science* 275:1490

Op deze plaats wil ik iedereen bedanken die heeft bijgedragen aan de totstandkoming van dit proefschrift en de afgelopen vier jaar voor mij tot een leerzame en waardevolle periode hebben gemaakt. Enkele personen wil ik graag met name noemen.

Allereerst mijn promotor, Prof. Dr. Carel van Os. Beste Carel, bedankt voor je enthousiasme en optimisme wanneer het weer eens tegen zat. Jouw enorme fysiologische kennis en overzicht was onontbeerlijk wanneer wij dreigden te verzanden in details.

Ook wil ik mijn co-promotor, Dr. Peter Deen, bedanken. Beste Peter, onze samenwerking verliep vaak moeizaam, maar ik hoop dat we er allebei veel van geleerd hebben. Bedankt voor je aanstekelijke enthousiasme en dat je altijd voor me klaar stond.

Dr. René Bindels wil ik graag bedanken voor de vele goede adviezen en belangstelling, en niet te vergeten voor de strakke laborganisatie, wat absoluut bevordelijk was voor het werkplezier. Alle mensen van de afdeling Celfysiologie wil ik bedanken voor de plezierige samenwerking en de gezellige sfeer. We hebben samen veel gekletst, gelachen, en gemopperd. Hanneke van Boxtel en Annemiete van der Kemp wil ik bedanken voor hun bijdrage aan hoofdstuk 3. Annemiete, bedankt voor je enorme inzet tijdens de laatste, hectische weken. Anita Hartog wil ik graag bedanken voor haar bijdrage aan de schitterende coupes van de oöcyten. Maarten de Jong wil ik bedanken voor de isolatie van oöcyten, wat in 'de slechte tijden' van de padden niet altijd even dankbaar werk was. Johan Rijss ben ik erg dankbaar voor de geweldige samenwerking. Jammer dat je je werk aan de aquaporines niet voortzet, maar heel veel succes met je nieuwe baan! Erik-Jan Kamsteeg wens ik veel succes met de voortzetting van het aquaporine-werk. Ik hoop dat je er met net zoveel plezier aan zult werken als ik. Martijn Driessen en Sylvie Terlouw wil ik bedanken voor hun inzet en waardevolle bijdrage aan dit werk tijdens hun stage.

Ron Engels van de vakgroep Experimentele Dierkunde wil ik bedanken voor de zorg voor 'onze' padden en de bereidheid om even te assisteren wanneer dat nodig was. Ik heb dit zeer gewaardeerd!

Ook 'de overkant': Prof. Dr. Leo Monnens, Dr. Anita van Lieburg en Dr. Nine Knoers, van de afdelingen Kindergeneeskunde en Antropogenetica ben ik erg dankbaar voor de plezierige samenwerking. Het klinische aspect van mijn onderzoek was voor mij heel waardevol en maakte het nog interessanter.

I would also like to thank Peter Agre from the Johns Hopkins University in Baltimore, for the very interesting stay in his laboratory. I feel so lucky to have had the opportunity to work in such an inspiring environment.

Lieve pap en mam, ontzettend bedankt voor de onvoorwaardelijke steun en de nooit aflatende interesse. Lieve Ellen en Bas, ik vind het heel speciaal dat jullie mijn paranimfen willen zijn. Ellen, bedankt voor de prachtige vormgeving van dit proefschrift, ook al moest het in recordtijd af.

Lieve Remco, bedankt voor dat waar het uiteindelijk allemaal om gaat: gelukkig zijn. Na een periode van hard werken is het nu tijd voor iets heel anders!

Sabine Mulders werd 5 april 1969 geboren in Silvolde. In 1987 werd het ongedeeld VWO diploma behaald aan het Isala College te Silvolde. Aansluitend studeerde zij Gezondheidswetenschappen aan de Faculteit der Medische Wetenschappen, Katholieke Universiteit Nijmegen. Voor de afstudeerrichting Toxicologie liep zij stage bij de afdeling Biochemie (Prof. J.J.H.H.M. de Pont) en de afdeling Farmacologie (Dr. F.G.M. Russel). In augustus 1991 behaalde ze het doctoraal diploma (cum laude).

Vervolgens liep ze twee extra stages in het kader van een aanvullend doctoraalexamen Gezondheidswetenschappen bij de afdeling Celbiologie (Prof. B. Wieringa) en het Department of Physiology, University of Michigan, Ann Arbor, USA (Prof. J.A. Williams). Aansluitend startte zij in mei 1993 als Onderzoeker in Opleiding (OIO), in dienst van de Nederlandse Organisatie voor Wetenschappelijk Onderzoek, bij de afdeling Celfysiologie van de Faculteit der Medische Wetenschappen, Katholieke Universiteit Nijmegen. Hier voerde zij onder leiding van Prof. C.H. van Os en Dr. P.M.T. Deen het in dit proefschrift beschreven onderzoek uit. Van februari 1994 tot juli 1994 werd een werkbezoek gebracht aan de groep van P. Agre, MD, Departments of Biological Chemistry, Medicine, and Physiology, The Johns Hopkins University School of Medicine, Baltimore, USA.

Graphic design: Ellen Mulders, Nijmegen
Printed by: Thoben Offset Nijmegen
With thanks to: Thoben Offset Nijmegen

Stellingen

behorende bij het proefschrift

Structure and function of aquaporins in health and disease

Het zandlopermodel (hourglass model) blijkt een realistisch model te zijn voor de structuur van de waterporie in zowel AQP1 als AQP2. De structuur van de waterporie van AQP4 en AQP5 zal waarschijnlijk vergelijkbaar zijn, gezien de grote homologie met AQP1 en AQP2.

AQP3 vertoont meer homologie met de glycerol transporters dan met de aquaporines en zou een waterporie kunnen hebben die structureel anders is.

Het integreren van resultaten uit twee verschillende disciplines, electron crystallografie en *in vitro* mutagenese, zal uiteindelijk moeten leiden tot een gedetailleerd 3-dimensionaal structuur-functie model voor aquaporines.

De ontdekking van individuen bij wie een functioneel AQP1 ontbreekt en desondanks fenotypisch normaal zijn (*Preston et al. (1994) Science 265:1585-1587*), was een eerste aanwijzing dat het fysiologisch belang van sommige aquaporines niet zo groot is als werd gedacht.

AQP2 is gevoeliger voor een verstoring van het transport van het eiwit naar de plasmamembraan ten gevolge van structurele veranderingen dan AQP1, dit maakt AQP2 minder geschikt voor plaats-gerichte mutagenese studies.

Conductantiemetingen aan geïsoleerde kanaaleiwitten die in planaire lipide bilagen zijn gereconstitueerd (*Ehring et al. (1990) J Gen Physiol 96:631-664*) kunnen resultaten opleveren die niet in overeenstemming zijn met de *in vivo* situatie.

De bevinding dat AQP1 een forskoline-geïnduceerde conductantie veroorzaakt in *Xenopus* oöcyten (*Yool et al. (1996) Science 273:1216-1218*), kon door 6 verschillende groepen niet worden gereproduceerd, en berust waarschijnlijk op een artefact in de conductantiemetingen.

De tijdwinst die wordt behaald door gebruik van oöcyten van de klauwpad als expressiesysteem voor membraaneiwitten, vergeleken met transfectie van zoogdiercellen, wordt vaak teniet gedaan door het feit dat de oöcyten minimaal 3 maanden per jaar onbruikbaar zijn doordat de vrouwelijke padden de lente in hun kop hebben.

Bij de metabole labeling van eiwitten met behulp van ^{35}S-gelabeld methionine, moet men bedacht zijn op het vrijkomen van radioaktieve gassen die de werkomgeving sterk radioaktief kunnen besmetten (*Meisenhelder and Hunter (1988) Nature 335:120*).

Door de grote druk om te publiceren komt de onderzoeker/assistent 'in opleiding' (OIO/AIO) vaak te weinig toe aan het volgen van onderwijs.

De stijging in salaris van een AIO of OIO gedurende de 4 jaar is noodzakelijk om uiteindelijk in staat te zijn de promotie te kunnen betalen.

Het succes van de Tamagotchi (computereitje om lief te hebben) is een teken dat we in deze snelle maatschappij onze zorginstincten niet meer kunnen bevredigen, of dat een deel van de mensheid zich stierlijk verveelt (*De Gelderlander*).

Bij de weersvoorspelling op de televisie is het een trend om in steeds meer tijd steeds minder nuttige informatie te verschaffen.

Uit respect voor de lokale bevolking zou de vakantieganger zich qua kleding redelijkerwijs moeten aanpassen aan het vakantieland. Het opkomend massatoerisme in afgelegen streken zal dit echter niet bevorderen.

Met betrekking tot het draagcomfort van sokken is het onlogisch dat de naad van het teenstuk zich aan de binnenkant bevindt in plaats van aan de buitenkant.

Niemand weet hoe laat het is, leef dus je leven als het allerlaatste uur (*Youp van 't Hek*).

Sabine Mulders, Nijmegen, 10 oktober 1997

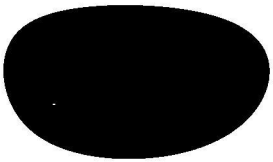

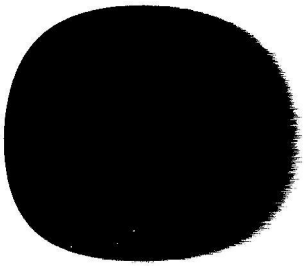

ISBN 90-9010904-8